UNIVERSITY OF CALIFORNIA, SAN DIEGO

The CREB Coactivator dTORC is Required for Metabolic Stress Resistance and Maintenance of Cardiac Function in *Drosophila*

A dissertation submitted in partial satisfaction of the requirements for the degree Doctor of Philosophy

in

Biomedical Sciences

by

Jason Thomas Goode

Committee in charge:

Professor Marc R. Montminy, Chair

Professor Christopher K. Glass, Co-Chair

Professor James R. Feramisco

Professor Bruce A. Hamilton

Professor Mark A. Lawson

Professor John B. Thomas

2010

This Dissertation of Jason Thomas Goode is approved, and it is acceptable in quality and form for publication on microfilm and electronically

_____

_____

_____

_____

_____

Co-Chair

_____

Chair

University of California, San Diego

2010

DEDICATION

To my wife and best friend, Taryn.

I couldn't have done it without you.

And with you, there is nothing I can't do.

TABLE OF CONTENTS

LIST OF FIGURES

LIST OF TABLES

ACKNOWLEDGEMENTS

I would like to acknowledge my advisor Dr. Marc Montminy for his guidance and patience. His insight and drive should be an example for all aspiring scientists.

I feel lucky to have worked with such talented and productive people in the Montminy Lab. First, I would like to thank Susan Hedrick for keeping the show rolling. She kept up her end of the bargain and is now free to retire. I would especially like to thank Jennifer Best-Martin for teaching me so much about flies and leaving me a challenging project. I am grateful to Michael Conkright for taking the time to teach me new techniques and for all the critical discussions over a beer. I would also like to thank Robert Screaton, Shawn Jeffries, Gianluca Canettieri, Jose Heredia, Henri Kester, and the rest of Marc's "boy toys", for welcoming me into the lab. I'm grateful to all the more recent members of the lab for continuing the tradition of camaraderie with the "lunch club" and the occasional pub trips. Not surprisingly, some of our most fruitful discussions occurred outside of the lab. I would like to thank Grant Miura for bringing a measure of levity to the lab and for critical reading of portions of this manuscript (as well as a good deal of my previous ramblings). I guess what I'm trying to say is: "Thank you for being a friend..."

I would like to acknowledge Dr. John Thomas who opened up his lab and his door to me. He always made the time to discuss the latest results and

to teach me something new. His passion and excitement about discovery are infectious.

I'm also grateful to all the members of the Thomas lab, past and present, who were generous with their time and knowledge.

I would like to thank the rest of my committee members, Dr. Christopher Glass, Dr. Mark Lawson, Dr. Bruce Hamilton, and Dr. James Feramisco for their feedback and advice.

I'm indebted to Dr. Rolf Bodmer and Dr. Karen Ocorr for welcoming me into their lab and teaching me that: yes, flies do have a heart. Karen has been especially generous with her time and expertise. Much of the heart data presented in Chapter 3 was collected shoulder to shoulder with Karen. I would also like to thank Georg Vogler for all of the help collecting, preparing, staining and imaging the embryos presented in Chapter 3. I'm also grateful for the critical discussions. I would like to thank Nakissa Alayari for generously sharing her superhuman dissecting skills and collecting scores of Drosophila hearts for me, which were used in the microarray experiments in Chapter 3. Thanks to all of the members of the Bodmer Lab for the stimulating discussions and boisterous lab meetings.

I would like to thank Leanne Nordeman for handling all of the administrative problems that come with a graduate program, so that I could concentrate on the scientific ones.

I'm extremely lucky to have a caring and supportive family. I would like to thank them for their encouragement throughout the years and for constantly asking me when I would be finished.

It is impossible to acknowledge everything that my wonderful wife, Taryn, has done for me. She has picked me up in the worst times; she is the reason for the best times. I want to thank her for her support, love and friendship that have carried me to this point. And this one.

Chapter 2 has been published and appears in Cell Metabolism 2008. Biao Wang, Jason Goode, Jennifer Best, Jodi Meltzer, Pablo E. Schilman, Jian Chen, Dan Garza, John B. Thomas, and Marc Montminy.

VITA

EDUCATION

2003-2010: University of California, San Diego
Ph.D., Graduate Program in Biomedical Sciences

2002: University of California, San Diego Extension
Course in Applied Immunology

1995-1999: New Mexico State University
B.S. Biochemistry

AWARDS

2004-2006: Genetics Training Program, University of California, San Diego
1999: University Honors Certificate, New Mexico State University
1999: Graduated with Honors, , New Mexico State University
1999: Alpha Chi Honor Society, New Mexico Alpha Chapter
1995-1999: Regents Scholarship, New Mexico State University,
1995-1999: Crimson Scholar, New Mexico State University,
1995-1999: Dean's List, College of Arts and Sciences,

PUBLICATIONS

Song Y, Altarejos J, Goodarzi MO, Inoue H, Guo X, Berdeaux R, Kim JH, Goode J, Igata M, Paz J, Hogan MF, Singh P, Goebel N, Miller N, Cui J, Jones MR, Taylor KD, Hsueh WA, Rotter JI, Montminy M. The CREB Coactivator CRTC3 Links Catecholamine Signaling to Energy Balance. Nature. *In Press*

Wang B, Goode J, Best J, Meltzer J, Schilman PE, Chen J, Garza D, Thomas JB, Montminy M.The insulin-regulated CREB coactivator TORC promotes stress resistance in *Drosophila*.Cell Metab. 2008 May;7(5):434-44.

Greten FR, Arkan MC, Bollrath J, Hsu LC, Goode J, Miething C, Goktuna SI, Neuenhahn M, Fierer J, Paxian S, Van Rooijen N, Xu Y, O'Cain T, Jaffee BB, Busch DH, Duyster J, Schmid RM, Eckmann L, Karin M. NF-kappaB is a negative regulator of IL-1beta secretion as revealed by genetic and pharmacological inhibition of IKKbeta. Cell. 2007 Sep 7;130(5):918-31.

Tabeta K, Hoebe K, Janssen EM, Du X, Georgel P, Crozat K, Mudd S, Mann N, Sovath S, Goode J, Shamel L, Herskovits AA, Portnoy DA, Cooke M, Tarantino LM, Wiltshire T, Steinberg BE, Grinstein S, Beutler B. The Unc93b1

mutation 3d disrupts exogenous antigen presentation and signaling via Toll-like receptors 3, 7 and 9. Nat Immunol. 2006 Feb;7(2):156-64.

Tabeta K, Georgel P, Janssen E, Du X, Hoebe K, Crozat K, Mudd S, Shamel L, Sovath S, Goode J, Alexopoulou L, Flavell RA, Beutler B. Toll-like receptors 9 and 3 as essential components of innate immune defense against mouse cytomegalovirus infection. Proc Natl Acad Sci U S A. 2004 Mar 9;101(10):3516-21.

Hoebe K, Du X, Goode J, Mann N, Beutler B.
Lps2: a new locus required for responses to lipopolysaccharide, revealed by germline mutagenesis and phenotypic screening. J Endotoxin Res. 2003;9(4):250-5.

Hoebe K, Du X, Georgel P, Janssen E, Tabeta K, Kim SO, Goode J, Lin P, Mann N, Mudd S, Crozat K, Sovath S, Han J, Beutler B. Identification of Lps2 as a key transducer of MyD88-independent TIR signalling. Nature. 2003 Aug 14;424(6950):743-8.

ABSTRACT OF THE DISSERTATION

The CREB Coactivator dTORC is Required for Metabolic Stress Resistance and Maintenance of Cardiac Function in *Drosophila*

by

Jason Thomas Goode

Doctor of Philosophy in Biomedical Sciences

University of California, San Diego, 2010

Professor Marc R. Montminy, Chair

Professor Christopher K. Glass, Co-Chair

Transducers of Regulated CREB (TORCs) are a recently characterized family of coactivators that enhance CRE-dependent transcription by interacting with the cAMP and calcium responsive transcription factor, CREB. TORC has

been shown to mediate the CREB-regulated transcription program of gluconeogenic genes in the mammalian liver. In response to fasting signals, TORC is dephosphorylated and transported to the nucleus where it binds CREB and activates transcription. Feeding promotes the phosphorylation and degradation of TORC through insulin signaling. We have found that *Drosophila* possess a single member of this family (dTORC) that behaves identically to its mammalian counterparts. In order to investigate the physiological role of TORC in an intact organism, we created TORC-null mutant flies. These animals display reduced glycogen and lipid stores and are sensitive to starvation and oxidative stress. Remarkably, neuronal expression of dTORC can rescue these phenotypes, suggesting the existence of an unknown pathway in the brain that controls metabolic stress resistance. dTORC mutant flies also display profound cardiac pathology that can be reversed by expression of dTORC in the heart, but not in neurons. These results suggest that TORC may function in many physiological processes beyond metabolic control. This work represents the first description of a completely TORC-null organism.

CHAPTER 1 Introduction

1.1 cAMP Response Element –Binding Protein (CREB)

It is a universal feature of all cells on earth, that they store their characteristic blueprint in the form of deoxyribonucleic acid (DNA). In order to express the instructions encoded in the blueprint, all cells transcribe portions of the DNA into ribonucleic acids (RNAs), which may catalyze chemical reactions themselves, or be translated into proteins. The regulation of these DNA (or gene) products is controlled by a class of sequence-specific DNA-binding molecular switches, called transcription factors. While some genetic programs may run autonomously, cells must be able to respond to changing intracellular conditions and their environment. Transcription factors control nearly all biological processes, and must be able to respond to external signals. In fact, flipping one of these molecular switches can often be thought of as the final step in a signal transduction pathway. Here we will focus on one of the best studied transcription factors: CREB.

1.1.1 The CREB Protein Family

3'-5'-Cyclic adenosine monophosphate (cAMP) response element-binding (CREB) protein is so named because it was originally identified as a 43 kiloDalton (kDa) phosphoprotein that binds to an eight base pair, palindromic sequence in the promoter of the somatostatin gene, called the

cAMP response element (CRE) (Montminy and Bilezikjian 1987), (Montminy, Sevarino et al. 1986). Subsequently, the related proteins, cAMP response element modulator (CREM), and activating transcription factor-1 (ATF-1) were identified, comprising a subgroup of the large family of basic region leucine zipper (bZIP) transcription factors (Lee, Hai et al. 1987) (Foulkes, Borrelli et al. 1991). The bZIP transcription factors dimerize through a heptad of leucine repeats along an alpha-helix that also contains the basic region that contacts DNA (Figure 1.1).

The basic structure of the CREB family proteins is composed of a carboxy-terminal bZIP dimerization and DNA-binding domain, a centrally located kinase-inducible domain (KID), and one or two constitutively active glutamine-rich domains (Q1 and Q2) (Figure 1.2). CREB, ATF-1 and CREM are highly identical in the bZIP region. CREB shares 91% identity with ATF-1 in the bZIP domain, and 95% with one of CREM's alternatively spliced bZIP domains and 75% with the other.(Hai, Liu et al. 1989), (Rehfuss, Walton et al. 1991), (Foulkes, Borrelli et al. 1991). The KID contains the Protein Kinase A (PKA) consensus phosphorylation site, as well as sites for several other protein kinases and confers sensitivity to cAMP. (Brindle, Linke et al. 1993), (de Groot, den Hertog et al. 1993), (Quinn 1993). The glutamine rich Q1 and Q2 domains are important for transcriptional activity in the absence of a stimulus and thus are termed constitutively active domains (CAD) (Brindle, Linke et al. 1993). The contribution of the Q2 domain to this constitutive

activation is greater than that of the Q1 domain (Gonzalez, Menzel et al. 1991). It should be noted that ATF-1 lacks a Q1 domain altogether.

CREB family proteins bind as dimers to the palindromic CRE sequence (5'-TGACGTCA-3') or, at lower affinity, to the half site (CGTCA/TGACG) in DNA. CREB, CREM and ATF-1 have all been shown to bind as homodimers, or heterodimers in various combinations (Laoide, Foulkes et al. 1993), (Hai, Liu et al. 1989; Loriaux, Brennan et al. 1994). Complexes with at least one CREB monomer appear to be the most stable, as ATF-1/CREB heterodimers have a longer half-life than ATF-1 homodimers while CREB/CREB homodimers have the longest half-life of all (Hurst, Totty et al. 1991) (Kobayashi and Kawakami 1995) (Kvietikova, Wenger et al. 1995). Little is known about the importance of heterodimerization in determining the nature of transcriptional activation by this family of proteins.

The CREB and CREM genes are both made up of many alternatively spliced exons which yield a number of variant proteins. (Foulkes and Sassone-Corsi 1992),(Ruppert, Cole et al. 1992) (Walker, Girardet et al. 1996), (Mayr and Montminy 2001)(Figure-1.3). To date, seventeen potential isoforms of CREB have been identified in humans, thirteen of which are known or believed to produce a protein product. However, only three of these transcripts are consistently annotated across all of the major public sequence databases, and are therefore included in the Consensus Coding Sequence Project (CCDS) (Pruitt, Harrow et al. 2009). Human CREM is alternatively spliced to form as

many as fifty-seven transcript variants, fourteen of which are included in the CCDS. ATF-1 has just one known transcript in humans. Alternative splicing in both CREB and CREM produces transcripts that encode either activator or repressor forms of these proteins (Foulkes and Sassone-Corsi 1992), (Walker, Girardet et al. 1996). The major activator forms of CREB are the 341 amino acid (aa) CREB-alpha and the 327aa CREB-delta which lacks the 14-residue alpha-peptide (Figure 1.3), (Hoeffler, Meyer et al. 1990). CREB-alpha and CREB-delta are widely expressed in all tissues. Inhibitory isoforms of CREB are produced by splice forms containing premature stop codons that allow translation reinitiation downstream. These isoforms are particularly important in the development of male germ cells (Walker, Girardet et al. 1996), (Girardet, Walker et al. 1996). CREM-tau is the major activator form of CREM, containing the Q1, KID, Q2, and bZIP domains like activator forms of CREB. Several CREM transcript variants have been shown to act as transcriptional repressors (Foulkes, Borrelli et al. 1991) (Molina, Foulkes et al. 1993). Of particular interest is the CREM isoform known as Inducible cAMP Early Repressor (ICER). ICER is a truncated bZIP domain which can repress CRE-mediated transcription. ICER transcription is itself activated by cAMP, due to mulitple CREs present in its intronic promoter. This negative feedback mechanism has been shown to be important in tissues such as T cells, pituitary gland, and heart (Bodor, Fehervari et al. 2007), (Mazzucchelli and Sassone-Corsi 1999), (Tomita, Nazmy et al. 2003).

1.1.2 Activation of CREB

CREB was originally discovered as a factor that binds to the CRE in the somatostatin gene and is phosphorylated by PKA in response to an increase in cAMP (Montminy and Bilezikjian 1987). PKA is a heterotetrameric kinase, composed of two regulatory (R) subunits and two catalytic (C) subunits, that is located in the cytoplasm in the inactive state. Upon stimulation with cAMP, the catalytic subunits passively diffuse into the nucleus where they bind and phosphorylate CREB (Mayr and Montminy 2001). Kinetic analysis of CREB phosphorylation confirmed that nuclear accumulation of catalytic PKA subunits, parallels the phosphorylation of CREB and transcriptional activation (Montminy 1997). PKA phosphorylates CREB at serine 133 within the kinase-inducible domain (Gonzalez and Montminy 1989). Phosphorylation at this residue is required for activation of transcription in response to cAMP, as mutation of this serine to alanine completely abolishes cAMP-induced transcription (Gonzalez and Montminy 1989). Furthermore, injection of CREB-specific neutralizing antibodies into cells, blocked expression of a CRE reporter gene, illustrating the requirement of CREB for cAMP dependent transcription (Meinkoth, Montminy et al. 1991).

The majority of cAMP-activated genes are transiently induced. (Hagiwara, Alberts et al. 1992). In the case of somatostatin, transcription peaks at thirty minutes after induction, and declines to basal levels after four hours. Inactivation of CREB, following cAMP induction, is achieved through

dephosphorylation by the serine/threonine phosphatases PP-1 and PP-2A (Hagiwara, Alberts et al. 1992), (Wadzinski, Wheat et al. 1993). The rate of dephosphorylation at serine 133 mirrors a decline in cAMP-induced transcription

Phosphorylation at serine 133 has been shown to recruit the CREB-binding protein (CBP)(Chrivia, Kwok et al. 1993). CBP is a 265-kDa nuclear protein that possesses histone acetyltransferase (HAT) activity and is involved in recruiting the RNA polymerase II (Pol II) transcription complex. Histone acetyltransferases catalyze the acetylation of lysine residues in the N-termini of histones. This leads to alteration of chromatin structure, making the DNA more accessible to the transcriptional machinery (Struhl 1998).

The N-terminus of CBP contains a 94 amino acid region known as the KID interaction domain (KIX) that is required to bind to the phosphorylated KID in CREB (Chrivia, Kwok et al. 1993). The structure of phosphorylated KID complexed to the KIX domain of CBP has been solved by nuclear magnetic resonance spectroscopy (Radhakrishnan, Perez-Alvarado et al. 1997). This structure reveals that the KID is not highly ordered and assumes a random-coil formation when not phosphorylated. Once phosphorylated at serine 133 and bound to KIX domain, the KID transitions to a two-helix structure with a kink close to the phosphorylation site that positons the two helices nearly perpendicular to each other (Figure 1.4). The KIX domain of CBP is made up of three alpha-helices that form a hydrophobic pocket, in which the carboxy-

terminal helix of the KID is bound. The phosphate at serine 133 stabilizes the complex by hydrogen bonding with residues in the KIX domain.

CBP also contains a C-terminal region required for interaction with Pol II known as the cysteine/histadine-rich 3 (C/H3) domain. The C/H3 domain interacts with RNA helicase A (RHA), and RHA interacts directly with Pol II. Coexpression of CBP along with RHA greatly enhances CREB induced transcription (Nakajima, Uchida et al. 1997).

A second, highly similar protein, known as p300 is also recruited by CREB. p300 shares most of the functional domains of CBP, including the KIX region, the C/H3 domain and also exhibits HAT activity. CBP and p300 appear to function very similarly in regards to CREB, however there is evidence that these coactivators have distinct roles in certain systems. For example, F9 carcinoma cells treated with a p300-specific ribozyme become resistant to retinoic-acid-induced differentiation, while knockdown of CBP has no effect (Kawasaki, Eckner et al. 1998). Furthermore, the mouse knockouts of CBP and p300 show somewhat distinct phenotypes (Vo and Goodman 2001). It should also be noted that in fibroblasts derived from p300 knockout mice, cAMP-induced activation of CRE-dependent gene expression is not affected (Yao, Oh et al. 1998).

The KID has been shown to be both necessary and sufficient for stimulus-induced activation of CREB. A fusion of the KID to the Gal4 DNA

binding domain is still able to activate transcription in the absence of other domains of CREB. However, the level of the response is greatly diminished compared to full-length CREB (Brindle, Linke et al. 1993), (Quinn 1993). Under certain conditions, CREB can activate transcription in the absence of stimulus. In these situations, the glutamine-rich region, Q2, has been shown to be important (Xing and Quinn 1994). The Q2 domain of CREB promotes transcriptional activation by recruiting the basal transcription factors, Transcription Factor IIB (TFIIB) and the TAFII130 subunit of Transcription Factor IID (TFIID) (Ferreri, Gill et al. 1994),(Xing, Gopal et al. 1995) .

Taken together, these results show that CREB uses multiple mechanisms to recruit and interact with the Pol II transcriptional machinery. The KID interacts with CBP, which recruits Pol II via an interaction with RHA, while the Q2 domain of CREB interacts with the basal transcription factors TFIIB and TFIID. CBP further enhances transcriptional activation through its HAT activity (Figure 1.5).

In addition to cAMP, CREB is also stimulated by another second messenger: Calcium (Ca^{2+}). Increasing intracellular Ca^{2+} concentration by membrane depolarization in the PC12 pheochromocytoma cell line has been shown to activate transcription of the CREB target gene *c-fos* . Activation of c-fos transcription requires a promoter element (TGACGTTT) that is very similar to the CRE (TGACGTCA) and in fact contains a CRE half site. This element has been named the Ca^{2+}-Responsive Element (CaRE) and was found to bind

CREB. Furthermore, CREB was required to activate transcription from the CaRE in response to elevated Ca^{2+}.

A variety of cellular signaling pathways that raise intracellular Ca^{2+} concentration have been shown to activate CREB through serine 133 phoshphorylation (Johannessen, Delghandi et al. 2004). However, the Ca^{2+}/calmodulin-dependent protein kinase II (CaMKII) phosphorylates CREB at a second site within the KID, serine 142, in addition to serine 133 (Sun, Enslen et al. 1994). There is some evidence that phoshphorylation of serine 142 is inhibitory to CREB activity. For example, in a fusion of CREB to the Gal4 DNA binding domain (GAL4-CREB), mutation of serine 142 to alanine permitted CaMKII-activation of a GAL4-reporter (Sun, Enslen et al. 1994). There is also evidence that phoshphorylation at serine 142 can disrupt the KID/KIX interaction (Parker, Jhala et al. 1998). On the contrary, several studies have suggested that serine 142 phosphorylation, may in fact stimulate CREB activity. One study finds that mice harboring a homozygous serine 142 to alanine (Ser142Ala) mutation in CREB, exhibit decreased expression of the CREB target genes *c-fos* and *mPer1 (*Gau, Lemberger et al. 2002). A second study finds that Ca^{2+} influx activates phoshphorylation at serine 142 (as well as serine 143) along with serine 133 and that phoshphorylation at these sites increases CREB activation. However, they confirm that serine 142 phosphorylation disrupts the CREB/KIX interaction and suggest that activation of CREB may occur independent of CBP recruitment in this system

(Kornhauser, Cowan et al. 2002). Further investigation will be necessary to resolve this controversy.

Many studies have identified serines other than Ser133, Ser142, and Ser143, as phosphoacceptor sites in CREB. These include Ser 89, Ser98, Ser108, Ser111, Ser114, Ser117, Ser121, Ser129, and Ser156. However, there is little evidence that any of these phoshphorylation sites are biologically relevant.

In addition to the second messengers, cAMP and Ca^{2+}, a very large number of stimuli have been shown to induce phoshphorylation of CREB (many of which themselves increase cAMP and Ca^{2+} levels) (Figure 1.6). Although, more than 300 different stimuli that lead to phosphorylation at serine 133 are described, not all of these have been shown to activate transcription via CREB (Johannessen, Delghandi et al. 2004). Therefore, while serine 133 phosphorylation is often necessary, it is not always sufficient for transcriptional activation. Perhaps the best illustration of this principal is the induction of CREB activity by growth factors. CREB is able to independently activate transcription of the immediate early gene, *c-fos*, in response to cAMP or calcium signals. However, treatment of the pheochromocytoma cell line, PC12, with Nerve Growth Factor (NGF) results in serine 133 phosphorylation of CREB, but transcription of c-fos does not occur in the absence of additional promoter-bound factors (Bonni, Ginty et al. 1995).

1.1.3 CREB Target Genes

CREB functions in a large number of cellular process including proliferation, survival, stress response, and regulating energy homeostasis. Being a transcription factor, it is generally believed that CREB exerts its influence on these processes by regulating the transcription of target genes. Two studies, using different methods, recently attempted to define all of the target genes that make up the CREB transcriptome. One group combined chromatin immunoprecipitation (ChIP) with a modified version of Serial Analysis of Gene Expression (SAGE), in a method they termed Serial Analysis of Chromatin Occupancy (SACO) (Impey, McCorkle et al. 2004). In this method, large numbers of concatemerized, 21 base-pair genomic signature tags (GSTs) derived from CREB ChIPs are sequenced and compared to DNA sequence databases to identify their chromosomal locations. This study identified 41,000 unique loci bound by CREB, but only 6,302 loci were detected with high confidence. Of the high confidence loci, 72% were found within one kilobase (kb) of a CRE, and 40% were within two kilobases of an annotated transcriptional start site (Impey, McCorkle et al. 2004).

The second study used multiple bioinformatic analyses, along with gene expression microarrays and ChIP on Chip assays to examine CREB function in different tissues (Zhang, Odom et al. 2005). Three independent bioinformatic algorithms identified 4,084 putative CREB target genes *in silico*. Gene ontology analysis of these putative CREB target genes revealed a very

strong enrichment of transcription factors, as well as genes involved in metabolism, cell cycle control, and the secretory pathway (Zhang, Odom et al. 2005). DNA obtained from CREB ChIP was hybridized to microarrays containing putative promoter regions for 16,000 human genes, in order to identify genes that are occupied by CREB *in vivo*. In this ChIP on chip study, approximately 3,000 promoters, representing nearly 20% of protein-coding genes were found to bind CREB. The authors suggest that this number is likely underestimated, due to the lack of sensitivity of the ChIP on chip assay. The actual number of promoters occupied by CREB may exceed 5,000 (Zhang, Odom et al. 2005). Contrary to the promoter-binding studies, gene expression profiling experiments find that only about 100 genes are activated by cAMP in any of the tissues considered. Moreover, there is very little overlap between the collections of genes activated in each tissue type. On the other hand, phoshphorylation of serine 133 was nearly uniform across all CREB-positive promoters, in all tissues tested, after stimulation with cAMP. Taken together, these results suggest that transcriptional activation by CREB requires more than DNA binding and serine 133 phosphorylation. Indeed, the authors find that CBP is selectively recruited to cAMP responsive genes, and absent from promoters of nonresponsive genes (Zhang, Odom et al. 2005). This result indicates that additional CREB regulatory partners may be required for activation of transcription.

1.1.4 Physiological Roles For CREB

Given that CREB binds up to one quarter of all human promoters, it is not surprising that CREB has been implicated in a diverse range of physiological processes. Knockout and transgenic models illustrate the broad role of CREB family members in organismal physiology. CREB null (CREB -/-) mice are found at reduced Mendelian ratios and die shortly after birth due to respiratory distress (Rudolph, Tafuri et al. 1998). These animals are also smaller, having birth weights only 70% that of their wild-type littermates. The observed respiratory distress is attributed to impaired production of a surfactant protein which leads to collapse of alveoli of the lung. No impairment of brain stem structure or expression of marker genes was observed in the CREB -/- animals, which may have been an alternate explanation for the respiratory impairment. However, the corpus callosum and anterior commissure were clearly reduced in CREB -/- mice compared to wild-type controls. Development of the αβ subpopulation of T cells and overall thymic cellularity was also severely impaired in CREB null animals.

Mouse knockouts of the CREM and ATF1 genes show a much less severe phenotype than CREB -/- animals. CREM null mice survive through adulthood and appear developmentally normal. However, male CREM knockouts are sterile due to postmeiotic arrest in spermiogenesis, and an increase in apoptosis of germ cells (Blendy, Kaestner et al. 1996), (Nantel, Monaco et al. 1996). ATF1 knockout mice appear to be phenotypically normal.

However ATF +/-, CREB -/- double mutant animals die around embryonic day 9.5, suggesting that other CREB family members can compensate for loss of ATF1 (Bleckmann, Blendy et al. 2002).

Use of constitutively active and dominant negative CREB transgenes has revealed further roles for CREB in different physiological processes. For example, expression of constitutively active VP16-CREB fusion protein in hippocampal neurons has been shown to lower the threshold for late phase long-term potentiation (Barco, Alarcon et al. 2002). Studies expressing unphosphorylatable, Ser133Ala CREB in the pituitary or, dominant negative ACREB in growth plate chondrocytes both lead to dwarfism in the mouse (Struthers, Vale et al. 1991), (Long, Schipani et al. 2001).

A large number of studies have focused on CREB's role in the nervous system (Benito and Barco 2010), (Lonze and Ginty 2002). CREB has been shown to be involved in the growth and survival of neurons as well as synaptic plasticity that affects learning and memory formation (Riccio, Ahn et al. 1999), (Yin, Wallach et al. 1994), (Bourtchuladze, Frenguelli et al. 1994), (Bartsch, Ghirardi et al. 1995). Recent studies have found that CREB can also affect the excitability of neurons (Dong, Green et al. 2006), (Lopez de Armentia, Jancic et al. 2007). Furthermore, both CREB and CREM appear to be involved in the maintenance of normal circadian rhythms (Gau, Lemberger et al. 2002), (Foulkes, Borjigin et al. 1997).

CREB is also known to regulate metabolism and energy homeostasis. Heterozygous mutant CREB +/- mice, as well as transgenic mice expressing the dominant-negative CREB inhibitor, ACREB, in the liver, exhibit fasting hypoglycemia and reduced expression of gluconeogenic enzymes (Herzig, Long et al. 2001). Furthermore, these mice display significantly increased plasma triglyceride levels and a fatty liver phenotype when fed a high-fat diet (Herzig, Hedrick et al. 2003).

CREB has been implicated in a remarkably large number of physiological processes. However, despite over two decades of research on this molecule, this aspect of CREB's function is probably the least well understood. Further studies are sure to find even more roles for CREB.

1.1.5 *Drosophila* CREB

Drosophila melanogaster have a single PKA responsive member of the CREB family called CrebB-17A or dCREB2. At the sequence level, this gene closely resembles both mammalian CREB and CREM. dCREB2 is alternatively spliced to form nine transcript variants. Similar to mammalian CREB and CREM, dCREB2 is transcribed as both a PKA responsive activator form and a transcriptional inhibitor isoform (Yin, Wallach et al. 1995). Expression of dCREB2 was detected throughout development of the fly, and in all tissues tested. dCREB2 was found to bind to the consensus CRE site in

electrophoretic mobility shift assays (EMSA), and to transactivate a CRE-reporter in the presence of PKA (Yin, Wallach et al. 1995). Taken together, these data suggest that dCREB2 is a *bona fide* member of the CREB family of transcription factors.

Like its mammalian counterparts, dCREB2 has been shown to be important for learning and memory and control of circadian rhythms. Transgenic expression of an inducible dominant-negative form of dCREB2 (dCREB2-b), blocked formation of long term memory in flies (Yin, Wallach et al. 1994). Another study went on to show that expression of the activator form of dCREB2 (dCREB2-a) could actually enhance formation of long term memory in the fly (Yin, Del Vecchio et al. 1995). However, the validity of this claim was called into question when it was discovered that the construct used to generate the transgenic flies contained a premature stop codon that resulted in truncation of the dCREB2 protein at amino acid 79. Overexpression of either the truncated dCREB2-a transgene, or a corrected full-length dCREB2-a transgene did not enhance long term memory formation in this study (Perazzona, Isabel et al. 2004). However, they were able to confirm that expression of the dominant negative dCREB2-b did, in fact, block formation of long term memory. These results may indicate that overexpression of CREB in the absence of stimulus is insufficient to enhance transcription of CREB target genes, or that increases in these target genes are incapable of enhancing long term memory formation.

Recent studies have also implicated dCREB2 in regulating energy balance and feeding behavior (Honjo and Furukubo-Tokunaga 2005), (Iijima, Zhao et al. 2009). Overexpression of the dominant-negative dCREB2-b in flies, reduced glycogen and lipid stores and increased food intake. These studies further confirm the similarities between dCREB2 and mammalian CREB and validate *Drosophila* as an excellent model organism in which to study CREB function.

1.2 Transducer of Regulated CREB (TORC)

1.2.1 Discovery of TORC/CRTC

CREB regulates a wide variety of genes that control processes such as cellular growth, metabolism, stress response and memory. As discussed in the previous section, CREB phosphorylation in response to stimulus is uniform across all of its bound target genes, yet only a subset of these genes is transcribed in a given cell type (Zhang, Odom et al. 2005). These results suggested that CREB is regulated by a process in addition to phosphorylation. In order to find additional CREB regulatory partners, two groups carried out high-throughput expression screens using full-length human cDNAs (Conkright, Canettieri et al. 2003), (Iourgenko, Zhang et al. 2003). These cDNAs were tested for their ability to activate CRE-containing luciferase reporters in HEK293 or HeLa cells. Both groups identified a new family of

CREB coactivators termed Transducers of Regulated CREB (TORC) or CREB Regulated Transcriptional Coactivators (CRTC). The screens identified two human TORC genes (TORC1 and TORC2), while DNA database searches revealed a third human TORC (TORC3) and single fly TORC gene (dTORC) (Conkright, Canettieri et al. 2003; Iourgenko, Zhang et al. 2003). Gene profiling experiments revealed TORC expression in nearly all tissues, however TORC1 was found to be more abundant in the brain, while TORC2 was highly expressed in B and T lymphocytes. All of the identified TORC genes were found to strongly coactivate expression of CRE-containing, cAMP-responsive promoters. Conversely, TORCs had almost no effect on promoters containing AP-1, heat shock, serum response, NF-κB, or glucocorticoid receptor response elements. Furthermore, mutating the CRE in the responsive promoters, completely abolished TORC-dependent transcriptional activation. Similar loss of CRE reporter activity was observered upon expression of a dominant-negative CREB protein (A-CREB) that blocks binding of CREB to DNA (Conkright, Canettieri et al. 2003). These results demonstrate that TORCs specifically transactivate CRE-containing genes, and that CREB is essential for these effects.

Induction of CRE reporter activity by elevation of cAMP and expression of TORC was additive, suggesting that TORC and PKA regulate CREB activity independently. Surprisingly, TORCs appear to potentiate CREB independently of Serine 133 phosphorylation. While TORC is unable to induce CRE activity

in mouse embryonic fibroblasts (MEFs) lacking CREB, expression of either wild-type or serine 133 to alanine (Ser133Ala) mutant CREB, restored TORC-induced CRE-activation.

TORCs were found to physically interact with the bZIP domain of CREB by Glutathione-S-Transferase (GST) pull-down assays, while other CREB domains (Q1, Q2, KID) exhibit no affinity for TORC. TORC strongly induced GAL4 reporter activity in HEK293T cells expressing full-length GAL4-CREB, as well as GAL4 fused to just the bZIP domain of CREB (GAL4-bZIP). However, TORC had no effect on cells expressing a GAL4-CREBΔbZIP protein which lacks the C-terminal bZIP binding domain of CREB (Conkright, Canettieri et al. 2003). Mutating charged residues in the bZIP domain to alanine revealed that arginine 314 is required for binding TORC. The Arg314Ala mutant CREB bZIP was unable to interact with TORC in GST pull-down assays and gel mobility shift assays (Screaton, Conkright et al. 2004). GST pull down assays demonstrated that a highly conserved, N-terminal coiled-coil domain of TORC is sufficient for binding CREB, and that binding occurs even in the absence of DNA (Conkright, Canettieri et al. 2003).

A fusion of the fourty-two N-terminal amino acids of TORC1 to the Notch coactivator Mastermind-like 2 (MAML2) was identified in a study of a common DNA translocation in mucoepidermoid carcinomas (Tonon, Modi et al. 2003). This fusion, termed MECT1-MAML2, to activated expression of the Notch target gene Hairy-Enhancer of Split-1 (HES-1) independent of the

presence of Notch ligand. The MECT1-MAML2 fusion protein was found to interact with CREB in coimmunoprecipitation assays, and potentiated CRE-reporter activity, while MAML2 alone had no effect. Furthermore, expression of the dominant-negative ACREB polypeptide blocked activation by the MECT1-MAML2 fusion protein. A luciferase reporter derived from the promoter of the Notch target gene HES-1, was also found to be activated by MECT1-MAML2 in a Notch ligand-independent, CREB-dependent manner. Moreover, this reporter was found to be strongly coactivated by full-length TORC as well. These results suggest that the TORC1-MAML2 fusion protein may interfere with Notch signaling by co-opting MAML2 to activate CREB target genes.

1.2.2 TORC is cAMP and Ca^{2+} Coincidence Detector

CREB has been shown to respond to both cAMP and calcium via phosphorylation at Ser133. However, studies with Gal4-CREB fusion proteins suggested that the bZIP domain may also play a role in integrating these two signals (Sheng, Thompson et al. 1991). The discovery of the TORC family of transcriptional coactivators revealed another potential mechanism by which CREB might respond to these two second messengers.

One study looked at the role of TORC in regulating cAMP and calcium signals in pancreatic islet β cells (Screaton, Conkright et al. 2004). Increased blood glucose levels lead to membrane depolarization, and elevation of

intracellular calcium levels in β cells, while gut hormones such as glucagon-like peptide 1 (GLP-1) cause increases in intracellular cAMP. These two signals are believed to synergize at the level of gene transcription. (Hinke, Hellemans et al. 2004).

Treatment of MIN6 insulinoma cells with high glucose and the GLP-1 analog, exendin-4, was shown to cooperatively increase the expression of CREB target genes. This effect could be mimicked by using the adenylate cyclase agonist, forskolin (FSK), and depolarizing concentrations of potassium chloride (KCl), which increase intracellular levels of cAMP and Ca^{2+} respectively. Conversely, this cooperativity was blocked by knockdown of TORC2 using RNA interference (RNAi), or by treatment with cyclosporine A (CsA) which inhibits the calcium-activated serine/threonine phosphatase, calcineurin/PP2B. (Screaton, Conkright et al. 2004).

1.2.3 Control of TORC2 Subcellular Localization

TORC2 is found primarily in the cytoplasm of resting MIN6 and HIT insulinoma cells. Treatment of these cells with compounds that raise either intracellular cAMP (i.e. FSK, Exendin-4) or Ca^{2+} (i.e. KCl, Glucose), had no effect on subcellular localization of TORC2. However, activation of both pathways simultaneously, resulted in primarily nuclear localization of TORC2.

Administration of cyclosporine A inhibited TORC2 nuclear entry (Screaton, Conkright et al. 2004).

Interestingly, TORC2 (as well as TORC3) is constitutively nuclear in resting HeLa epithelial carcinoma cells, while TORC1 is cytoplasmic (Bittinger, McWhinnie et al. 2004). Furthermore, in this cell line, TORC1 nuclear entry can be induced by increasing intracellular cAMP alone. In contrast, all three mammalian TORCs are found in the cytoplasm of HEK293 cells. In these cells, TORC2 and TORC3 rapidly accumulates in the nucleus in response to cAMP alone, while TORC1 requires both cAMP and the CRM1/exportin-1-mediated nuclear export inhibitor, leptomycin B (LMB) (Bittinger, McWhinnie et al. 2004). These results suggest that TORC family members are differentially regulated in different tissues. This property of TORCs was used to identify regions of the protein involved in nuclear import and export. Fusions of truncated TORC polypeptides, with green fluorescent protein (GFP) were used in ATYB1 human fibroblast cells to identify a nuclear localization sequence (NLS), and two nuclear export sequences (NES1 and NES2) in TORC2. These domains are highly conserved in the three mammalian TORC family members. In ATYB1 cells, TORC1 and TORC2 were cytoplasmically localized and shuttled into the nucleus in response to either forskolin or leptomycin B. Mutagenesis of individual leucines within NES1 and NES2 lead to nuclear localization of these proteins. However, TORC3 was found to be constitutively nuclear in ATYB1 cells. This is due to a single variant residue in the NES1

region of TORC3, which contains a tyrosine (Tyr) in place of the phenylalanine (Phe) found in TORC1 and TORC2. Mutating this residue from Tyr to Phe in TORC3, promoted cytoplasmic retention of the protein which could be reversed by treatment with forskolin (Screaton, Conkright et al. 2004). These results suggest that signal-dependent shuttling of TORC proteins is mediated in part by the NES sequences.

1.2.4 Regulation of TORC Activity by Phosphorylation

Immunoblotting TORC isolated from nuclear and cytoplasmic cellular fractions revealed that nuclear TORC2 migrates as a single band while cytoplasmic TORC2 migrates as a doublet containing a slower migrating band in addition to the band seen in the nuclear fraction. The slower migrating band collapsed into the faster species when treated with phosphatase, suggesting that this band represents phosphorylated TORC2. Treatment of HIT cells with FSK and KCl also resulted in accumulation of the faster migrating, unphosphorylated form of TORC2. Furthermore, this shift in mobility could be blocked by pretreatment with the calcineurin inhibitor, cyclosporine A (Screaton, Conkright et al. 2004). Taken together, these results suggest that cAMP and Ca^{2+} stimulate calcineurin-dependent dephosphorylation, and nuclear accumulation of TORC2.

Several phosphorylation sites were identified on TORC2, using tandem mass spectrometry and two-dimensional tryptic mapping. Mutagensis of individual serine residues revealed that Ser171 is particularly sensitive to cAMP, while a second region of TORC2 (aa 243-428) was dephosphorylated in response to KCl. However, a phospho-Ser171 specific antiserum revealed that FSK and KCl reduced phosphorylation at Ser171 cooperatively, suggesting that the cAMP and Ca^{2+} pathways may converge on this site.

1.2.5 TORC Binding Partners

Mass spectrometry revealed an association of the phosphoprotein-binding 14-3-3 proteins with TORC2 in two separate studies (Screaton, Conkright et al. 2004), (Jin, Smith et al. 2004). 14-3-3 proteins have been shown to bind a large number of proteins and to regulate them in a variety of ways, including serving as adapters, allosteric regulators of enzymes and sequestering proteins in particular subcellular compartments (Jin, Smith et al. 2004). Mutation of serine 171 to alanine reduced the interaction of TORC2 with 14-3-3, as did treatment of cells with KCl or FSK. However, none of these treatments reduced the interaction as much as complete dephosphorylation of TORC2 with calf intestinal phosphatase (CIP) (Screaton, Conkright et al. 2004). This suggests that 14-3-3 binds to multiple phosphorylation sites on TORC2 (Figure 1.7).

As noted, cyclosporine A (CsA) was able to inhibit dephosphorylation of TORC2 as well as potentiation of CRE reporters by TORC2. Furthermore, cyclosporine A blocked the release of TORC2 from 14-3-3 proteins. These observations suggest a potential role for the serine/threonine phosphatase calcineurin in regulating TORC activity. Indeed, calcineurin A and TORC2 were found to interact in pull-down assays as well as Far Western blotting assays.

Sequence analysis of the TORC2 protein revealed three potential calcineurin binding motifs (consensus PXIXIT). Two of these motifs were shown by mutagenesis, to enhance binding of calcineurin A to TORC2. Mutation of one these motifs decreased the ability of TORC2 to activate a CRE reporter. Conversely, the unphosphorylatable Ser171Ala mutant TORC2 was found to be more active on a CRE reporter (Screaton, Conkright et al. 2004). Therefore, calcineurin-mediated dephosphorylation of TORC promotes its nuclear translocation and activation, while phosphorylation (particularly at Ser171) enhances TORC's interaction with 14-3-3 in the cytoplasm, and inhibits its transcriptional activity (Figure 1.8).

1.2.6 Inhibition of TORC Activity by SIK

A search for the kinase that might be responsible for phosphorylation of TORC2 at Ser171 revealed a potential candidate in immunoprecipitates of TORC2 prepared from HEK293T cell cytoplasmic lysates. The salt-inducible

kinase 2 (SIK2) is a member of the sucrose non-fermenting-1 (snf1) family of serine/threonine kinases and has been shown to inhibit transcription of cAMP inducible genes in a CREB bZIP-dependent manner (Doi, Takemori et al. 2002). TORC2 and SIK2 were found to interact in coimmunoprecipitation (CoIP) assays, and coexpressing SIK2 with TORC2 led to decreased mobility of TORC2 in Western blot assays. Furthermore, SIK2 phosphorylated wild-type TORC2, but not Ser171Ala mutant TORC2 *in vitro*. Additionally, overexpression of SIK2 increased the binding of wild-type TORC2 peptides to 14-3-3, while this effect was blocked in the Ser171Ala mutant.

SIK2 is phosphorylated and inactivated by PKA at Ser587 in response to cAMP elevation (Okamoto, Takemori et al. 2004). Coexpression of SIK2 with TORC2 in ATYB1 cells enhanced the cytoplasmic localization of TORC2. However, treatment of these cells with forskolin lead to the nuclear translocation of TORC2. Forskolin was unable to induce the nuclear translocation of TORC2 in cells expressing a constitutively active Ser587Ala mutant SIK2. In contrast, Ser171Ala mutant TORC2 was found to be nuclear localized in both basal and forskolin stimulated conditions (Screaton, Conkright et al. 2004). Taken together, these results suggest that SIK2 phosphorylates TORC2 at Ser171 and promotes its cytoplasmic localization and transcriptional inactivation (Figure 1.8).

1.2.7 Additional Sites of TORC Regulation

The fact that Ser171Ala mutant TORC2 was still able to interact with 14-3-3 suggested that additional 14-3-3-binding phosphorylation sites might be present on TORC2. Mutating a series of serines to alanine in TORC2 revealed that in addition to Ser171, Ser275 and Ser369 also interact with 14-3-3. A TORC2 triple serine 171, 275 and 369 to alanine mutant is completely unable to bind 14-3-3 (Jansson, Ng et al. 2008). Given that at least two signals are required to drive nuclear translocation of TORC in certain cell types, and that Ser171 is efficiently dephosphorylated in response to cAMP alone, it is possible that the second signal is acting at another site.

Cellular immunofluorescence assays revealed that while wild-type or TORC2 harboring alanine mutations at serines 171, 275 or 369 alone were cytoplasmically localized, Ser171Ala, Ser275Ala double mutants were nuclear in HIT insulinoma cells. Mutation of Ser369, in combination with the other mutations, had no effect on nuclear localization in these assays (Jansson, Ng et al. 2008). A phosphoserine 275 specific antiserum revealed that serine 275 is dephosphorylated in response to glucose treatment, but not cAMP alone, in MIN6 cells and isolated mouse pacreatic islets. However, treatment with both glucose and cAMP enhanced dephosphorylation at Ser275. It should also be noted that cyclosporine A blocked dephosphorylation at Ser275, suggesting that calcineurin is the phosphatase acting at this site. (Jansson, Ng et al. 2008).

Parallel arrayed in vitro kinase assays were used to identify the AMPK family member, MAP/microtubule affinity-regulating kinase 2 (MARK2) as the kinase responsible for phosphorylating Ser275 in TORC2 (Fu and Screaton 2008; Jansson, Ng et al. 2008). Indeed, MARK2 is able to block TORC2-induced CREB activity on a CRE reporter (Jansson, Ng et al. 2008).

1.2.8 Summary of Regulation of TORC Activity

These studies indicate that TORCs are regulated by phosphorylation and nuclear shuttling. In the basal state, TORCs are sequestered in the cytoplasm by a phosphorylation-dependent interaction with 14-3-3 proteins. Calcium and cAMP pathways trigger release from 14-3-3 proteins by promoting dephosphorylation of TORC, which can then shuttle to the nucleus and associate with CREB. These two pathways act synergistically to increase nuclear TORC accumulation and target gene activation. This is accomplished by calcium activating the phosphatase calcineurin, and cAMP inhibiting an AMP kinase family member, Salt Inducible Kinase 2 (SIK2). In the absence of stimulus, SIK2 and MARK2 phosphorylate TORC at key regulatory serines and promotes 14-3-3 binding. An increase in cAMP inactivates SIK2 via the PKA-mediated phosphorylation at Ser587, while an increase in calcium counteracts MARK2, and activates calcineurin, which dephosphorylates TORC and leads to nuclear translocation (Figure 1.9).

1.2.9 Physiological Roles for TORCs

Given that CREB regulates a large number of physiological processes, it is likely that TORC is also involved in some or all of these processes. Although the TORC family was discovered relatively recently, it has already been implicated in the regulation of glucose homeostasis(Canettieri, Koo et al. 2005; Koo, Flechner et al. 2005; Shaw, Lamia et al. 2005; Dentin, Liu et al. 2007; Dentin, Hedrick et al. 2008), obesity (Altarejos, Goebel et al. 2008; Qi, Saberi et al. 2009; Ryu, Oh et al. 2009), fertility (Altarejos, Goebel et al. 2008), cancer (Hishiki, Ohshima et al. 2007; Canettieri, Coni et al. 2009; Jaskoll, Htet et al. 2010; Wang, Iwasaki et al. 2010), mitochondrial biogenesis (Wu, Huang et al. 2006), long-term memory (Zhou, Wu et al. 2006; Kovacs, Steullet et al. 2007), viral reactivation (Murata, Sato et al. 2009), salivary gland development (Jaskoll, Htet et al. 2010), cocaine addiction (Hollander, Im et al. 2010), and RNA splicing (Amelio, Caputi et al. 2009).

1.2.10 Gluconeogenesis

Perhaps the best studied aspect of TORC in physiological processes is its role in regulating glucose homeostasis. Circulating glucose levels are regulated systemically by the pancreatic hormones, insulin and glucagon. Insulin stimulates tissues such as muscle, adipose and liver to take up glucose from the blood. Conversely, under fasting conditions, glucagon raises blood

glucose levels by inducing glycogenolysis (the breakdown of glycogen) and gluconeogenesis (the production of new glucose from three and four carbon precursors) in the liver (Vander, Sherman et al. 1998). Glucagon is known to activate CREB in the liver, which contributes to gluconeogenesis and fatty acid oxidation in part by activating target genes such as glucose-6-phosphatase (G6Pase), phosphoenol pyruvate carboxykinase (PEPCK) and the peroxisome-proliferation-activated receptor γ coactivator-1 (PGC-1α) (Herzig, Long et al. 2001) (Herzig, Hedrick et al. 2003). However, CREB is equally phosphorylated in the liver in response to both glucagon and insulin treatment suggesting that the CREB-CBP pathway is unable to discriminate between these two signals (Koo, Flechner et al. 2005). In contrast, hepatic TORC2 is dephosphorylated, nuclear localized and binds to the promoters of gluconeogenic genes in response to glucagon or fasting conditions, but not in response to insulin or feeding. Furthermore, overexpression of TORC2 in the liver promotes fasting hyperglycemia, while RNAi knockdown of hepatic TORC2 causes fasting hypoglycemia (Koo, Flechner et al. 2005).

Approximately three hours after stimulation with glucagon, gluconeogenic transcript levels return to baseline, and TORC2 is inactivated by phosphorylation at Ser171. The salt-inducible kinase family member, SIK1, appears to be primarily responsible for this phosphorylation in hepatocytes. Interestingly, SIK1 expression itself is regulated by CREB and TORC2 suggesting that SIK1 functions as part of a negative feedback loop in which

fasting activates TORC to induce its own inhibitor (Koo, Flechner et al. 2005). AMP-activated protein kinase (AMPK) was also found to inactivate hepatic TORC2 through Ser 171 phosphorylation. Unlike SIK1, the ability of AMPK to inactivate TORC2 is not blocked by cAMP, suggesting that this kinase may override the stimulatory effects of glucagon on TORC2 in gluconeogenesis (Koo, Flechner et al. 2005). Supporting this hypothesis, mice lacking the AMPK activating kinase, LKB1 in the liver, exhibit hyperglycemia and increased expression of gluconeogenic and lipogenic genes. TORC2 is dephosphorylated and nuclear in the livers of these mice, and knockdown of TORC2 normalizes blood glucose (Shaw, Lamia et al. 2005). Therefore, TORC may be regulated by a number of AMPK family members in the liver.

Supporting the role of TORC2 in activating the gluconeogenic program, TORC2 -/- mice exhibit reduced hepatic glucose production, along with reduced expression of gluconeogenic genes, resulting in lower fasting blood glucose levels (Wang, Inoue et al. 2010). These mice also have lower circulating insulin, triglycerides, and cholesterol, and are more insulin sensitive (Wang, Inoue et al. 2010). These results suggest that TORC2 may be involved in the development of insulin resistance that occurs in disorders like type 2 diabetes.

A second group also generated a TORC mutant mouse that exhibited a reduction in gluconeogenic CREB target genes. Yet, this mutant maintained normal blood glucose levels in feeding and fasting (Le Lay, Tuteja et al. 2009).

However, this mutant may not be a TORC2 null because the targeting strategy used would allow for the generation of TORC2 polypeptide containing the N-terminal CREB binding domain fused directly to the C-terminal transactivation domain. A similar truncated TORC2 polypeptide, lacking the central regulatory domain can efficiently activate a CRE-reporter, suggesting that it may maintain much of the activity of the wild-type protein.

1.2.11 Regulation by Insulin

Counteracting the role of glucagon in increasing hepatic glucose output through activation of TORC2, insulin inhibits gluconeogenic gene expression by activating the kinase SIK2. In fact, the insulin-stimulated kinase AKT phosphorylates and activates SIK2, which leads to the phosphorylation and ubiquitin-dependent degradation of TORC2 in the liver. Degradation of TORC2 is mediated by ubiquitination of Lys628, through the E3 ubiquitin ligase, constitutive photomorphic protein-1 (COP1). Remarkably, TORC2 degradation seems to depend on initial activation by cAMP agonists such as glucagon, as evidenced by the inability of insulin alone to trigger degradation, as well as the insensitivity of the Ser171Ala mutant TORC2 to degradation (Dentin, Liu et al. 2007). This has the effect of allowing inactive TORC to remain in the cytoplasm in the fed state. However, in the case of refeeding that follows a period of fasting in which TORC was activated, TORC would be ubiquitinated

and degraded to prevent further increases in blood glucose through the gluconeogenic program.

TORC also enhances insulin signaling in the liver by inducing the expression of the insulin receptor substrate-2 (IRS2) gene in concert with CREB. The importance of this molecule in transducing the insulin signal is apparent in mice with acute knockdown or overexpression in the liver. Knocking down IRS2 results in glucose intolerance, whereas overxpression reduces fasting glucose levels by lessening gluconeogenic gene expression (Canettieri, Koo et al. 2005). These results suggest that TORC2 may prime its own insulin-driven degradation by activating transcription of IRS2.

1.2.12 Protein Modifications of TORC2

The degradation of TORC2 is blocked by acetylation of Lys628 by the histone acetytransferase p300 (Liu, Dentin et al. 2008). After a long term fast, TORC2 is deacetylated by the nutrient-sensing deacetylase sirtuin-1 (SIRT1). Deacetylation of TORC2, allows ubiquitination of Lys628 and subsequent degradation. Interestingly, SIRT1 upregulates the activity of the forkhead box protein O1 (FOXO1), suggesting that this transcription factor may assume control of the gluconeogenic program after prolonged fasting (Liu, Dentin et al. 2008).

In addition to the hormones glucagon and insulin, an elevated blood glucose level itself may regulate hepatic TORC2. One study showed that hepatocytes treated with high concentrations of glucose or glucosamine exhibit increased expression of CREB target genes and nuclear localization of TORC2 (Dentin, Hedrick et al. 2008). This was shown to be due to the O-glycosyl transferase (OGT)-dependent O-glycosylation of TORC2 on Ser171 and Ser70. O-glycosylation of these sites blocks their phosphorylation and therefore activates TORC2. Furthermore, insulin resistant db/db diabetic mice, as well as mice fed on a high-fat diet, have elevated levels of O-glycosylation on TORC2 in the lver. The increased expression of gluconeogenic genes, increased blood glucose levels, and increased O-glycosylation of TORC2 could all be reversed by overexpression of the degylcosylating enzyme, O-GlcNAcase in the liver. The metabolic phenotypes observed in the db/db and high-fat diet fed mice could be mimicked by overexpression of OGT in the livers of wild-type mice (Dentin, Hedrick et al. 2008). Knockdown of TORC2 reversed these phenotypes, suggesting that TORC2 may play a role in exacerbating hyperglycemia by activating gluconeogenesis in response to high glucose.

1.2.13 ER Stress

In addition to its role in coactivating gluconeogenic CREB target genes, TORC2 serves a second role in the liver in responding to endoplasmic reticulum (ER) stress. Interestingly, ER stress induced by thapsigargin or tunicamycin causes dephosphorylation and nuclear entry of TORC2 in hepatocytes, but not activation of a CRE-reporter, even in the presence of the cAMP agonist forskolin (Wang, Vera et al. 2009). However, TORC2 appears to activate the expression of ER stress genes (Xbp1, Grp78, Chop) by interacting with activating transcription factor 6 alpha (ATF6α). Association of TORC2 with ATF6α disrupts the interaction of TORC2 with CREB and inhibits the activation of gluconeogenic genes, reducing hepatic glucose output (Wang, Vera et al. 2009). These results suggest that TORC2 may function as a switch between fasting and ER stress signals. This would be of particular interest in obesity which causes chronic ER stress and increased hepatic glucose production. Dysregulation of TORC activity may play a role in this process.

1.2.14 TORC1 in Obesity and Fertility

In contrast to its role in liver, TORC function in other tissues is only beginning to be elucidated. TORC1 is expressed primarily in the brain where it is required to control feeding behavior and fertility. TORC1$^{-/-}$ mice are hyperphagic, obese and infertile (Altarejos, Goebel et al. 2008). Mutant mice

progressively gain more weight than wild-type animals, because they eat more and expend less energy. Obesity in TORC1-/- mice is accompanied by hyperglycemia, hypertriglyceridemia and insulin resistance. Notably, TORC1-/- mice are relatively insensitive to the anorexigenic effects of the adipose derived hormone leptin. Experiments in leptin mutant *ob/ob* mice revealed that TORC1 is dephosphorylated and activated in the arcuate cells of the hypothalamus in response to leptin (Altarejos, Goebel et al. 2008).

Activation of TORC1 drives expression of the neuropeptides cocaine and amphetamine-regulated transcript prepropeptide (Cartpt) and kisspeptin (Kiss1). Cartpt inhibits food intake in response to leptin, while Kiss1 regulates fertility by stimulating secretion of hypothalamic gonadotropin-releasing hormone. TORC1-/- mice, like Kiss1-mutant mice, have decreased circulating leuteinizing hormone, abnormal uterine morphology and are infertile (Altarejos, Goebel et al. 2008). However, the fertility phenotype of TORC1-/- mice is in question, because a second group using an identical targeting strategy observed only a mild reproductive phenoptype (smaller litter size) in TORC1-/- intercrosses (Breuillaud, Halfon et al. 2009). This observed discrepancy in the phenotype may reflect subtle differences in the genetic background of the mice in each lab. This controversy aside, these results indicate that TORC1, in conjuction with CREB, regulates the central effects of hormones on energy balance and fertility.

Several other studies have demonstrated the importance of TORC in the brain. Two groups have shown that TORC1 is required for late-phase, long-term potentiation (L-LTP) in hippocampal neurons (Zhou, Wu et al. 2006; Kovacs, Steullet et al. 2007), and a third study has revealed that TORC1 is required in BDNF-regulated dendritic growth (Finsterwald, Fiumelli et al. 2010).

1.3 Conclusions

CREB is among the best studied transcription factors, however much about its function and regulation remains unknown. The discovery of the TORC family of CREB coactivators has answered some old questions and opened up new frontiers of previously unexplored areas of the biology of CREB. In the short time since the discovery of TORC, much progress has been made in describing its regulation and response to cellular signaling. However, with the exception of the role of TORC2 in regulating glucose homeostasis in the liver, very little is known about the physiological processes TORC is involved in. One complication of investigating the physiological role of TORC in mammals, is compensation by family members. Mammals express three separate TORC genes, often in overlapping patterns. Flies, however, express only a single TORC gene. Additionally, flies share many of the same regulatory mechanisms that control energy homeostasis in mammals. For

example, mobilization of glycogen and lipid stores in response to starvation in flies, is controlled by a glucagon-like peptide called adipokinetic hormone (AKH) (Kim and Rulifson 2004) (Lee and Park 2004). Furthermore, the insulin signaling pathway is well conserved, and like in mammals, controls growth and circulating sugar levels (Broughton, Piper et al. 2005) (Puig, Marr et al. 2003). These similarities, along with their genetic tractability and quick generation time, make flies an ideal organism to study the physiology of the CREB-TORC pathway.

1.4 Figures

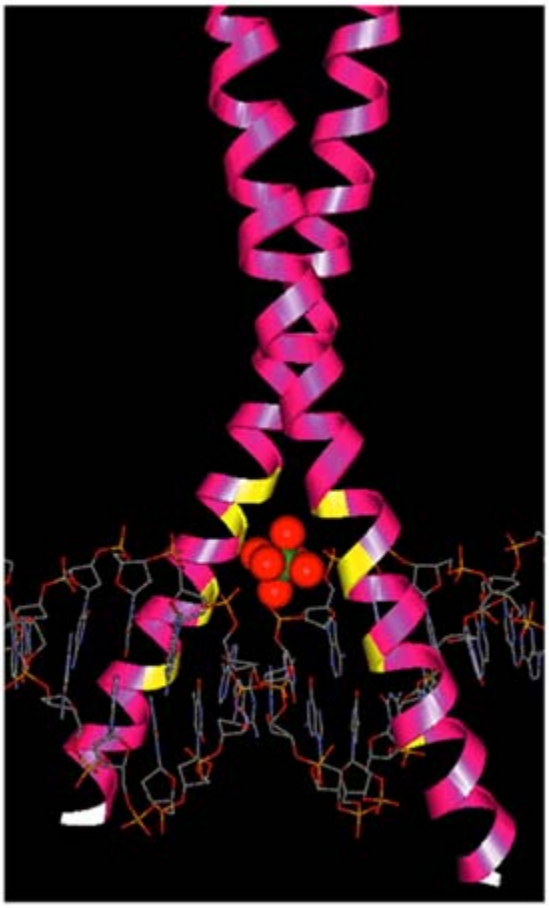

Figure 1.1. The bZIP Domain of CREB Binds the CRE in DNA

The structure of the basic region/leucine zipper domain of CREB (pink helices) is shown binding to a cAMP response element in DNA (wireframe). The surface of the helix that contains residues involved in DNA recognition is highlighted in yellow. In the cavity between the DNA and CREB bZIP domain, is a magnesium ion (green) with surrounding water molecules (red). Figure adapted from Mayr et. al., 2001.

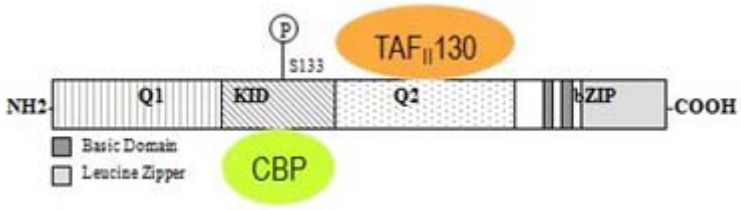

Figure1.2. The Major Functional Domains of CREB

Structure of CREB showing major functional domains and regulatory phosphorylation site (S133). Q2 is the constitutively active domain which interacts with TAFII130. The KID binds CBP in a phspho-dependent manner. The bZIP domain consists of basic regions involved in DNA binding and a leucine zipper domain responsible for dimerization. Q1 and Q2, Gluatmine-rich regions, KID, Kinase inducible domain, bZIP, Basic region/leucine zipper domain.

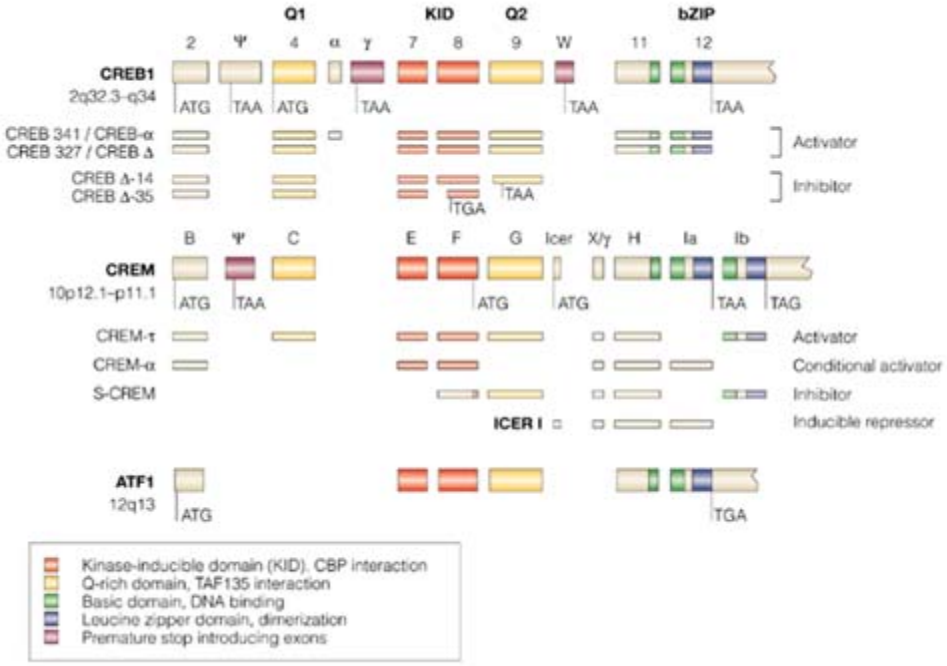

Figure 1.3. Exon Structure of The Members of the Human CREB Family

All exons for human CREB1, CREM, and ATF1 are shown. Selected splice products for CREB and CREM are shown below their respective exon structure. Their activating properties are displayed on the right. In-frame stop codons (TAA, TGA) and alternative start codons (ATG) are indicated. Homologous exons are in matching color. Figure adapted from Mayr et. al., 2001.

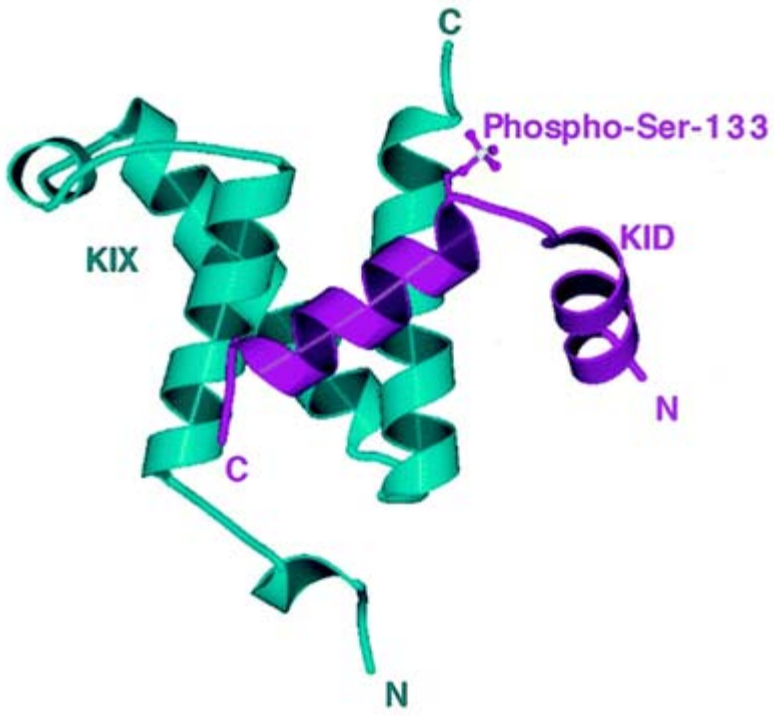

Figure 1.4. Structure of the KID/KIX Interaction

The ribbon diagram shows the interaction between kinase inducible domain of CREB (KID) (purple) and the KID interaction domain (KIX) (cyan) of CBP deduced from NMR spectroscopy. The KIX domain is made up of residues 586-666 of CBP, and forms three alpha helices. The KID domain here is comprised of residues 119-146 which form two perpendicular helices. Phosphoserine 133 is indicated. Figure adapted from Shaywitz et. al., 1999.

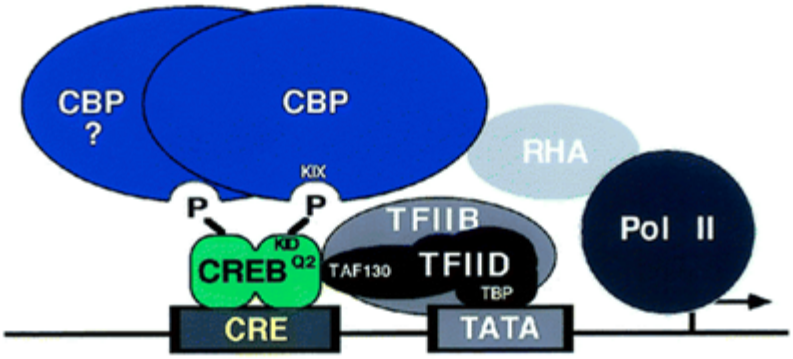

Figure 1.5. CREB Coordinates The Recruitment of the Transcriptional Machinery Through its Multiple Domains.

CREB uses multiple mechanisms to recruit and interact with the Pol II transcriptional machinery. Phosphorylated CREB bound to a CRE in DNA recruits the CREB binding protein (CBP) through its KID domain. In turn, CBP interacts indirectly with RNA Polymerase II (Pol II) via the RNA helicase A (RHA) protein. CREB can associate with the basal transcription factor complexes TFIIB and TFIID via the Q2 domain. Figure adapted from Shaywitz et. al., 1999.

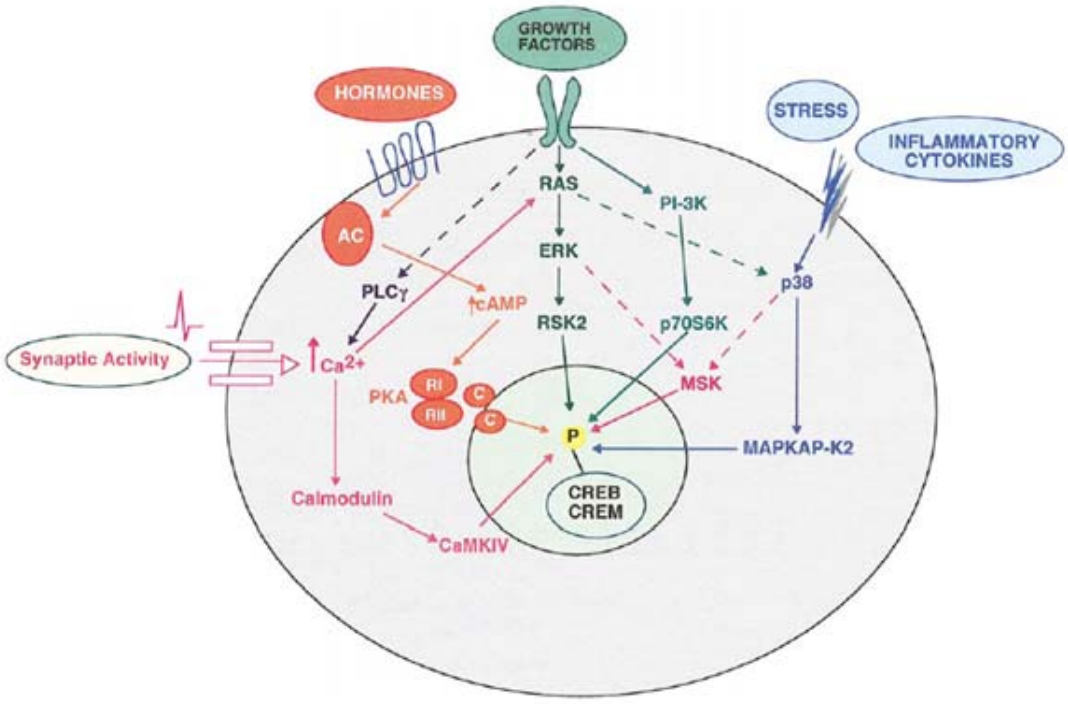

Figure 1.6. Signaling Pathways That Lead to Phosphorylation of CREB

CREB is phosphorylated by a large number of kinases in response to a variety of signaling pathways. Pathways involving intermediate kinases are indicated by dashed lines. CaMKIV, Calcium-calmodulin-dependent kinase IV; ERK, extracellular regulated kinase;p70S6K, p70 S6 kinase; MAPKAP-K2, MAP-kinase-activated protein kinase 2; MSK, mitogen- and stress-activated kinase ;PI-3K, phosphoinositide-3 kinase; PLC, phospholipase C; RSK-2, ribosomal S6 kinase 2; PKA, cAMP-dependent protein kinase. Figure adapted from Servillo et. al., 2002.

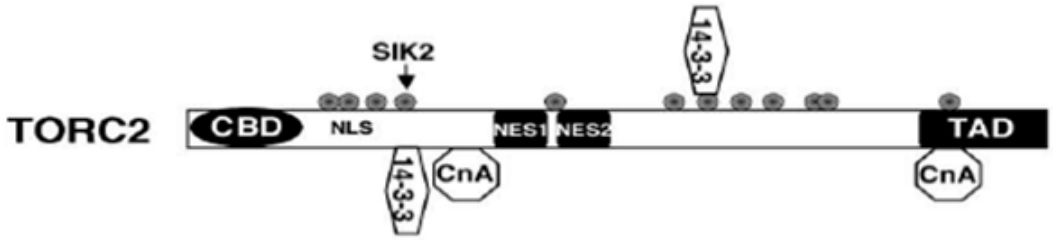

Figure 1.7. Major regulatory domains of TORC2

The diagram shows the relative positions of the major regulatory domains of TORC2. CREB binding domain (CBD), nuclear localization sequence (NLS), nuclear export sequence (NES), transactivation domain (TAD). Phosphorylation sites are indicated by circled Ps. 14-3-3 and calcineurin (CnA) binding sites are shown. Figure adapted from Screaton et. al. 2004.

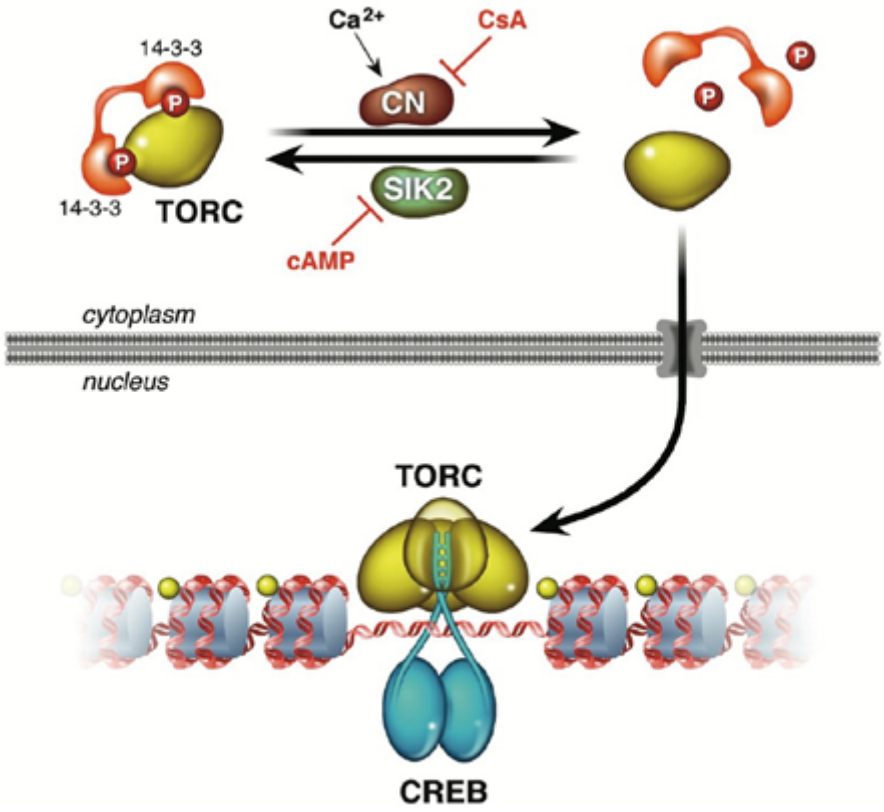

Figure 1.8. Regulation of TORC2 Nuclear Shuttling

TORC2 is sequestered in the cytoplasm via a phosphorylation-dependent interaction with dimeric 14-3-3 proteins. Calcium and cAMP pathways trigger release from 14-3-3 proteins by activating the TORC phosphatase calcineurin (CN), and inhibiting the TORC kinase SIK2. Dephosphorylated TORC migrates into the nucleus and is recruited to the promoter via an interaction with the bZIP domain of CREB. CsA, Cyclosporine A. Figure adapted from Screaton et. al. 2004.

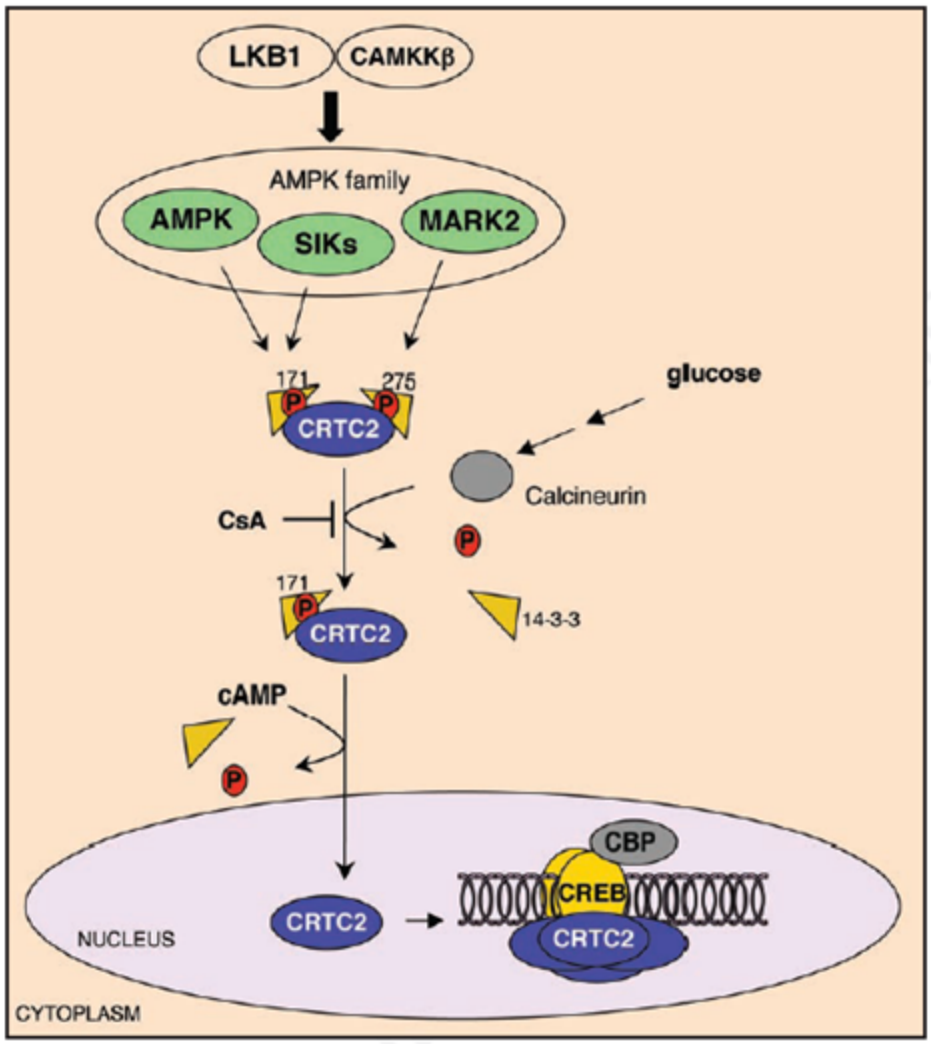

Figure 1.9. Regulation of TORC2 in Pancreatic Beta Cells

TORC2 (CRTC2) is maintained in the cytoplasm through phosphorylation by AMPK family kinases (AMPK, SIKs, MARK2). Membrane depolarization, calcium influx and activation of calcineurin are stimulated by glucose. Calcineurin dephosphorylates Ser275 which can be blocked by cyclosporine A (CsA). Ser171 is dephosphorylated in response to cAMP after being "primed" by glucose. Dephosphorylated TORC2 (CRTC2) releases from 14-3-3 and translocates to the nucleus. The AMPK kinases LKB1 and CAMKKβ activate AMPKs via phosphorylation of the activation loop. Figure adapted from Fu et. al.2008.

CHAPTER 2

TORC: an Insulin-Regulated CREB Coactivator that Promotes Stress Resistance in *Drosophila*

2.1 Abstract

In fasted mammals, glucose homeostasis is maintained through activation of the cAMP responsive CREB coactivator TORC2, which stimulates the gluconeogenic program in concert with the forkhead transcription factor FOXO1 (Koo, Flechner et al. 2005). Here we show that starvation also triggers TORC activation in *Drosophila*, where it maintains energy balance by promoting the expression of CREB target genes in the brain. *TORC* mutant flies have reduced glycogen and lipid stores, and they are sensitive to starvation as well as oxidative stress. Neuronal TORC expression rescued starvation and oxidative stress sensitivity as well as CREB target gene expression in *TORC* mutants. During refeeding, increases in insulin signaling inhibited TORC activity in wild type flies by stimulating the Salt Inducible Kinase 2 (SIK2)-mediated phosphorylation and subsequent degradation of TORC. Depletion of neuronal SIK2 increased TORC activity and enhanced resistance to starvation and oxidative stress in adult flies. As disruption of insulin signaling, either by ablation of insulin-producing cells (IPCs)

(Broughton, Piper et al. 2005) or by mutation of the insulin receptor adaptor gene *chico*, also increased TORC activity, our results illustrate the importance of an insulin-regulated pathway in brain for energy balance in *Drosophila*.

2.2 Introduction

Fasting triggers concerted changes in behavior, physical activity, and metabolism that are remarkably well conserved through evolution. In mammals, such responses are often coordinated by transcriptional coactivators that are themselves targets for regulation by environmental cues (Spiegelman and Heinrich 2004), but the extent to which these coactivators function in model organisms such as *Drosophila* is less clear.

In the basal state, mammalian TORCs are phosphorylated by Salt Inducible Kinases (SIKs) and sequestered in the cytoplasm via phosphorylation-dependent association with 14-3-3 proteins (Screaton, Conkright et al. 2004; Koo, Flechner et al. 2005). During fasting, elevations in circulating pancreatic glucagon promote TORC dephosphorylation via the PKA-mediated phosphorylation and inhibition of SIK2.

Increases in intracellular calcium have also been found to stimulate CREB target gene expression through the activation of calcineurin/PP2B, a calcium/calmodulin dependent Ser/Thr phosphatase that binds directly to and dephosphorylates mammalian TORCs (Screaton, Conkright et al. 2004; Koo, Flechner et al. 2005). Following their liberation from 14-3-3 proteins,

dephosphorylated TORCs shuttle to the nucleus where they mediate cellular gene expression by associating with CREB over relevant promoters.

TORC2 is thought to function in parallel with FOXO1 to maintain energy balance during fasting. Knockdown and knockout studies support a critical role for both proteins in regulating catabolic programs in the liver (Koo, Flechner et al. 2005; Dentin, Liu et al. 2007; Matsumoto, Pocai et al. 2007). In *Drosophila*, starvation promotes the mobilization of glycogen and lipid stores in response to increases in circulating adipokinetic hormone (AKH), the fly homolog of mammalian glucagon (Kim and Rulifson 2004; Lee and Park 2004). In parallel, decreases in insulin-IGF signaling (IIS) also stimulate the de-phosphorylation and nuclear translocation of *Drosophila* FOXO (Junger, Rintelen et al. 2003; Puig, Marr et al. 2003), which in turn stimulates a wide array of nutrient-regulated genes (Zinke, Schutz et al. 2002; Gershman, Puig et al. 2007).

The accumulation of lipid and glycogen stores in adult flies is highly correlated with resistance to starvation in *Drosophila* (Djawdan, Chippindale et al. 1998). Indeed, disruption of the IIS pathway promotes lipid accumulation and correspondingly increases resistance to starvation and oxidative stress (Clancy, Gems et al. 2001; Broughton, Piper et al. 2005). Although FOXO does not appear to be required for starvation resistance in adult flies (Junger, Rintelen et al. 2003), over-expression of FOXO has been found to mimic the starvation phenotype in larvae (Kramer, Davidge et al. 2003).

Here we address the importance of *Drosophila* TORC, the single homolog of mammalian TORCs, in metabolic regulation. We found that increases in TORC activity during starvation enhance survival through the activation of CREB target genes in the brain. During feeding, increases in insulin signaling inhibit TORC activity through phosphorylation by a *Drosophila* homolog of mammalian SIK2. These studies indicate that TORC is part of an insulin-regulated pathway that functions in parallel with FOXO to promote energy balance and stress resistance.

2.3 Results

Drosophila TORC shares considerable sequence homology with mammalian TORCs, in the CREB binding and trans-activation domains (TAD), calcineurin (Cn) recognition motif, and regulatory site (Ser157), which is phosphorylated by members of the AMPK family of stress and energy sensing Ser/Thr kinases in mammals (figure 2.1a, top). *Drosophila* TORC protein is expressed at low levels during larval and pupal stages, with highest amounts detected in adults (figure. 2.1a, bottom). TORC mRNA levels are also increased in adults relative to larvae, although to a lesser extent.

In the basal state, *Drosophila* TORC is highly phosphorylated at Ser157 and localized to the cytoplasm in *Drosophila* S2 cells and *Drosophila* KC-167 cells (figure 2.1b, top and figure 2.1c). Demonstrating the importance of

Ser157 phosphorylation in sequestering TORC, S157A mutant TORC shows only low-level binding to 14-3-3 proteins relative to wild-type TORC in HEK293T cells (figure 2.1b, bottom). Exposure to the adenyl cyclase activator Forskolin (FSK) or to Staurosporine (STS), an inhibitor of SIKs and other protein kinases (Ravnskjaer, Kester et al. 2007; Takemori, Kanematsu et al. 2007), promotes TORC dephosphorylation, liberation from 14-3-3 proteins, and nuclear translocation (figure 2.1b,c).

Consistent with these changes, over-expression of wild type *Drosophila* TORC potentiates CRE-luciferase (CRE-luc) reporter activity following exposure of HEK293T cells to FSK, whereas phosphorylation-defective (S157A)-TORC stimulates CRE-luc activity under basal as well as FSK induced conditions (figure 2.1d). CRE-luc activity is blocked by co-expression of the dominant negative CREB inhibitor ACREB (Ahn, Olive et al. 1998). Taken together, these results indicate that *Drosophila* TORC modulates CREB target gene expression following its dephosphorylation at Ser157 and nuclear entry in response to cAMP.

Based on the ability for mammalian TORCs to promote fasting metabolism (Koo, Flechner et al. 2005), we examined whether *Drosophila* TORC performs a similar function in adult flies. Amounts of de-phosphorylated, active TORC increased progressively during water-only starvation (figure 2.1e). Feeding adult flies paraquat, a respiratory chain inhibitor that stimulates the production of reactive oxygen species, also

promoted the accumulation of dephosphorylated TORC (figure 2.1f), suggesting a broader role for this coactivator in stress resistance. Similar to mammalian TORCs (Dentin, Liu et al. 2007), the up-regulation of TORC in *Drosophila* appears to reflect an increase in TORC protein stability as amounts of *TORC* mRNA did not change significantly in response to fasting or paraquat treatment (figure 2.1e,f).

To evaluate the role of TORC in energy homeostasis, we mutated the *TORC* gene by excising EY00004, a P element insertion from the Berkeley *Drosophila* Genome Project, located 2.9 kb downstream of the TORC coding region (CG6064; sup. figure 2.1). One line, referred to as $TORC^{25\text{-}3}$, contains a 10 kb deletion that removes the entire transcribed region of *TORC*. TORC mRNA and protein were not detected in $TORC^{25\text{-}3}$ compared to wild type controls, where TORC protein is expressed primarily in the brain, and at lower levels in other parts of the body (figure 2.2a, not shown). *TORC* mRNA amounts were more comparable between head and body, however, supporting the idea that TORC activity in different tissues is also controlled primarily at the level of protein stability (sup. figure 2.2).

Individuals homozygous for $TORC^{25\text{-}3}$ are viable and fertile. However, in response to water-only starvation, $TORC^{25\text{-}3}$ flies lived an average of less than 36 hours while wild type flies lived an average of 72 hours (figure 2.2b, top). Starvation had similar effects on a second independent TORC mutant line (A4-32; not shown). $TORC^{25\text{-}3}$ flies were also sensitive to oxidative stress; following

exposure to paraquat their mean survival time was reduced by 50% relative to controls (figure 2.2b, bottom). Arguing against a more general “sickly” effect of TORC disruption, *TORC*$^{25\text{-}3}$ flies had similar food intake, as determined using the CAFÉ method (Ja, Carvalho et al. 2007); and they exhibited comparable or elevated physical activity compared to controls, particularly during fasting (sup. figure 2.3, not shown).

Respiratory quotients were indistinguishable between TORC mutant and wild-type flies, indicating that glucose oxidation was appropriately induced during feeding, transitioning to fat burning in response to starvation (sup. figure 2.3). Consistent with their starvation sensitivity, however, *TORC*$^{25\text{-}3}$ mutant flies had lower amounts of stored glycogen and lipid relative to wild-type (figure 2.2c). These reductions appear specific for adults, because wild type and *TORC*$^{25\text{-}3}$ mutant larvae and pupae had comparable lipid levels (sup. figure 2.4).

We examined effects of TORC disruption on insulin signaling. In line with increases in glucose oxidation, amounts of phosphorylated AKT during feeding were comparable between wild-type and *TORC*$^{25\text{-}3}$ flies (figure 2.2d; sup. figure. 2.5). By contrast, amounts of de-phosphorylated, active FOXO as well as 4E-BP, a FOXO target gene, were actually elevated in starved *TORC*$^{25\text{-}3}$ flies, likely reflecting a secondary response to the depletion of lipid and glycogen (figure 2.2d; sup. figure 2.s5). While removal of one copy of *FOXO* had no effect on survival or lipid accumulation in starved *TORC*$^{25\text{-}3}$ flies

(sup. figure 2.s6), removal of both copies of *FOXO* was lethal in the TORC mutant background. By contrast with $TORC^{25\text{-}3}$ flies, however, FOXO null flies ($FOXO^{21}/FOXO^{25}$) had normal lipid levels, and they were as resistant to starvation as wild-type flies (sup. figure 2.s7) (Junger, Rintelen et al. 2003).

We performed gene profiling studies on mRNAs from heads of fasted wild type and $TORC^{25\text{-}3}$ mutant flies to evaluate the mechanism by which TORC mediates starvation resistance. This analysis revealed a set of 169 genes that are down-regulated 4-fold or better in $TORC^{25\text{-}3}$ mutants (Sup. Table 1). Many of the genes that were down-regulated in $TORC^{25\text{-}3}$ flies appear to function in glucose and lipid metabolism, proteolysis, amino acid transport, and mitochondrial respiration.

Similar to the role of mammalian TORCs in promoting mitochondrial gene expression (Wu, Huang et al. 2006), mRNAs for mitochondrial respiration (*citrate synthase (CS), cytochrome C oxidase subunit IV (COX)*) and reactive oxygen scavenging (*UCP4c*, *catalase*, *TrxT*, *Cyp4g1*) were reduced in $TORC^{25\text{-}3}$ flies. Correspondingly, cytochrome oxidase and citrate synthase enzymatic activities, markers of mitochondrial function, are also lower in *TORC* mutants compared to wild type (sup. figure 2.s8).

We examined whether genes that are down-regulated in *TORC* mutants are directly modulated by TORC. When TORC was over-expressed in a heat-inducible manner using the GAL4/UAS bipartite transactivation system (Brand and Perrimon 1993), a number of fasting-inducible genes, including *COX*, *CS*,

and *CAT*, were up-regulated (sup. figure 2.s9). Indeed, many of the genes that are down-regulated in *TORC*$^{25\text{-}3}$ flies contain CREB binding sites (sup. figure 2.s10). For example, the *Cyp4g1* promoter contains CREs at –375 and –100, and exposure to FSK correspondingly increased *Cyp4g1*-luciferase reporter activity 10-20 fold in human HEK293T cells (figure 2.2f). *Cyp4g1* reporter activity in these cells was further enhanced by expression of wild type *Drosophila* TORC, and to a greater extent by phosphorylation defective S157A TORC. Expression of the dominant negative mouse CREB polypeptide ACREB disrupted effects of TORC on reporter activity, demonstrating the importance of CREB for induction of this gene (sup. figure 2.s11). CRE-luciferase reporter activity (Iijima-Ando and Yin 2005) was effectively eliminated in *TORC*$^{25\text{-}3}$ compared to wild type flies, demonstrating the importance of TORC for CREB- mediated transcription in *Drosophila* (figure 2.2g).

We used the GAL4/UAS transactivation system to supply wild type TORC in a cell-type specific manner to *TORC*$^{25\text{-}3}$ flies. Panneuronal expression of TORC using *ELAV-GAL4* to drive expression of *UAS-TORC* rescued both the starvation and paraquat sensitivity phenotypes (figure 2.3a). Similarly, driving neuronal expression of TORC using *SCRATCH-GAL4* also rescued the starvation phenotype (sup. figure 2.s12). In contrast, TORC expression in fat body using *r*^{4}*-GAL4* (Lee and Park 2004) did not rescue

starvation sensitivity (not shown), arguing for a specific requirement for TORC in neurons.

In keeping with this increase in starvation resistance, total lipid amounts were elevated in TORC rescue compared to mutant flies (figure 2.3b, top). Interestingly, however, while neuronal TORC fully rescued starvation sensitivity of *TORC* mutants, lipid levels were only partially restored, raising the possibility that starvation sensitivity in this setting does not depend exclusively on lipid stores. Consistent with the improvements in these metabolic parameters, FOXO activity and 4E-BP expression in TORC rescued individuals were commensurately down-regulated to wild type levels (figure 2.3b, bottom). Moreover, neuronal TORC also rescued CRE reporter activity and fasting-inducible gene expression (figure 2.3c,d).

Based on the activation of TORC during starvation, we examined whether increases in insulin signaling inhibit *Drosophila* TORC activity during refeeding. In contrast to fasting, refeeding triggered TORC phosphorylation after 1 hour and degradation after 4 hours in wild-type flies (figure 2.4a). TORC did not undergo phosphorylation during refeeding in flies with defective insulin signaling caused either by mutation of *chico*, the *Drosophila* ortholog of the insulin receptor substrate (IRS) protein, or by ablation of the insulin producing cells (IPCs) (figure 2.4b). Indeed, CRE-luciferase activity and fasting-inducible TORC target gene expression were correspondingly elevated in insulin-signaling mutant flies compared to wild type (figure 2.4c,d). These

data support the notion that TORC acts down-stream of the insulin signaling pathway in *Drosophila*.

We considered that neuronal TORC may affect systemic resistance to starvation through feedback inhibition of insulin like peptides (*ilps*). In that event, $TORC^{23\text{-}5}$ flies might be predicted to exhibit starvation sensitivity as a consequence of increased *ilp* expression. However, mRNA amounts for *ilp2*, *ilp3*, and *ilp5* were either comparable or modestly reduced in $TORC^{23\text{-}5}$ relative to wild-type flies fed ad libitum (figure 2.4e). Moreover, IPC ablation did not affect starvation sensitivity in $TORC^{23\text{-}5}$ flies, arguing against a significant role for *ilps* in this setting (figure 2.4f).

Mammalian SIK2 has been shown to mediate inhibitory effects of insulin on CREB target gene expression in refed mice, by phosphorylating TORC2 and promoting its subsequent proteasomal degradation (Dentin, Liu et al. 2007). SIK2 kinase activity is inhibited during fasting by the PKA-mediated phosphorylation of SIK2 at Ser 587. The presence of a single putative SIK2 homolog (CG4290) in *Drosophila* (Okamoto, Takemori et al. 2004) prompted us to test its role in regulating TORC activity. Over-expression of *Drosophila* SIK2 increased amounts of Ser157-phosphorylated *Drosophila* TORC in HEK293T cells (figure 2.5a). Mutation of the inhibitory PKA phosphorylation site at Ser1032 to Alanine in *Drosophila* SIK2 further increased amounts of phosphorylated TORC. Consistent with these effects, *Drosophila* SIK2 inhibited *Drosophila Cyp4g1*-luciferase reporter activity in HEK293T cells

expressing *Drosophila* TORC; and mutant S1032A SIK2 inhibited reporter activity to a greater extent relative to wild-type (figure 2.5b).

We examined whether depletion of SIK2 increases TORC activity in flies. Neuronal expression of *UAS-SIK2* RNAi from an *ELAV-GAL4* driver reduced amounts of Ser157-phosphorylated TORC during refeeding, when SIK2 is predicted to be active (figure 2.5c; sup. figure 2.s13). Consistent with the increase in amounts of de-phosphorylated, active TORC protein, mRNA amounts for the TORC-regulated genes Cyp4g1 and AcBP were substantially up-regulated in SIK2-RNAi flies (figure 2.5d). Correspondingly, SIK2-RNAi flies were more resistant to starvation and paraquat feeding relative to controls (figure 2.5e, f).

We performed genetic epistasis experiments to evaluate the mechanism by which TORC activity is regulated (figure 2.6, Table 2.1). Eye-specific over-expression of TORC using a *GMR-GAL4* driver led to a rough eye phenotype (figure 2.6a-c; Table 2.1). TORC transcriptional activity appeared critical for these effects since reduction of *Drosophila* CrebB expression, using either the chromosomal deficiency *Df(1)N19* or the *CrebB*^{S162} mutation (Belvin, Zhou et al. 1999) suppressed the rough-eye phenotype in TORC expressing flies (figure 2.6d,e; Table 2.1).

We evaluated the role of the Ser/Thr kinase AKT, which has been shown to inhibit mammalian TORC2 activity through the phosphorylation and activation of SIK2 during feeding (Koo, Flechner et al. 2005; Dentin, Liu et al.

2007; Matsumoto, Pocai et al. 2007). Depletion of AKT by RNAi mediated knockdown enhanced the TORC-mediated rough-eye phenotype (figure 2.6f; Table 2.1), arguing that this component of the insulin signaling pathway inhibits TORC activity.

Based on the presence of a conserved calcineurin/PP2B binding motif in *Drosophila* TORC (figure 2.1a) plus the ability of calcineurin to activate mammalian TORC, we tested whether this *Drosophila* Ser/Thr phosphatase also promotes TORC activation. Eye-specific expression of active PP2B alone promoted a rough eye phenotype (figure 2.6g; Table 2.1). This phenotype was completely suppressed in a *TORC* mutant background (figure 2.6g'), demonstrating the importance of endogenous TORC in this context. In further support of the ability for PP2B to promote TORC activation, eye-specific over-expression of TORC strongly potentiated the effects of PP2B on eye morphology (figure 2.6g).

Because FOXO activity is increased in *TORC* mutant flies, we tested whether this forkhead protein is required for the TORC eye phenotype. TORC over-expressing flies in which FOXO is reduced or eliminated using $FOXO^{21}$ and $FOXO^{25}$ alleles (Junger, Rintelen et al. 2003), still exhibited a rough-eye phenotype (figure 2.6h). $FOXO^{21}/FOXO^{25}$ null flies also had wild-type levels of TORC protein amounts and activity, as measured by immunoblot and CRE-luc reporter assays, indicating that FOXO is not required for TORC activation in this setting (sup. figure 2.s14).

2.4 Discussion

Insulin signaling regulates lipid and glucose metabolism in both *C. elegans* and *Drosophila* in part by inhibiting FOXO-dependent transcription (Giannakou and Partridge 2007). Lipid stores are increased in flies with mutations in the IIS pathway; they are resistant to starvation as well as oxidative stress (Clancy, Gems et al. 2001; Broughton, Piper et al. 2005). We found that TORC enhances survival during starvation in part by stimulating CREB target gene expression in neurons. Although TORC appears to act in parallel with FOXO, the increase in FOXO activity we observed in *TORC* mutant flies indicates that TORC likely impacts on this pathway at least indirectly.

TORC appears to be required for the expression of genes that promote lipid and glucose metabolism, amino acid transport, and proteolysis. Consistent with this idea, paralogs for a number of TORC-regulated genes (*TrxT, CAT, UCP4c*) appear to be required for starvation and oxidative stress resistance (Mockett, Bayne et al. 2003; Chen, Rio et al. 2004; Fridell, Sanchez-Blanco et al. 2005; Svensson and Larsson 2007). Superimposed on these effects, neuronal TORC may also promote systemic resistance to starvation and oxidative stress by modulating the expression of neuropeptide hormones and other circulating factors, which in turn regulate peripheral glucose and lipid metabolism.

In mammals, refeeding has been found to decrease TORC activity through the AKT-mediated phosphorylation and activation of SIK2 (Dentin, Liu et al. 2007). Phosphorylated TORC2 is ubiquitinated by the E3 ligase COP1 and subsequently degraded via the 26S proteasome. Supporting a similar mechanism in *Drosophila*, RNAi-mediated knockdown of AKT in *Drosophila* was sufficient to increase TORC activity. Likewise, depletion of neuronal SIK2 enhanced TORC activity and increased resistance to both starvation and paraquat feeding. Although a *Drosophila* homolog for COP1 has not been identified, we imagine that the ubiquitin-dependent degradation of *Drosophila* TORC is also critical in modulating its activity in brain as well as other tissues.

Based on its ability to potentiate CREB target gene expression in neurons, TORC may function in a variety of biological settings. Indeed, *Drosophila* CREB appears to have an important role in learning and memory, circadian rhythmicity, rest homeostasis, and addictive behavior (Belvin, Zhou et al. 1999; Hendricks, Williams et al. 2001; Perazzona, Isabel et al. 2004; Sakai, Tamura et al. 2004). Future studies should reveal the extent to which TORC participates in these contexts as well.

2.5 Materials and Methods

Fly stocks

All *Drosophila melanogaster* lines were maintained at 25^{o}C on standard food medium. *P{EPgy2}EY00004*, *UAS-rp*r, *chico*^{1}, *actin-GAL4*, and *ELAV-*

gal4 were obtained from the Bloomington *Drosophila* Stock Center. CRE-luc reporter flies (Iijima-Ando and Yin 2005) were obtained from Jerry Yin. *UAS-Pp2b-14D*^{act} flies were kindly provided by Toshiro Aigaki. *Dilp2-GAL4* flies were obtained from U. Heberlien, and *chico*^{2} , *FOXO*^{21}, and *FOXO*^{25} flies were obtained from E. Hafen. IPC^{-} flies were generated by crossing *dilp2-GAL4* with *UAS-rpr*. *r*^{4}*-GAL4* flies were from J. Park. Chico mutants were generated by crossing *chico*^{1}*/Cyo* with *chico*^{2}*/Cyo* flies. SIK2 RNAi and AKT RNAi flies were obtained from the Vienna *Drosophila* RNAi Center. TORC RNAi flies were generated by inserting a 600bp *TORC* coding region fragment into the pWIZ vector. *UAS-TORC-GFP* flies were generated as described (Bittinger, McWhinnie et al. 2004).

Generation of *TORC* null mutant and *UAS-TORC* flies

TORC deletion alleles were generated by mobilization of the P{EPgy2} insertion EY00004 with a Δ2-3 source of transposase (Robertson, Preston et al. 1988). Potential deletions were screened by PCR. One deletion line, 25-3, was found to have ~10kb deletion removing the entire *TORC* coding sequence; the 25-3 deletion break points were confirmed by sequencing. A second mutant line, A4-32, contains a P{EPgy2} element inserted 1877 bp 3' to the *TORC* start codon, resulting in an in-frame stop codon after aa 625 of TORC. For mis-expression constructs, the *TORC* coding region was cloned into pUAST and transgenic lines generated.

Starvation and oxidative stress

For starvation assay, 3~5 day-old flies were transferred to vials of 1% Agar/PBS with filter papers soaked with H_2O. Dead flies were scored every 4-8 hours. For oxidative stress, 3~5 day-old flies were starved in 1%Agar/PBS for 4 hours, then transferred to vials of 20 mM Paraquat/10% sucrose/1%1 Agar/PBS, and deaths were scored every 4-8 hours.

Lipid and glycogen measurement

Fly total lipid and glycogen levels were measured as previously described (Van Handel 1985; Van Handel 1985). For lipids, single flies were crushed in 0.2 ml of chloroform-methanol (1:1). After evaporating solvent, 0.2 ml of sulfuric acid was added, and samples were heated at 37^{o}C for 10 min. After cooling, 2 ml vanillin reagent (0.12% vanillin in 68% phosphoric acid) was added and samples were allowed to develop for 5 min. Absorbance was measured at 525nM. Sesame oil (Sigma, S-3547) was used to generate a standard curve. For glycogen content, single flies were crushed in 0.2 ml of 2% Sodium sulfate, followed by addition of methanol (1ml), and centrifugation (1 min). Supernatants were evaporated and 2 ml anthrone reagent (0.14% anthrone in 28% sulfuric acid) was added to each sample. Reactions were

incubated at 37^0C for 15 min, and absorbance (625 nM) was measured. Purified glycogen (Roche) was used to generate a standard curve.

Respirometry

A Sable Systems International TR-2 system (SSI; Las Vegas, Nevada, USA) was used for flow-through respirometry with a Li-6251 CO_2 analyzer (Li-Cor, Lincoln, NE, USA; resolution < 0.1 p.p.m. CO_2), supplemented with a SSI's differential oxygen analyzer Oxzylla II, a SSI's ExpeData data acquisition software with UI-2 16-bit measurement interface (basic accuracy 0.03%), and SSI Expedata data analysis software. Activity was constantly monitored using an SSI AD-2 optical activity detector. Room temperature and air flow rate were also measured and recorded via an A/D converter (UI-2). Bev-A-Line (Thermoplastic Processes Inc., Georgetown, DE, USA) low-permeability tubing was used throughout to minimize CO_2 and H_2O absorbance errors. Room-air from a carboy was pulled by an SSI TR-SS3 sub-sampler through a Drierite/Ascarite/Drierite drying column to remove CO_2 and H_2O, at an STP-corrected flow rate of about 50 ml/minute. The prepared air then entered the glass/aluminum respirometry chamber (volume ca. 3 ml; SSI TRRM). During each recording the CO_2 produced and the O_2 consumed by the group of 25 flies together with the activity, the flow rate and room temperature were recorded.

During a typical run, a group of 25 flies was cooled for about 10 min at 5 °C and transferred to the respirometric chamber. The flies in the chamber were left at least 10 min for temperature acclimatization (room temperature *ca.* 25 °C). Recording was started to establish a 4-min baseline for the CO_2 and O_2 analyzers with an empty chamber. Each recording consisted of a variable number of data points taken at 1-second intervals, using finite impulse response digital filtration to reduce short-term noise (Lighton 1991).

Data analysis and statistics

Recordings were analyzed using SSI ExpeData software. For each recording, the CO_2 and O_2 baselines were subtracted assuming a linear drift. CO_2 in ppm and O_2 in % were converted to $\mu l\ h^{-1}$ using the recorded flow rate. The activity (measured as volts) was transformed to the absolute difference sum (ADS) of the activity. The ADS is the cumulative sum of the absolute difference between all adjacent data points (Lighton and Turner 2004). The slope and intercept of the lineal regression of the ADS values of activity was calculated as a function of time for each recording. The ADS value reached after 10 minutes was compared across groups. Data are presented as means and standard errors (SE). *TORC*$^{25\text{-}3}$ and wild type flies were compared by two-tail unpaired Student's *t*-test. A probability of error $P < 0.05$ was considered statistically significant.

Q-PCR measurement

Fly heads were collected and RNA was extracted using RNease Mini Kit (QIAGEN). Total RNA (1ug) was reverse-transcribed by Superscript II transcriptase (Invitrogen) and the generated cDNA used for real time PT-PCR (Roche LightCycler 480 Real-Time PCR system, SYBRGreen), using 2 ng of cDNA template and a primer concentration of 400 nM. Values were normalized to rp49.

q-PCR primers

Sequences for each primer shown below.

TORC-F	GGAGGAGGTCTGACCAACGGTTAC
TORC-R	ATCCCACCACACCATTGCTCAAC
rp49-F	gctaagctgtcgcacaaatg
rp49-R	gttcgatccgtaaccgatgt
COX CG10396-F	GCCAGTGGAGGAGATGGTAT
COX CG10396-R	TATATGGGTCGCCCATTGAT

CS CG14740-F	CGTTCATATCCCGACTGCAA
CS CG14740-R	CTTGCCGTGCAGACACTTT
TrxT CG3315-F	AGCTCTTCGTTGGCTGCAATT
TrxT CG3315-R	CATCGATATGGACGGCCTTA
Cyp4g1 CG3972-F	CAAGGTGGTCAAGGATCGTAA
Cyp4g1 CG3972-R	GTGCTGGCAACAGGTGTAGAA
UCP4c CG9064-F	GGAGGGTGTCCTCACGTTAT
UCP4c CG9064-R	GCTCGACGGACAGCCAAA
ACBP CG5804-F	GGAGGTGTACCTGGAGTTCT
ACBP CG5804-R	ACTTCTCGTACAGGGCGACGTA
Cat CG9314-F	CGATACGGCGTCAAATCAA
Cat CG9314-R	TCCACTGGATGTCGTGATCT
dSIK2 CG4290-F	TTCCGGTCGCTTTCGCATTC
dSIK2 CG4290-R	CCAGATTGTACTTGGCTATCAG

Cell culture and transfection

HEK293T cells were maintained and transfections were carried out as previously described (Ravnskjaer, Kester et al. 2007). For promoter studies, 50 ng of promoter and 50 ng of β-galactosidase plasmids were used per well, and total amount was kept constant at 300 ng by adding indicated plasmids or empty vector pcDNA3. After 24h transfection, cells were treated with FSK (10 μM) for 4 hours and luciferase activity was measured. S2 and KC-167 cells were cultured in Schneider's media (Invitrogen) with 10% FCS at room temperature, and transfections were preformed using Fugene 6 according to manufacture instruction. Cells were treated with FSK (10 μM), IBMX (4μg/ml), or staurosporine (STS, 100 nM).

Western blotting

Cells or flies were lysed on ice in lysis-buffer (50 mM Tris-HCl, 150 mM NaCl, 1 mM EDTA, 6 mM EGTA, 20 mM NaF, 1% TritonX-100, and protease inhibitors) for 15-20 min. After centrifugation at 13000 rpm for 15 min, supernatants were reserved for protein determinations and SDS-PAGE analysis. The following antibodies were used: phospho-TORC 1 (Cell Signaling), dFOXO (generous gift of O. Puig), 4E-BP (generous gift of N. Sonenberg), HSP90 (Santa Cruz Biotechnology; SC-7947), Tubulin (Upstate; 05-829), Flag M2 (Sigma; A8592), phospho-AKT(Ser473) (Cell Signaling Technology; 9271), AKT (Cell Signaling Technology; 9272), HA (Santa Cruz

Biotechnology; SC-7392). TORC antibodies were raised against a synthetic TORC peptide (DYTREIFDSLSLSLG) by Covance Research Products. Sera were collected and purified using a peptide affinity resin.

Statistical analyses

Results are reported as mean SEM. The comparison of different groups was carried out using two-tailed unpaired Student's *t* test. Differences were considered statistically significant at $p<0.05$. Data are representative of at least two independent experiments.

ACKNOWLEDGEMENTS

We thank O. Puig for FOXO antiserum, N. Sonenberg for 4E-BP antiserum. We also thank Jerry Yin for CRE-luc reporter flies and the Bloomington *Drosophila* Stock Center and the Vienna *Drosophila* RNAi Center for fly stocks. We thank Sable Systems International for use of the open-flow respirometry equipment and John R. B. Lighton and R. Turner (Las Vegas) for advice. This work was supported by NIH grant GM037828. MM is supported by the Keickhefer Foundation.

2.6 Figures

Figure 2.1. *Drosophila* TORC is activated by starvation and oxidative stress.

a. Top, schematic of TORC showing CREB binding domain (CBD), trans-activation domain (TAD), nuclear import (NLS) and export (NES) sequences, calcineurin binding (Cn) motif, and regulatory phosphorylation site (S157). Alignment with mammalian TORC1 sequence and consensus motif for phosphorylation by SIKs and other members of the AMPK family of Ser/Thr kinases shown. Hydrophobic (Ψ) and Basic (B) residues indicated. Bottom left, immunoblot showing relative amounts of TORC protein in larvae (L1, L2, L3), pupae, and adult male flies. Bottom right, Q-PCR analysis of TORC mRNA amounts at different developmental stages. **b**. Top, Immunoblot of *Drosophila T*ORC protein in *Drosophila* S2 cells exposed to FSK+Isobutyl-methylxanthine (F/I), staurosporine (STS), or DMSO vehicle (CON). Amounts of phospho-(Ser157) TORC and total TORC protein recovered from anti-Flag epitope immunoprecipitates in cells expressing either wild type or S157A mutant *Drosophila* TORC shown. Bottom, Immunoblot of 14-3-3 proteins recovered from immunoprecipitates of wild type or S157A mutant TORC in HEK293T cells following exposure to FSK, STS, or control vehicle. Amounts of phospho (Ser157) and total TORC shown. **c**. Endogenous *Drosophila* TORC protein staining by immunofluorescence analysis of *Drosophila* KC-167 cells under basal conditions (CON) and following exposure to STS. DAPI staining shown to visualize nuclei. Scale bar (20 μm) shown. De-phosphorylation of TORC by STS in KC-167 cells was verified by immunoblot assay (not shown). **d**. CRE-luciferase reporter activity in HEK293T cells expressing wild type or Ser157Ala mutant *Drosophila* TORC. Effect of FSK or dominant negative CREB inhibitor A-CREB on CRE-luc activity shown. ($P<0.05$; $n=6$; data are means ± s.d.). **e**. and **f**. Top, immunoblots of *Drosophila* TORC protein in wild type (w^{1118}) flies exposed to water only starvation (**e**) or paraquat (PQT) feeding (**f**). For starvation assay, time after food withdrawal shown (in hours). Flies were maintained on paraquat-containing food for 24 hours before analysis. Phospho- and dephospho- TORC proteins indicated. Bottom, relative effect of starvation or paraquat feeding on TORC protein and mRNA amounts.

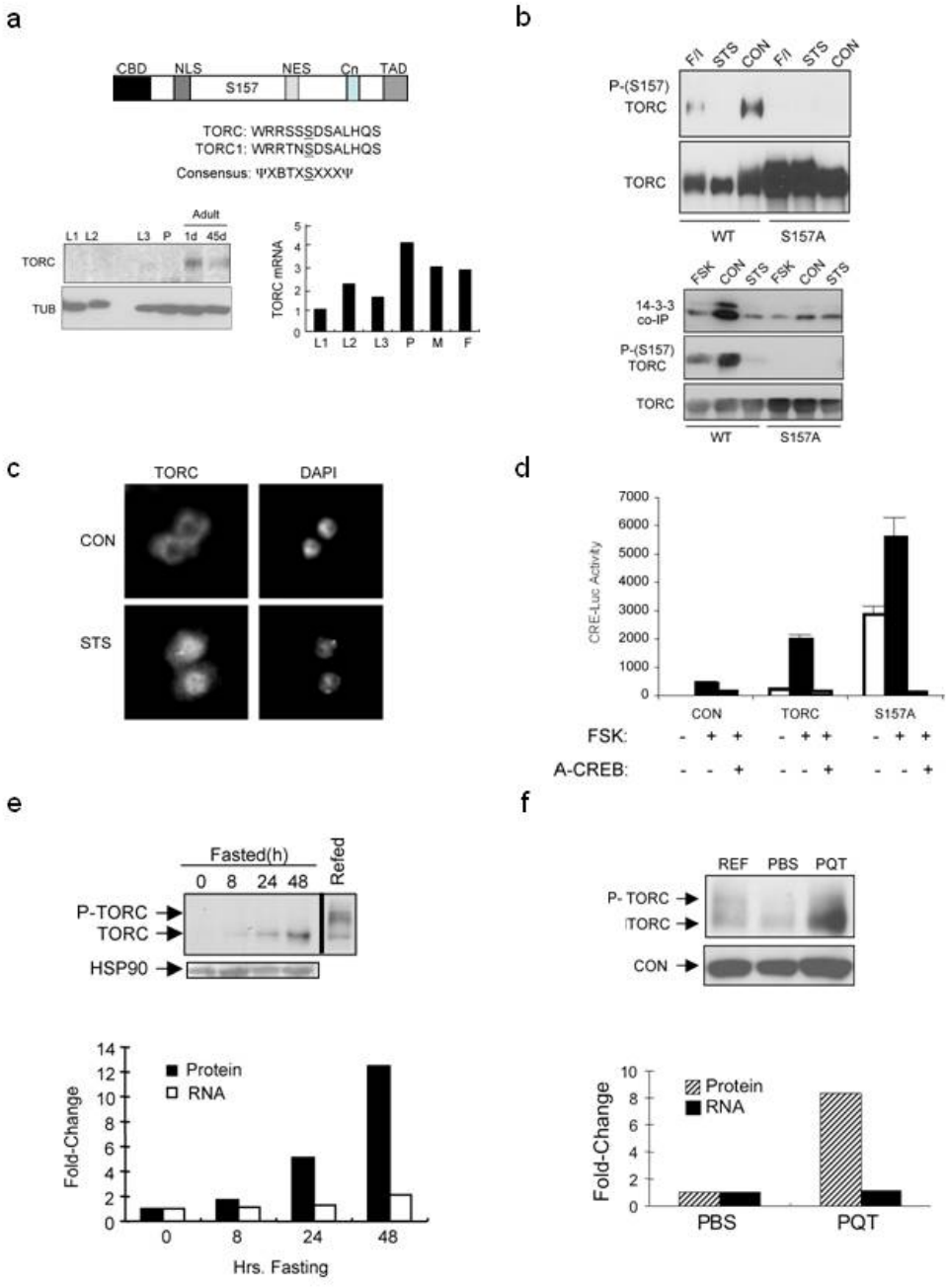
a
CBD
NLS
S157
NES
Cn
TAD
TORC: WRRSSSDSALHQS
TORC1: WRRTNSDSALHQS
Consensus: ΨXBTXSXXXΨ
Adult
L1 L2
L3
P
1d
45d
TORC
TUB
TORC mRNA
L1 L2 L3 P M F
b
F/I STS CON F/I STS CON
P-(S157) TORC
TORC
WT
S157A
FSK CON STS FSK CON STS
14-3-3 co-IP
P-(S157) TORC
TORC
WT
S157A
c
TORC
DAPI
CON
STS
d
CRE-Luc Activity
CON
TORC
S157A
FSK:
A-CREB:
e
Fasted(h)
0 8 24 48
Refed
P-TORC
TORC
HSP90
Protein
RNA
Fold-Change
Hrs. Fasting
f
REF PBS PQT
P- TORC
TORC
CON
Protein
RNA
Fold-Change
PBS
PQT

Figure 2.2. *TORC* mutant flies are sensitive to starvation and oxidative stress

a. Top, immunoblot of TORC in heads and bodies of wild type or *TORC*$^{25\text{-}3}$ flies. Bottom, relative amounts of TORC protein in fat bodies and brains of wild type and *TORC*$^{25\text{-}3}$ larvae. **b**. Relative survival of *TORC*$^{25\text{-}3}$ and wild type flies in response to starvation (top) or paraquat feeding (bottom). Percent survival at different times shown. ($p<0.05$; n= 50; data are means ± s.d.). Results are representative of three independent experiments. **c**. Total glycogen and lipid content, expressed as μg/mg body weight, in wild type and *TORC*$^{25\text{-}3}$ flies. (*; $p<0.05$; n= 6; data are means ± s.d.). **d**. Immunoblot of FOXO proteins in wild type and *TORC*$^{25\text{-}3}$ flies under ad libitum feeding (F), starvation (S) or refeeding (R) conditions. Amounts of total and phosphorylated AKT as well as 4E-BP indicated. **e**. Q-PCR analysis of head mRNAs from wild type and *TORC*$^{25\text{-}3}$ flies under fasted or fed conditions as indicated. Data are representative of two independent experiments (n=2; data are means ± s.d.). **f**. Representative of 2 independent experiments showing effect of wild type or S157A mutant TORC expression *Cyp4g1*-luc reporter activity in HEK293T cells. Exposure to FSK indicated. (n=3; data are means ± s.d.). **g**. CRE-luciferase reporter activity in wild type and *TORC*$^{25\text{-}3}$ flies. (*; $p<0.05$; n= 6; data are means ± s.d.).Comparable amounts and phosphorylation of *Drosophila* CREB (CREBB-17A) in wild type and *TORC*$^{25\text{-}3}$ flies confirmed by Western blot assay (not shown).

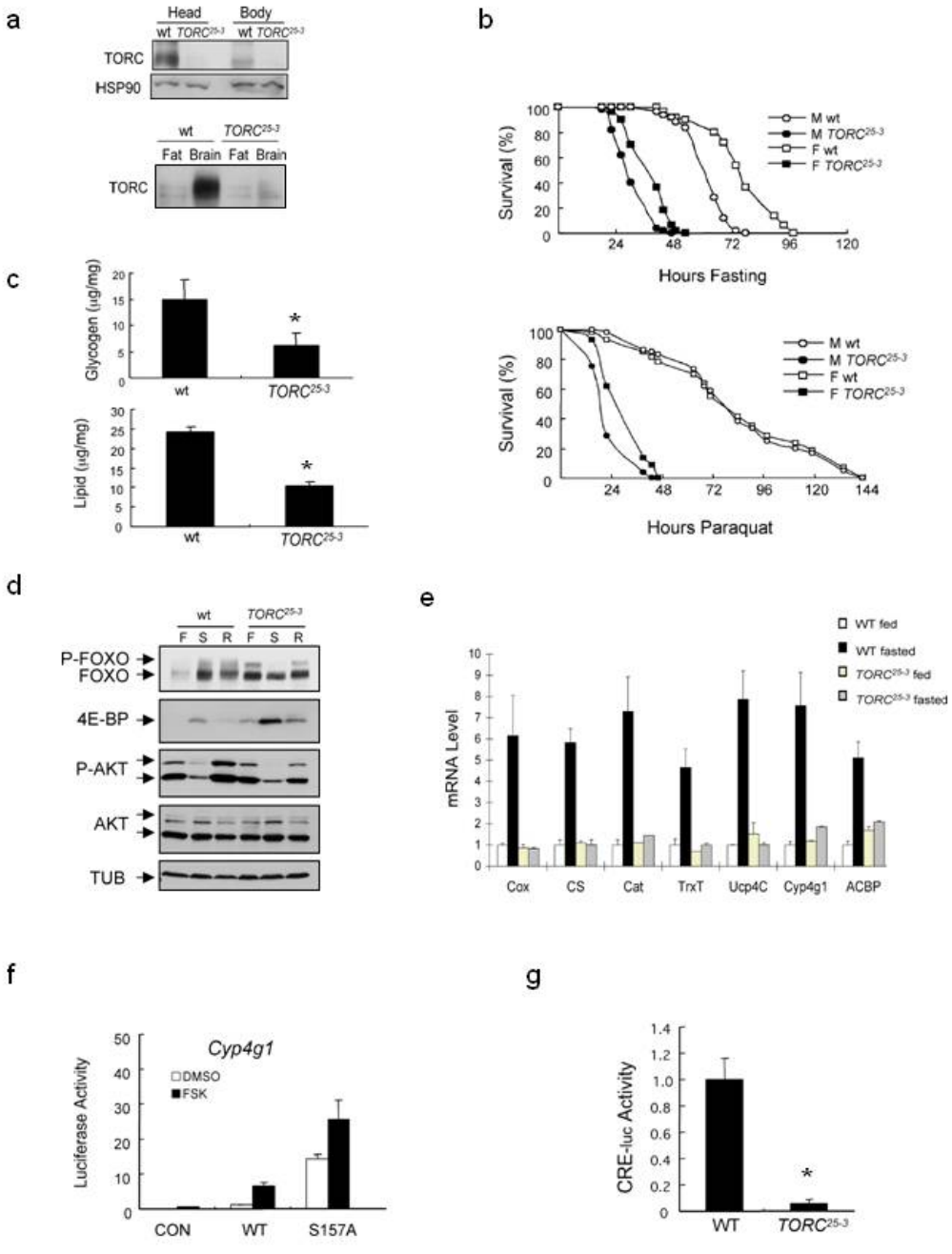
a
Head
Body
wt
TORC25-3
TORC
HSP90
Fat
Brain
b
Survival (%)
M wt
M TORC25-3
F wt
F TORC25-3
Hours Fasting
Hours Paraquat
c
Glycogen (μg/mg)
Lipid (μg/mg)
d
P-FOXO
FOXO
4E-BP
P-AKT
AKT
TUB
e
mRNA Level
WT fed
WT fasted
TORC25-3 fed
TORC25-3 fasted
Cox
CS
Cat
TrxT
Ucp4C
Cyp4g1
ACBP
f
Cyp4g1
DMSO
FSK
Luciferase Activity
CON
WT
S157A
g
CRE-luc Activity

Figure 2.3. Neuronal TORC expression rescues sensitivity of TORC25-3 flies to starvation and oxidative stress

a. Relative survival in response to starvation (top) or paraquat feeding (bottom) of wild type, *TORC*$^{25\text{-}3}$ flies, (*TORC*$^{25\text{-}3}$, *ELAV-GAL4*) control, and (*TORC*$^{25\text{-}3}$, *ELAV-GAL4*, *UAS-TORC*) rescued flies. ($p<0.05$; n=100; data are means ±s.d.). **b**. Top, relative lipid content of control (*TORC*$^{25\text{-}3}$, ELAV-GAL4) and rescued (*TORC*$^{25\text{-}3}$, *ELAV-GAL4*, UAS-*TORC*) flies. (*; $p<0.05$; n=6 flies per group; data are means ±s.d.). Bottom, Immunoblot of FOXO and 4E-BP proteins in TORC mutant (*TORC*$^{25\text{-}3}$, *ELAV-GAL4*), and rescue (*TORC*$^{25\text{-}3}$, *ELAV-GAL4*, *UAS-TORC*) flies under fed (F), starved (S), or refed (R) conditions. **c**. CRE-luciferase activity in control (*TORC*$^{25\text{-}3}$, *ELAV-GAL4*) and rescued (*TORC*$^{25\text{-}3}$, ELAV-*GAL4*, UAS-*TORC*) flies. (*; $p<0.05$; n= 6; data are means ± s.d.). **d**. Q-PCR analysis of TORC-regulated genes from head mRNAs of control (*TORC*$^{25\text{-}3}$, *ELAV-GAL4*) and rescued (*TORC*$^{25\text{-}3}$, *ELAV-GAL4*, UAS-*TORC*) flies under fasting conditions. Rescue genotype: *ELAV-GAL4, w*^{1118}*/Y; UAS-TORC/+; TORC*$^{25\text{-}3}$*.* Control genotype: *ELAV-GAL4, w*^{1118}*/Y; TORC*$^{25\text{-}3}$. Wild type: *w*^{1118}*.*

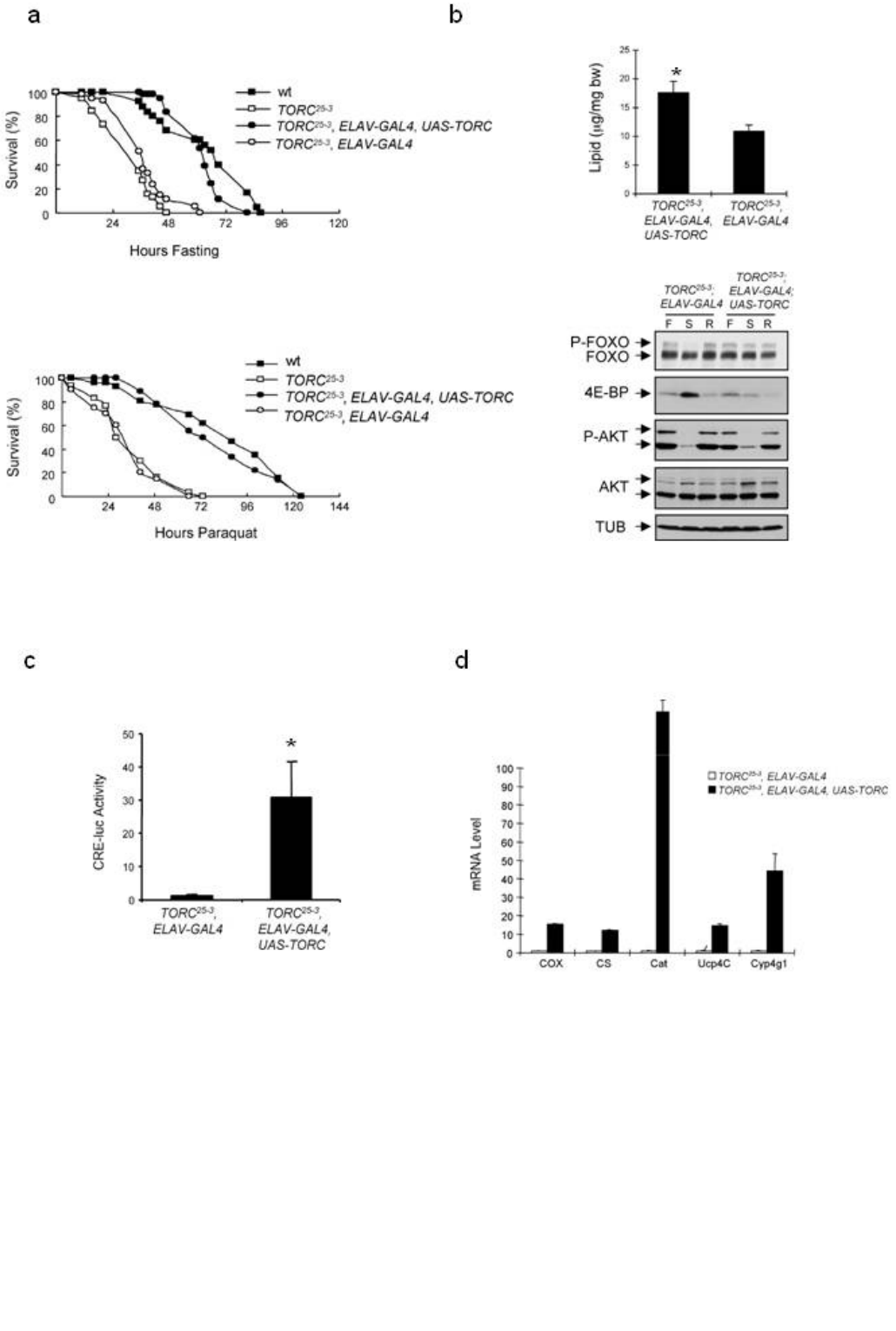
a
b
Survival (%)
Hours Fasting
wt
TORC25-3
TORC25-3, ELAV-GAL4, UAS-TORC
TORC25-3, ELAV-GAL4
Hours Paraquat
Lipid (µg/mg bw)
TORC25-3; ELAV-GAL4
TORC25-3; ELAV-GAL4; UAS-TORC
F S R F S R
P-FOXO
FOXO
4E-BP
P-AKT
AKT
TUB
c
d
CRE-luc Activity
mRNA Level
COX
CS
Cat
Ucp4C
Cyp4g1

Figure 2.4.The insulin signaling pathway regulates TORC activity in Drosophila

a. Immunoblot of phospho- and total TORC protein in fasted, or refed flies. Hours after refeeding indicated. Amounts of phospho-AKT shown. **b**. Immunoblot showing amounts of phospho- and total TORC in wild type and insulin producing cell ablated (IPC^-) flies (top) and *chico* mutant flies (bottom) under fasted or refed conditions. Loss of insulin like peptide (*ilp*) gene expression in IPC^- flies confirmed by Q-PCR analysis (not shown). **c**. Comparison of CRE-luciferase reporter activity in wild type and *chico* flies under fed or fasted conditions. ($p<0.05$; n=13 per group; data are means ±s.d.). **d**. Q-PCR analysis showing relative expression of TORC-regulated genes in wild type and IPC^- flies. **e**. Q-PCR analysis of *ilp*2, *ilp3*, and *ilp5* gene expression in wild-type and $TORC^{25\text{-}3}$ flies fed ad libitum. **f.** Effect of *ilp* cell ablation (IPC-) on starvation sensitivity in $TORC^{25\text{-}3}$ flies.

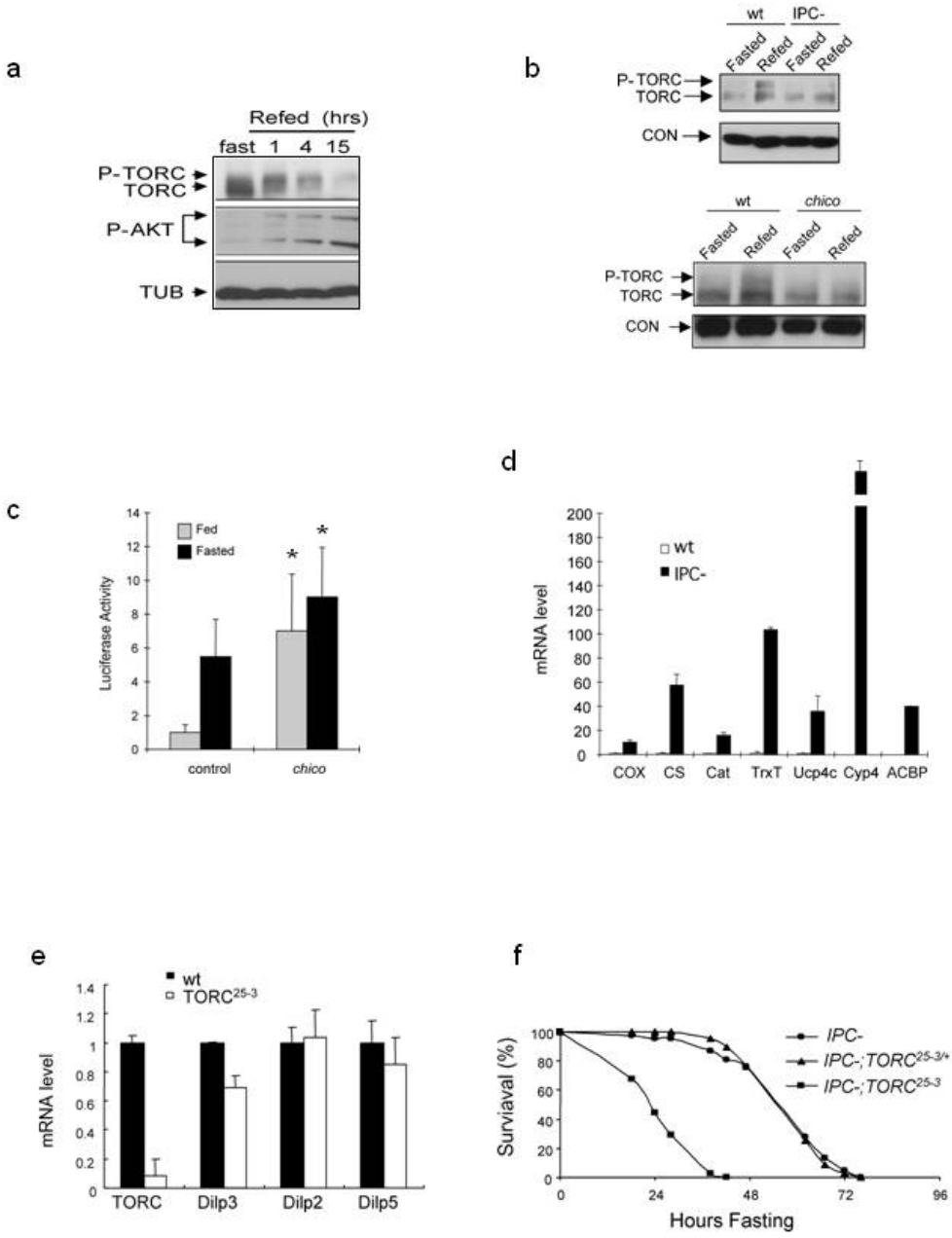
a
Refed (hrs)
fast 1 4 15
P-TORC
TORC
P-AKT
TUB
b
wt
IPC-
Fasted
Refed
Fasted
Refed
P-TORC
TORC
CON
wt
chico
Fasted
Refed
Fasted
Refed
P-TORC
TORC
CON
c
Fed
Fasted
Luciferase Activity
control
chico
d
wt
IPC-
mRNA level
COX
CS
Cat
TrxT
Ucp4c
Cyp4
ACBP
e
wt
TORC25-3
mRNA level
TORC
Dilp3
Dilp2
Dilp5
f
IPC-
IPC-;TORC25-3/+
IPC-;TORC25-3
Survival (%)
Hours Fasting

Figure 2.5. The Ser/Thr kinase SIK2 mediates effects of insulin signaling on TORC activity during refeeding

a. Immunoblot showing effect of wild-type and constitutively active S1032A *Drosophila* SIK2 on amounts of phosphorylated *Drosophila* TORC in transfected HEK293T cells. **b**. Transient assay of HEK293T cells showing effects of wild-type and S1032A mutant SIK2 on *Drosophila* Cyp4g1-luc reporter activity. Co-expression of *Drosophila* TORC and exposure to FSK indicated. **c**. Immunoblot showing effect of neuronal SIK2 RNAi expression on Ser157 phosphorylation of a neuronal TORC-GFP fusion protein in adult flies under starved (S) or refed (R) conditions. Genotypes: Control (-): *ELAV-GAL4/*+; *UAS-TORC-GFP/*+. SIK2 deficient (+): *ELAV-GAL4/*+; *UAS-TORC-GFP/ UAS-SIK2 RNAi*. **d.** Q-PCR analysis of TORC-regulated genes from head mRNAs of control and two independent strains expressing SIK2 RNAi in neurons. Genotypes are: **Con**: *ELAV-GAL4/Y*. **SIK RNAi I**: *ELAV-GAL4/Y; ; UAS-SIK2 RNAi I*. **SIK RNAi II**: *ELAV-GAL4/Y; ; UAS-SIK2 RNAi II*. **e. and f.** Effect of water only starvation (**e**) and paraquat (**f**) on survival of 5-day old female flies (n=100) expressing SIK2 RNAi in neurons relative to control. Genotypes are: **Con**: *Appl-GAL4/*+. **SIK RNAi I** *Appl-GAL4/+;;UAS-SIK2 RNAi I/*+. **SIK RNAi II**: *Appl-GAL4/+;;UAS-SIK2 RNAi II/+.*

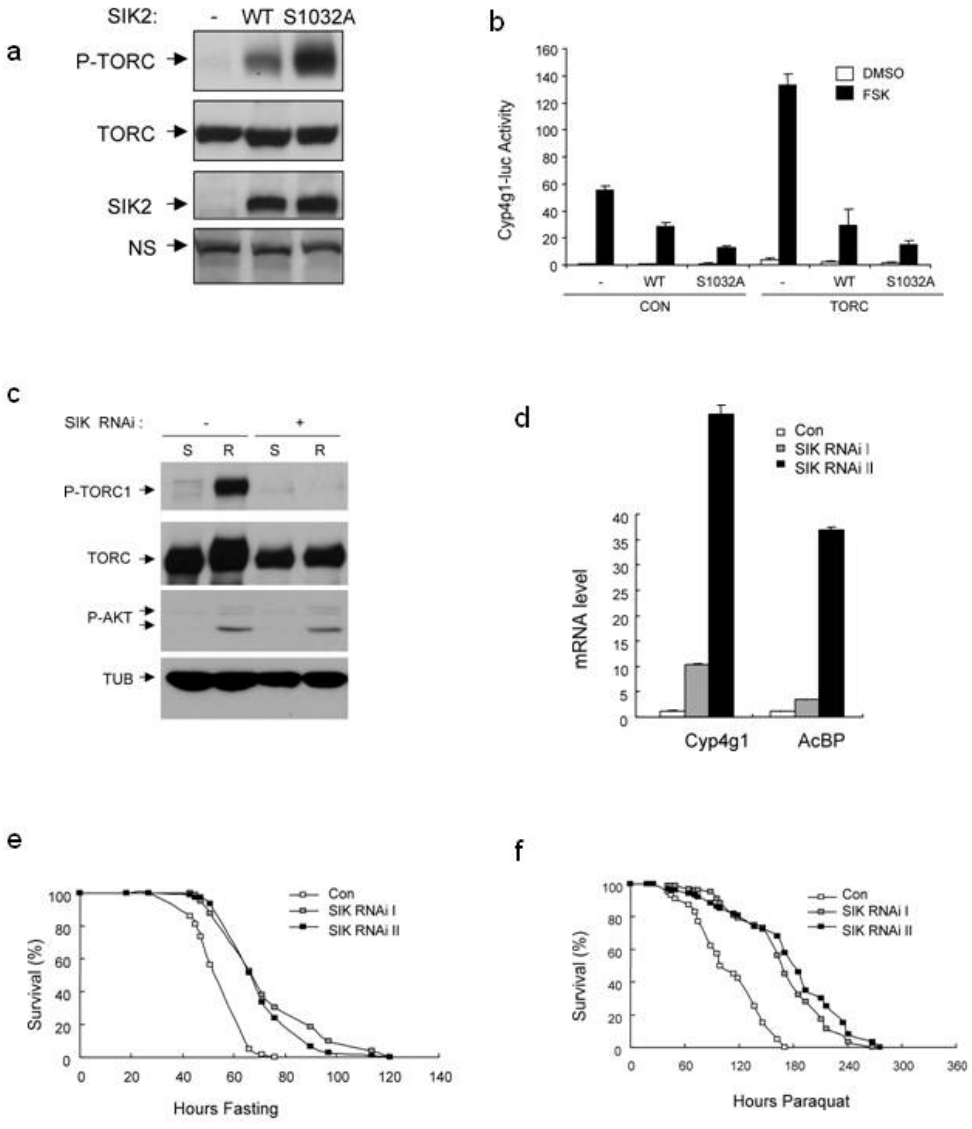
a
SIK2: - WT S1032A
P-TORC
TORC
SIK2
NS
b
Cyp4g1-luc Activity
DMSO
FSK
- WT S1032A - WT S1032A
CON
TORC
c
SIK RNAi : - +
S R S R
P-TORC1
TORC
P-AKT
TUB
d
Con
SIK RNAi I
SIK RNAi II
mRNA level
Cyp4g1
AcBP
e
Con
SIK RNAi I
SIK RNAi II
Survival (%)
Hours Fasting
f
Con
SIK RNAi I
SIK RNAi II
Survival (%)
Hours Paraquat

Figure 2.6. TORC acts down-stream of the Ser/Thr kinase AKT to regulate CREB activity

a. and **b**. Effect of TORC over-expression in post-mitotic cells of the eye imaginal disc shown relative to control. **c**. Effect of depleting TORC via RNAi mediated knockdown on eye morphology in TORC over-expressing flies. **d,e.** Effect of *CrebB* disruption, either via mutation in the *CrebB* gene ($CrebB^{S162}$; panel **d**) or in flies with a chromosomal deficiency (*Df (1) N19*; panel **e**) on eye phenotype in TORC transgenic flies. **f.** Eye morphology in TORC transgenic flies with reduced AKT (AKT RNAi) expression. **d'-f'**. Effect of each disruption (*CrebB, Df (1) N19, AKT*) on eye phenotype in the absence of TORC over-expression. **g-g''.** Effect of PP2b over-expression, alone (**g**), in TORC mutant flies (**g')**, and in TORC-over-expressing flies (**g''**). **h,h'.** Effect of mutation of FOXO ($FOXO^{21}/FOXO^{25}$) on the TORC over-expression phenotype (**h'**) compared to TORC over-expression alone (**h**). Genotypes are **a**. *GMR-GAL4/+; TM3/+*. **b**. *GMR-GAL4/+; 2X UAS-TORC/+*. **c**. *GMR-GAL4/UAS-TORC RNAi*; *2X UAS-TORC/+*. **d**. $CrebB^{S162}$*/+; GMR-GAL4/+*; *2X UAS-TORC/+*. **d'**. $CrebB^{S162}$*/+; GMR-GAL4/+*. **e**. *Df (1)N19/+; GMR-GAL4/+*; 2X *UAS-TORC/+.* **e**'. *Df (1)N19/+; GMR-GAL4/+*. **f.** *GMR-GAL4/ UAS-AKT RNAi; 2X UAS-TORC/+*. **f'**. *GMR-GAL4/ UAS-AKT RNAi.* **g.** *GMR-GAL4/UAS-Pp2b-14Dact/+* **g**'. *GMR-GAL4/UAS-Pp2b-14D*^{act}*;TORC*$^{25-3}$ **g''** *GMR-GAL4/UAS-Pp2b-14D*^{act}*;UAS-TORC/+*. **h.** *GMR-GAL4/2XUAS-TORC***. h'.** *GMR-GAL4/2XUAS-TORC;*$FOXO^{21}/FOXO^{25}$.

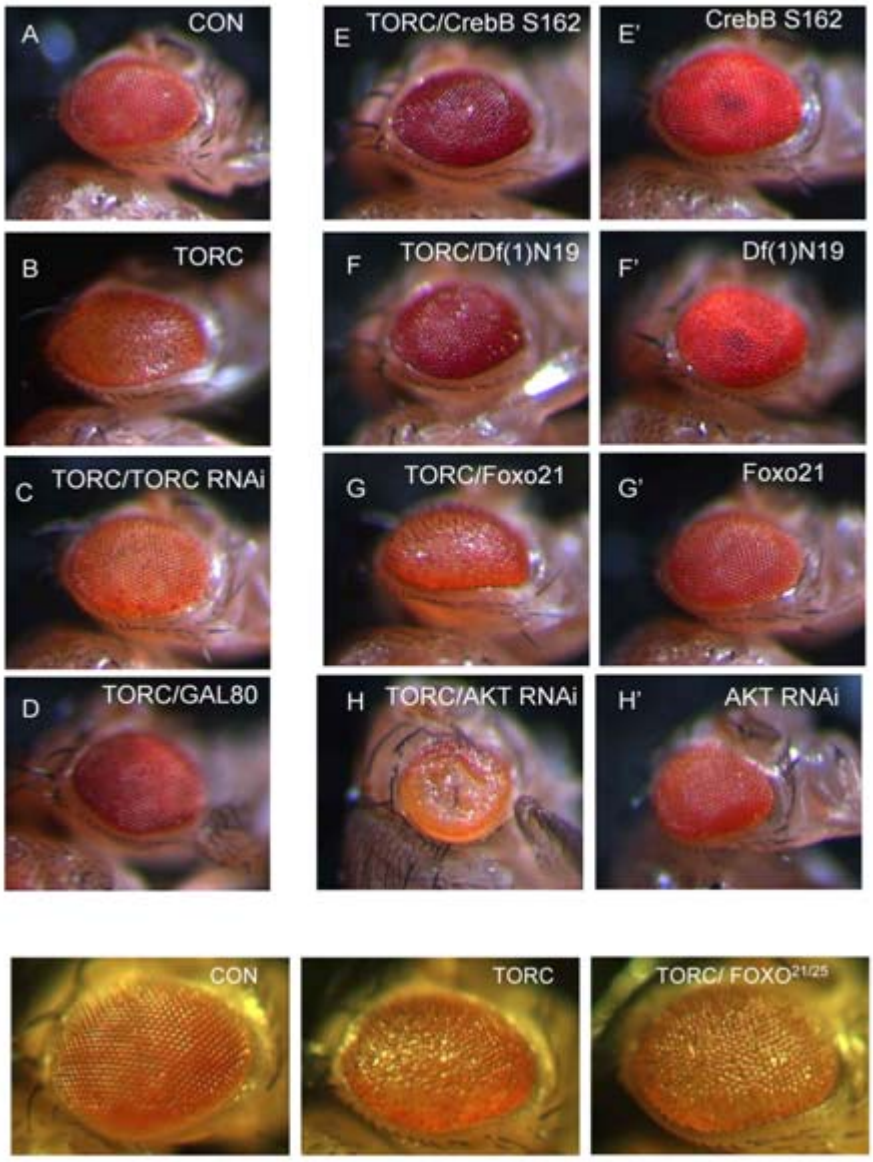
A
CON
E
TORC/CrebB S162
E'
CrebB S162
B
TORC
F
TORC/Df(1)N19
F'
Df(1)N19
C
TORC/TORC RNAi
G
TORC/Foxo21
G'
Foxo21
D
TORC/GAL80
H
TORC/AKT RNAi
H'
AKT RNAi
CON
TORC
TORC/ FOXO21/25

Figure 2.S1. Schematic representation of the TORC gene and the deletion by imprecise excision of the EY00004. The line: 25-3 removed ~10kB region containing *TORC* coding sequence. The deletion was verified by PCR of fly genomic DNA using two sets of primers (A, B).

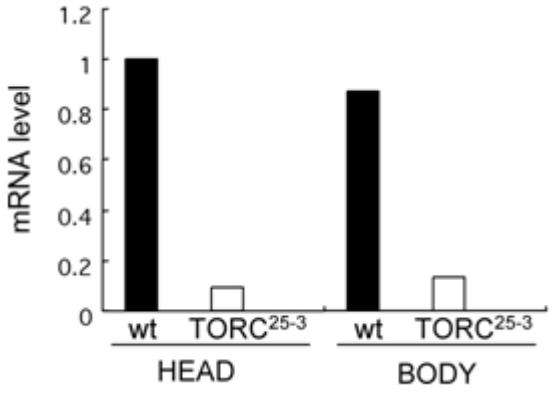

Figure 2.S2. Q-PCR analysis of TORC mRNA levels in heads and bodies of wild-type and *TORC$^{25-3}$* mutant flies.

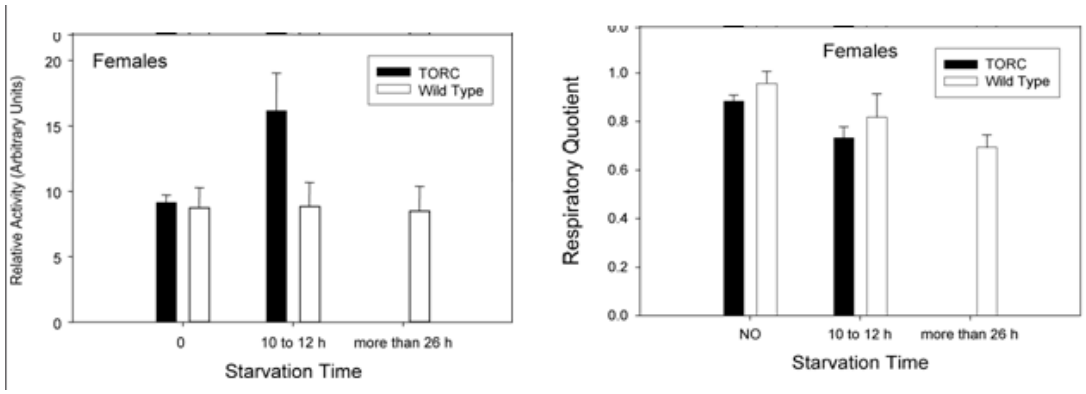

Figure 2.S3. Relative physical activity and respiratory quotients of wild-type and TORC25-3 mutant flies. Left, cumulative activity in ad libitum and fasted flies measured in arbitrary units. No significant differences in the activity of ad libitum fed *TORC*$^{25\text{-}3}$ and wild type female flies were observed (*t*-test, t_{10} = 0.812, *P* = 0.436). However, a significant increase in the activity of the *TORC*$^{25\text{-}3}$ flies compared with wild type flies appears after 10 to 12 hours of starvation (*t*-test, t_{10} = 2.942, *P* = 0.015). Right, Effects of starvation on the respiratory quotient (RQ; ratio of CO2 emitted to O2 consumed) of female *TORC*$^{25\text{-}3}$ and wild type flies. No significant differences in the RQ were observed under fed (*t*-test, t_{10} = 2.120, *P* = 0.060) or starved (*t*-test, t_8 = 0.801, *P* = 0.446) conditions.

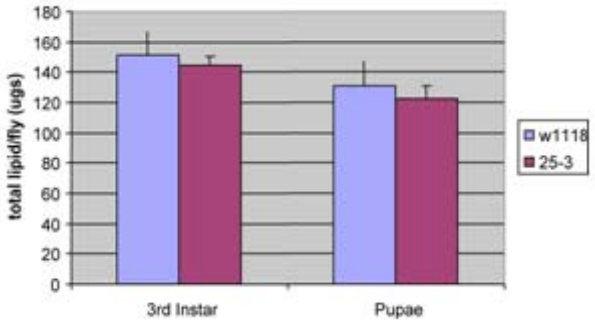

Figure 2.S4. Bar graph showing relative lipid levels in wild-type and *TORC*$^{25\text{-}3}$ larvae.

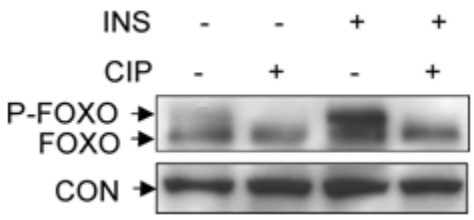

Figure 2.S5. Immunoblot of whole fly extracts showing effect of insulin injection on FOXO phosphorylation. Starved flies were injected intra-abdominally with insulin (1uM) and analyzed after 1 hour. Treatment of extracts with Calf alkaline phosphatase (CIP) indicated.

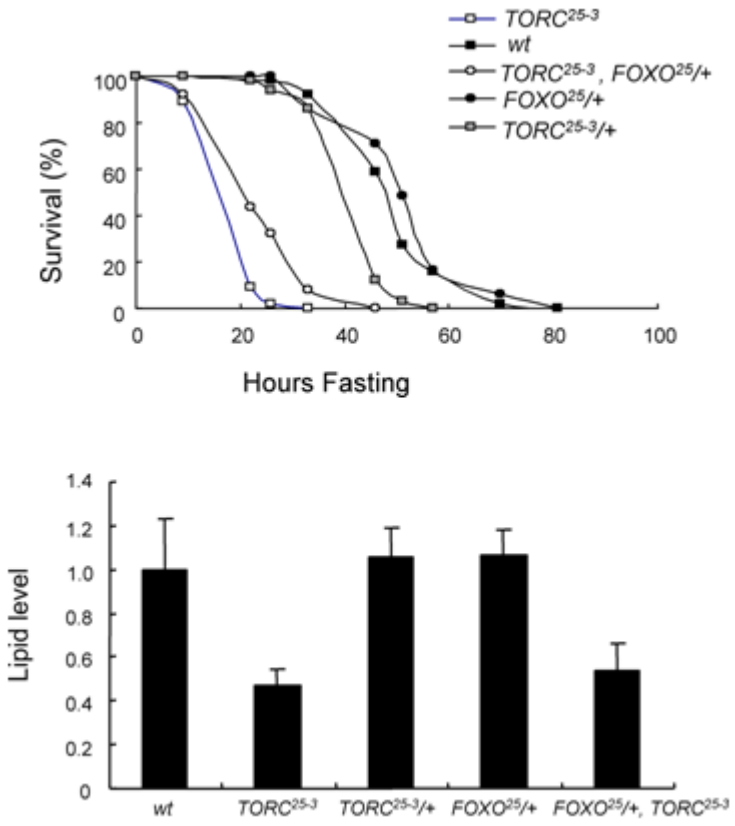

Figure 2.S6. Effect of FOXO disruption on starvation sensitivity of TORC25-3 flies. Survival curves (top) and lipid levels (bottom) for TORC homozygous (*TORC*$^{25\text{-}3}$) and heterozygous (*TORC*$^{25\text{-}3}$/+) mutants as well as FOXO mutant (FOXO^{25}/+) and double-mutant (*TORC*$^{25\text{-}3}$, FOXO^{25}/*TORC*$^{25\text{-}3}$) flies relative to wild-type. Starvation sensitivity was measured in 4-5 day old females (n=50). Similar results were obtained with males (not shown). Lipid levels were measured in 8-10 day old females (n=12).

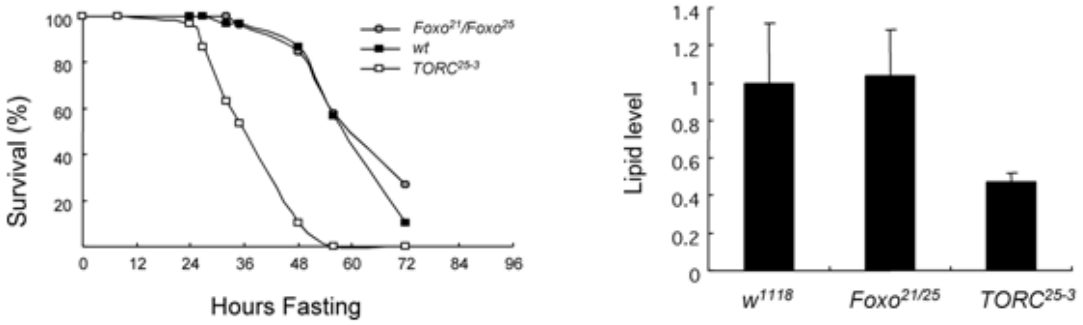

Figure 2.S7. Starvation sensitivity (left) and lipid levels (right) in wild-type, *TORC*$^{25-3}$ homozygous, FOXO$^{21/25}$ null, and wild-type flies.

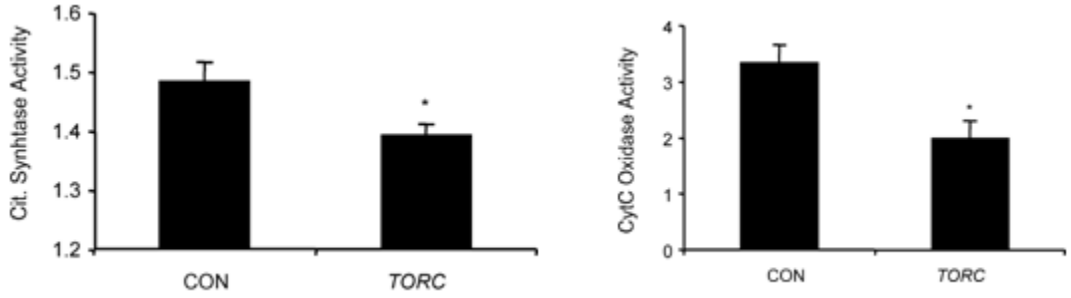

Figure 2.S8. Citrate Synthase (CS) and Cytochrome Oxidase (COX) enzymatic activities in *TORC*$^{25-3}$/*TORC*$^{A4-32}$ mutant flies (*TORC*) and *TORC*$^{25-3}$/*EY00004* control flies (CON). Both CS activity and COX activity are significantly reduced in *TORC* mutants ($p<0.05$; n= 8; data are means ± s.d.).

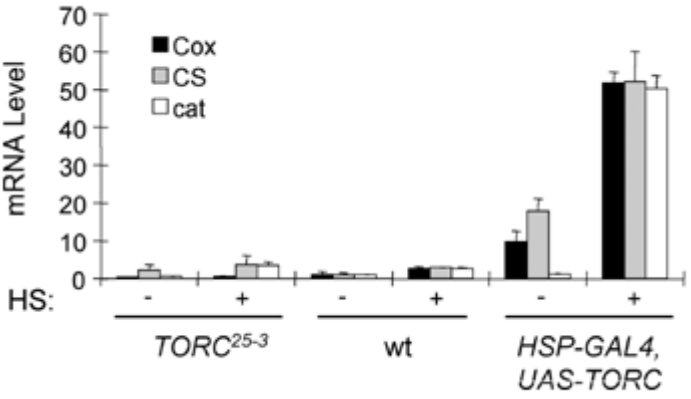

Figure 2.S9. Q-PCR analysis of COX (CG10396), Citrate Synthase (CG14740), and Catalase (CG9314) mRNAs in flies following over-expression of TORC by heat-shock (37^0C for 1hr, room temperature for 0.5hr, followed by 37^0C for 0.5hr).

GENE		CRE
Cytochrome C Oxidase (COX)	cg10396	-960
Citrate Synthase (CS)	cg14740	-26
Catalase (Cat)	cg9314	-314
TrxT	cg3315	-203
UCP4c	cg9064	-
Cyp4G1	cg3972	-375/-172
Acyl CoA Binding Protein (ACBP)	cg 5804	-202
NPF	cg10342	-625

Figure 2.S10. Presence of consensus cAMP Responsive Elements on fasting inducible genes that are down-regulated in TORC25-3 flies. Gene name and CG number shown. Position of CRE (TGACG or CGTCA) relative to transcriptional start site indicated.

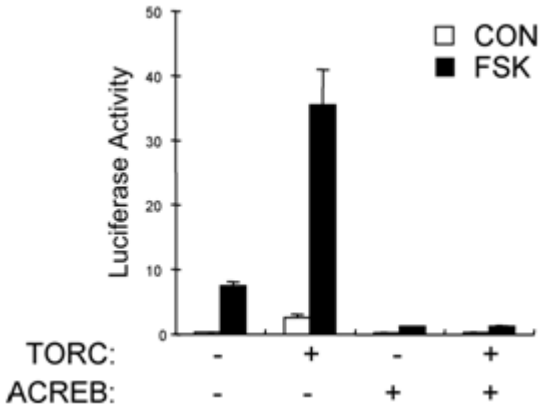

Figure 2.S11. Effect of TORC and ACREB on Cyp4g1-luciferase reporter activity in HEK293T cells. Exposure to FSK indicated. (n=3; results are means ± s.d.).

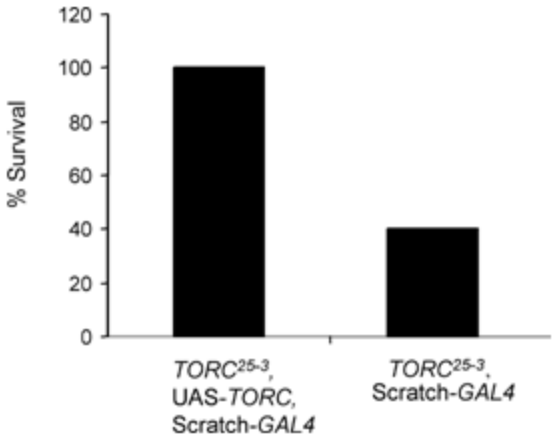

Figure 2.S12. Relative survival of mutant *TORC$^{25-3}$*, *SCRATCH-GAL4* and rescue *TORC$^{25-3}$*, *SCRATCH-GAL4*, *UAS-TORC* in response to 24 hour starvation.

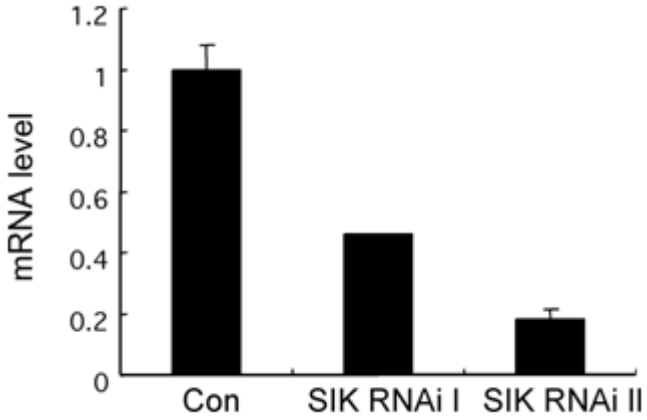

Figure 2.S13. Q-PCR analysis of *Drosophila* SIK2 mRNA levels in control and two different strains of SIK2 RNAi flies.

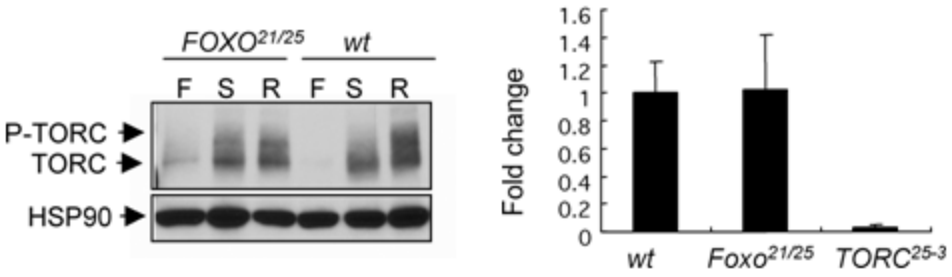

Figure 2.S14. Left, immunoblot showing TORC protein amounts in wild-type and *FOXO*$^{21/25}$ mutant flies under starvation (S), refeeding (R), or ad libitum fed (F) conditions. Right, CRE-luciferase activity in *FOXO*$^{21/25}$, *TORC*$^{25-3}$, and wild-type flies.

Table 2.S1. Results from Affymetrix Gene Profiling Analysis of Head mRNAs from Starved Wild-Type and TORC25-3 Flies
Genes (names and CG values) with average value scores of 100 or more in wild-type flies and downregulated 4-fold or better in *TORC25-3* flies are shown. The presence of a CREB binding sitefor each gene, identified by bioinformatics analysis, is indicated.

Gene Symbol	CRE Site within 3 kb of Promoter	Gene Ontology Biological Process
LvpH		006 // glucose metabolism // non-traceable author statement // 5975 // carbohydrate metabolism // inferred from electronic annotation
TpnC4		1539 // ciliary or flagellar motility // inferred from electronic annotation // 6936 // muscle contraction // inferred from electronic annotation // 19722 // calcium-mediated signaling // inferred from electronic annotation
Ucp4c	Y	15992 // proton transport // inferred from sequence or structural similarity // 6810 // transport // inferred from electronic annotation // 15992 // proton transport // inferred

Table 2.S1 Cont.

Gene Symbol	CRE Site within 3 kb of Promoter	Gene Ontology Biological Process
		from sequence similarity
CG10089	Y	165 // MAPKKK cascade // inferred from electronic annotation // 6470 // protein amino acid dephosphorylation // non-traceable author statement // 6468 // protein amino acid phosphorylation // inferred from electronic annotation // 6470 // protein amino acid dephosphorylation // inferred from electronic annotation
exu		1700 // embryonic development (sensu Insecta) // inferred from mutant phenotype // 7283 // spermatogenesis // traceable author statement // 7300 // nurse cell to oocyte transport (sensu Insecta) // traceable author statement // 8359 // regulation of bicoid mRNA localization // non-traceable author statement // 45450 // bicoid mRNA localization // inferred from expression pattern // 45450 //

Table 2.S1 Cont.

Gene Symbol	CRE Site within 3 kb of Promoter	Gene Ontology Biological Process
		bicoid mRNA localization // inferred from mutant phenotype // 45450 // bicoid mRNA localization // traceable author statement // 45451 // pole plasm oskar mRNA localization // traceable author statement // 7275 // development // inferred from electronic annotation
Mst57Dc		18991 // oviposition // non-traceable author statement // 45297 // post-mating behavior // non-traceable author statement // 7610 // behavior // inferred from electronic annotation
Acp26Ab		18991 // oviposition // non-traceable author statement // 45297 // post-mating behavior // non-traceable author statement // 7610 // behavior // inferred from electronic annotation // 7617 // mating behavior // inferred from electronic annotation
CG4434		19551 // glutamate catabolism to 2-oxoglutarate //

Table 2.S1 Cont.

Gene Symbol	CRE Site within 3 kb of Promoter	Gene Ontology Biological Process
		inferred from sequence or structural similarity // 6520 // amino acid metabolism // inferred from electronic annotation // 19551 // glutamate catabolism to 2-oxoglutarate // inferred from sequence similarity
CG5024	Y	19722 // calcium-mediated signaling // inferred from electronic annotation
CG3085	Y	226 // microtubule cytoskeleton organization and biogenesis // inferred from electronic annotation /// 7275 // development // inferred from electronic annotation /// 7276 // gametogenesis // inferred from electronic annotation /// 7283 // spermatogenesis // inferred from electronic annotation
fln		30241 // muscle thick filament assembly // inferred from mutant phenotype
CG14718	Y	3729 // mRNA binding // inferred from sequence or

Table 2.S1 Cont.

Gene Symbol	CRE Site within 3 kb of Promoter	Gene Ontology Biological Process
		structural similarity // 166 // nucleotide binding // inferred from electronic annotation // 3676 // nucleic acid binding // inferred from electronic annotation // 8270 // zinc ion binding // inferred from electronic annotation // 3729 // mRNA binding // inferred from sequence similarity
CG8565		398 // nuclear mRNA splicing, via spliceosome // inferred from electronic annotation // 6468 // protein amino acid phosphorylation // non-traceable author statement"
CG17221	Y	4024 // alcohol dehydrogenase activity, zinc-dependent // inferred from electronic annotation // 8270 // zinc ion binding // inferred from electronic annotation // 16491 // oxidoreductase activity // inferred from electronic annotation

Table 2.S1 Cont.

Gene Symbol	CRE Site within 3 kb of Promoter	Gene Ontology Biological Process
Acp32CD		45434 // negative regulation of female receptivity, post-mating // non-traceable author statement // 7610 // behavior // inferred from electronic annotation
Acp76A	Y	45861 // negative regulation of proteolysis // inferred from sequence or structural similarity // 45861 // negative regulation of proteolysis // inferred from sequence similarity
CG6289	Y	45861 // negative regulation of proteolysis // inferred from sequence or structural similarity // 45861 // negative regulation of proteolysis // inferred from sequence similarity
CG14305	Y	468 // protein amino acid phosphorylation // non-traceable author statement // 6468 // protein amino acid phosphorylation // inferred from electronic annotation

Table 2.S1 Cont.

Gene Symbol	CRE Site within 3 kb of Promoter	Gene Ontology Biological Process
Pen		59 // protein import into nucleus, docking // non-traceable author statement // 6606 // protein import into nucleus // non-traceable author statement // 6607 // NLS-bearing substrate import into nucleus // non-traceable author statement // 7291 // sperm individualization // inferred from mutant phenotype // 7301 // ovarian ring canal formation // inferred from mutant phenotype // 7303 // cytoplasmic transport, nurse cell to oocyte // non-traceable author statement // 8283 // cell proliferation // non-traceable author statement // 16482 // cytoplasmic transport // inferred from mutant phenotype // 48542 // lymph gland development (sensu Arthropoda) // inferred from mutant phenotype // 6606 // protein import into nucleus // inferred from electronic

Table 2.S1 Cont.

Gene Symbol	CRE Site within 3 kb of Promoter	Gene Ontology Biological Process
		annotation // 6810 // transport // inferred from electronic annotation // 6886 // intracellular protein transport // inferred from electronic annotation // 15031 // protein transport // inferred from electronic annotation
CG11669		5975 // carbohydrate metabolism // inferred from electronic annotation
CG30359	Y	5975 // carbohydrate metabolism // inferred from electronic annotation
Amy-d		5975 // carbohydrate metabolism // inferred from electronic annotation // 5975 // carbohydrate metabolism // traceable author statement
CG9466		5975 // carbohydrate metabolism // inferred from electronic annotation // 6013 // mannose metabolism // inferred from electronic annotation
CG17010		5975 // carbohydrate metabolism // inferred from electronic annotation

Table 2.S1 Cont.

Gene Symbol	CRE Site within 3 kb of Promoter	Gene Ontology Biological Process
		// 6014 // D-ribose metabolism // inferred from electronic annotation // 6413 // translational initiation // inferred from electronic annotation
CG6004		5975 // carbohydrate metabolism // inferred from electronic annotation // 6030 // chitin metabolism // inferred from electronic annotation // 6812 // cation transport // inferred from electronic annotation // 8643 // carbohydrate transport // inferred from electronic annotation
CG31169	Y	5975 // carbohydrate metabolism // inferred from electronic annotation // 6072 // glycerol-3-phosphate metabolism // inferred from sequence or structural similarity // 6629 // lipid metabolism // inferred from electronic annotation // 6072 // glycerol-3-phosphate

Table 2.S1 Cont.

Gene Symbol	CRE Site within 3 kb of Promoter	Gene Ontology Biological Process
		metabolism // inferred from electronic annotation // 46168 // glycerol-3-phosphate catabolism // inferred from electronic annotation // 6072 // glycerol-3-phosphate metabolism // inferred from sequence similarity
CG6484		5975 // carbohydrate metabolism // inferred from electronic annotation // 8643 // carbohydrate transport // inferred from electronic annotation // 6810 // transport // inferred from electronic annotation
CG11909		5976 // polysaccharide metabolism // inferred from electronic annotation // 5996 // monosaccharide metabolism // inferred from electronic annotation // 5975 // carbohydrate metabolism // inferred from electronic annotation
Hex-t1		6096 // glycolysis //

Table 2.S1 Cont.

Gene Symbol	CRE Site within 3 kb of Promoter	Gene Ontology Biological Process
		non-traceable author statement // 6096 // glycolysis // inferred from electronic annotation
CG7349		6099 // tricarboxylic acid cycle // inferred from electronic annotation // 6118 // electron transport // inferred from electronic annotation
CG14740	Y	6099 // tricarboxylic acid cycle // inferred from sequence or structural similarity // 6101 // citrate metabolism // inferred from sequence or structural similarity // 6092 // main pathways of carbohydrate metabolism // inferred from electronic annotation // 6099 // tricarboxylic acid cycle // inferred from sequence similarity // 6101 // citrate metabolism // inferred from sequence similarity
Cyp4g1	Y	6118 // electron transport // inferred from electronic annotation
Mst84Dc		6118 // electron transport // inferred

Table 2.S1 Cont.

Gene Symbol	CRE Site within 3 kb of Promoter	Gene Ontology Biological Process
		from electronic annotation
CG6279		6118 // electron transport // inferred from electronic annotation // 6364 // rRNA processing // inferred from electronic annotation
CG9314		6118 // electron transport // inferred from electronic annotation // 6800 // oxygen and reactive oxygen species metabolism // inferred from electronic annotation // 6952 // defense response // inferred from electronic annotation // 6979 // response to oxidative stress // inferred from electronic annotation
Cyt-c-d		6118 // electron transport // inferred from sequence or structural similarity // 6118 // electron transport // non-traceable author statement // 6119 // oxidative phosphorylation // inferred from sequence or structural similarity // 6919 // caspase activation // inferred

Table 2.S1 Cont.

Gene Symbol	CRE Site within 3 kb of Promoter	Gene Ontology Biological Process
		from mutant phenotype // 7291 // sperm individualization // inferred from mutant phenotype // 6118 // electron transport // inferred from electronic annotation // 6810 // transport // inferred from electronic annotation // 6118 // electron transport // inferred from sequence similarity // 6119 // oxidative phosphorylation // inferred from sequence similarity
TrxT		6118 // electron transport // non-traceable author statement // 6457 // protein folding // inferred from electronic annotation // 6790 // sulfur metabolism // inferred from electronic annotation // 6118 // electron transport // inferred from electronic annotation // 6810 // transport // inferred from electronic annotation
CG10396	Y	6123 // mitochondrial electron transport,

Table 2.S1 Cont.

Gene Symbol	CRE Site within 3 kb of Promoter	Gene Ontology Biological Process
		cytochrome c to oxygen // inferred from sequence or structural similarity // 6118 // electron transport // inferred from electronic annotation // 6123 // mitochondrial electron transport, cytochrome c to oxygen // inferred from sequence similarity
phr		6281 // DNA repair // inferred from sequence or structural similarity // 6281 // DNA repair // inferred from electronic annotation // 6281 // DNA repair // inferred from sequence similarity
CG5017	Y	6334 // nucleosome assembly // inferred from sequence or structural similarity // 6461 // protein complex assembly // inferred from electronic annotation // 6334 // nucleosome assembly // inferred from electronic annotation // 6334 // nucleosome assembly // inferred from sequence

Table 2.S1 Cont.

Gene Symbol	CRE Site within 3 kb of Promoter	Gene Ontology Biological Process
		similarity
CG7045		6355 // regulation of transcription, DNA-dependent // inferred from electronic annotation
cnc	Y	6357 // regulation of transcription from RNA polymerase II promoter // inferred from electronic annotation // 6950 // response to stress // inferred from electronic annotation // 6952 // defense response // inferred from electronic annotation // 7310 // oocyte dorsal/ventral axis determination // inferred from mutant phenotype // 7317 // regulation of pole plasm oskar mRNA localization // inferred from mutant phenotype // 7350 // blastoderm segmentation // inferred from mutant phenotype // 7498 // mesoderm development // inferred from electronic annotation // 8103 // oocyte microtubule cytoskeleton

Table 2.S1 Cont.

Gene Symbol	CRE Site within 3 kb of Promoter	Gene Ontology Biological Process
		polarization // inferred from mutant phenotype // 8359 // regulation of bicoid mRNA localization // inferred from mutant phenotype // 30097 // hemopoiesis // inferred from electronic annotation // 42070 // maintenance of oocyte nucleus localization during oocyte axis determination // inferred from mutant phenotype // 45450 // bicoid mRNA localization // inferred from mutant phenotype // 45451 // pole plasm oskar mRNA localization // inferred from mutant phenotype // 7287 // Nebenkern formation // inferred from mutant phenotype // 8053 // mitochondrial fusion // inferred from mutant phenotype // 7275 // development // inferred from electronic annotation // 7283 // spermatogenesis // inferred from electronic annotation // 8053 //

Table 2.S1 Cont.

Gene Symbol	CRE Site within 3 kb of Promoter	Gene Ontology Biological Process
		mitochondrial fusion // inferred from electronic annotation // 30154 // cell differentiation // inferred from electronic annotation // 6350 // transcription // inferred from electronic annotation // 6355 // regulation of transcription, DNA-dependent // inferred from electronic annotation // 7287 // Nebenkern formation // traceable author statement
Cdlc2		6403 // RNA localization // inferred from electronic annotation // 6886 // intracellular protein transport // inferred from electronic annotation // 7018 // microtubule-based movement // inferred from sequence or structural similarity // 7049 // cell cycle // inferred from electronic annotation // 16192 // vesicle-mediated transport // inferred from electronic annotation // 7017 // microtubule-based

Table 2.S1 Cont.

Gene Symbol	CRE Site within 3 kb of Promoter	Gene Ontology Biological Process
		process // inferred from electronic annotation // 7018 // microtubule-based movement // inferred from sequence similarity
CG3213	Y	6412 // protein biosynthesis // inferred from electronic annotation
Pof		6412 // protein biosynthesis // inferred from electronic annotation
CG8023		6412 // protein biosynthesis // inferred from electronic annotation // 6413 // translational initiation // inferred from electronic annotation
RpL3	Y	6412 // protein biosynthesis // inferred from sequence or structural similarity // 6412 // protein biosynthesis // non-traceable author statement // 6412 // protein biosynthesis // inferred from electronic annotation // 6412 // protein biosynthesis // inferred from sequence similarity

Table 2.S1 Cont.

Gene Symbol	CRE Site within 3 kb of Promoter	Gene Ontology Biological Process
CG8476	Y	6457 // protein folding // inferred from electronic annotation // 6605 // protein targeting // inferred from electronic annotation // 6810 // transport // inferred from electronic annotation // 15031 // protein transport // inferred from electronic annotation
CG9920	Y	6457 // protein folding // inferred from sequence or structural similarity // 6458 // 'de novo' protein folding // inferred from sequence or structural similarity // 6457 // protein folding // inferred from electronic annotation // 6457 // protein folding // inferred from sequence similarity // 6458 // 'de novo' protein folding // inferred from sequence similarity
CG7235		6457 // protein folding // inferred from sequence or structural similarity // 6458 // 'de novo' protein folding //

Table 2.S1 Cont.

Gene Symbol	CRE Site within 3 kb of Promoter	Gene Ontology Biological Process
		inferred from sequence or structural similarity // 6626 // protein targeting to mitochondrion // inferred from sequence or structural similarity // 6950 // response to stress // non-traceable author statement // 42026 // protein refolding // non-traceable author statement // 910 // cytokinesis // inferred from mutant phenotype // 6468 // protein amino acid phosphorylation // inferred from electronic annotation // 6457 // protein folding // inferred from electronic annotation // 44267 // cellular protein metabolism // inferred from electronic annotation // 6457 // protein folding // inferred from sequence similarity // 6458 // 'de novo' protein folding // inferred from sequence similarity // 6626 // protein targeting to

Table 2.S1 Cont.

Gene Symbol	CRE Site within 3 kb of Promoter	Gene Ontology Biological Process
		mitochondrion // inferred from sequence similarity
Hsp60B	Y	6457 // protein folding // inferred from sequence or structural similarity // 6458 // 'de novo' protein folding // inferred from sequence or structural similarity // 6626 // protein targeting to mitochondrion // inferred from sequence or structural similarity // 7286 // spermatid development // inferred from mutant phenotype // 9408 // response to heat // inferred from sequence or structural similarity // 42026 // protein refolding // inferred from sequence or structural similarity // 6457 // protein folding // inferred from electronic annotation // 44267 // cellular protein metabolism // inferred from electronic annotation

Table 2.S1 Cont.

Gene Symbol	CRE Site within 3 kb of Promoter	Gene Ontology Biological Process
		// 6457 // protein folding // inferred from sequence similarity // 6458 // 'de novo' protein folding // inferred from sequence similarity // 6626 // protein targeting to mitochondrion // inferred from sequence similarity // 9408 // response to heat // inferred from sequence similarity // 42026 // protein refolding // inferred from sequence similarity
CG16716		6464 // protein modification // inferred from electronic annotation // 19538 // protein metabolism // inferred from electronic annotation
CG3964	Y	6464 // protein modification // inferred from electronic annotation // 19538 // protein metabolism // inferred from electronic annotation
CG9602	Y	6464 // protein modification // inferred from electronic annotation // 6512 // ubiquitin

Table 2.S1 Cont.

Gene Symbol	CRE Site within 3 kb of Promoter	Gene Ontology Biological Process
		cycle // inferred from electronic annotation // 19538 // protein metabolism // inferred from electronic annotation
FucTB		6486 // protein amino acid glycosylation // inferred from electronic annotation
CG12374	Y	6508 // proteolysis // inferred from electronic annotation
CG13095	Y	6508 // proteolysis // inferred from electronic annotation
CG31198		6508 // proteolysis // inferred from electronic annotation
CG32063		6508 // proteolysis // inferred from electronic annotation
CG4439		6508 // proteolysis // inferred from electronic annotation
CG6372		6508 // proteolysis // inferred from electronic annotation
CG8564	Y	6508 // proteolysis // inferred from electronic annotation
CG13340	Y	6508 // proteolysis // inferred from electronic annotation // 19538 // protein metabolism // inferred from electronic annotation
CG32064	Y	6508 // proteolysis // inferred from

Table 2.S1 Cont.

Gene Symbol	CRE Site within 3 kb of Promoter	Gene Ontology Biological Process
		electronic annotation // 19538 // protein metabolism // inferred from electronic annotation
CG4750		6508 // proteolysis // inferred from electronic annotation // 19538 // protein metabolism // inferred from electronic annotation
Spn2		6508 // proteolysis // inferred from electronic annotation // 45861 // negative regulation of proteolysis // inferred from sequence or structural similarity // 45861 // negative regulation of proteolysis // inferred from sequence similarity
Spn3	Y	6508 // proteolysis // inferred from electronic annotation // 45861 // negative regulation of proteolysis // inferred from sequence or structural similarity // 45861 // negative regulation of proteolysis // inferred from sequence similarity
CG32351		6508 // proteolysis // inferred from

Table 2.S1 Cont.

Gene Symbol	CRE Site within 3 kb of Promoter	Gene Ontology Biological Process
		electronic annotation // 6508 // proteolysis // inferred from sequence or structural similarity // 19538 // protein metabolism // inferred from electronic annotation // 6508 // proteolysis // inferred from sequence similarity
CG6680		6508 // proteolysis // inferred from electronic annotation // 6915 // apoptosis // inferred from electronic annotation
CG17242	Y	6508 // proteolysis // inferred from electronic annotation // 8152 // metabolism // inferred from electronic annotation
CG30028		6508 // proteolysis // inferred from electronic annotation /// 6508 // proteolysis // non-traceable author statement /// 6508 // proteolysis // inferred from sequence or structural similarity /// 30422 // RNA interference, production of siRNA // inferred from mutant phenotype /// 30423 // RNA

Table 2.S1 Cont.

Gene Symbol	CRE Site within 3 kb of Promoter	Gene Ontology Biological Process
		interference, targeting of mRNA for destruction // inferred from mutant phenotype /// 35196 // miRNA-mediated gene silencing, production of miRNAs // inferred from mutant phenotype /// 35279 // miRNA-mediated gene silencing, mRNA cleavage // inferred from mutant phenotype /// 16246 // RNA interference // traceable author statement /// 6508 // proteolysis // inferred from sequence similarity
CG6462	Y	6508 // proteolysis // non-traceable author statement
Jonah 74E	Y	6508 // proteolysis // non-traceable author statement
CG10472	Y	6508 // proteolysis // non-traceable author statement // 6508 // proteolysis // inferred from electronic annotation
CG11037		6508 // proteolysis // non-traceable author statement // 6508 // proteolysis // inferred from electronic annotation

Table 2.S1 Cont.

Gene Symbol	CRE Site within 3 kb of Promoter	Gene Ontology Biological Process
CG18211		6508 // proteolysis // non-traceable author statement // 6508 // proteolysis // inferred from electronic annotation
CG18444		6508 // proteolysis // non-traceable author statement // 6508 // proteolysis // inferred from electronic annotation
Jon65Aiii	Y	6508 // proteolysis // non-traceable author statement // 6508 // proteolysis // inferred from electronic annotation
yip7		6508 // proteolysis // non-traceable author statement // 6508 // proteolysis // inferred from electronic annotation
sina		6508 // proteolysis // traceable author statement // 6511 // ubiquitin-dependent protein catabolism // inferred from mutant phenotype // 6511 // ubiquitin-dependent protein catabolism // non-traceable author statement // 7423 // sensory organ development // inferred from mutant phenotype // 7465 // R7 cell fate

Table 2.S1 Cont.

Gene Symbol	CRE Site within 3 kb of Promoter	Gene Ontology Biological Process
		commitment // traceable author statement // 16567 // protein ubiquitination // inferred from electronic annotation // 45676 // regulation of R7 differentiation // inferred from mutant phenotype // 6511 // ubiquitin-dependent protein catabolism // inferred from electronic annotation // 6512 // ubiquitin cycle // inferred from electronic annotation // 7275 // development // inferred from electronic annotation // 7601 // visual perception // inferred from electronic annotation // 50896 // response to stimulus // inferred from electronic annotation
CG33092		6537 // glutamate biosynthesis // inferred from sequence or structural similarity // 6562 // proline catabolism // inferred from sequence or structural similarity // 6561 // proline biosynthesis //

Table 2.S1 Cont.

Gene Symbol	CRE Site within 3 kb of Promoter	Gene Ontology Biological Process
		inferred from electronic annotation // 8152 // metabolism // inferred from electronic annotation // 6537 // glutamate biosynthesis // inferred from sequence similarity // 6562 // proline catabolism // inferred from sequence similarity
tomboy20	Y	6626 // protein targeting to mitochondrion // inferred from sequence or structural similarity // 6605 // protein targeting // inferred from electronic annotation // 6886 // intracellular protein transport // inferred from electronic annotation // 6626 // protein targeting to mitochondrion // inferred from sequence similarity
CG6277		6629 // lipid metabolism // inferred from electronic annotation
CG31872	Y	6629 // lipid metabolism // inferred from electronic annotation // 16042 // lipid

Table 2.S1 Cont.

Gene Symbol	CRE Site within 3 kb of Promoter	Gene Ontology Biological Process
		catabolism // inferred from electronic annotation
CG5932		6629 // lipid metabolism // inferred from electronic annotation // 16042 // lipid catabolism // inferred from electronic annotation
CG11426		6629 // lipid metabolism // inferred from electronic annotation // 16311 // dephosphorylation // non-traceable author statement
CG17097		6629 // lipid metabolism // inferred from electronic annotation // 6629 // lipid metabolism // inferred from sequence or structural similarity // 16042 // lipid catabolism // inferred from electronic annotation // 6629 // lipid metabolism // inferred from sequence similarity
CG18284		6629 // lipid metabolism // inferred from electronic annotation // 6629 // lipid

Table 2.S1 Cont.

Gene Symbol	CRE Site within 3 kb of Promoter	Gene Ontology Biological Process
		metabolism // inferred from sequence or structural similarity // 16042 // lipid catabolism // inferred from electronic annotation // 6629 // lipid metabolism // inferred from sequence similarity
CG16904		6629 // lipid metabolism // inferred from electronic annotation // 6631 // fatty acid metabolism // inferred from electronic annotation
CG15531		6631 // fatty acid metabolism // inferred from electronic annotation // 6633 // fatty acid biosynthesis // inferred from electronic annotation // 8610 // lipid biosynthesis // inferred from electronic annotation
CG17374	Y	6633 // fatty acid biosynthesis // inferred from electronic annotation // 8152 // metabolism // inferred from electronic annotation // 6633 // fatty acid biosynthesis //

Table 2.S1 Cont.

Gene Symbol	CRE Site within 3 kb of Promoter	Gene Ontology Biological Process
		inferred from sequence similarity
desat1	Y	6633 // fatty acid biosynthesis // non-traceable author statement // 6633 // fatty acid biosynthesis // inferred from electronic annotation // 8610 // lipid biosynthesis // inferred from electronic annotation
CG9389		6644 // phospholipid metabolism // inferred from electronic annotation // 7242 // intracellular signaling cascade // inferred from electronic annotation // 16311 // dephosphorylation // non-traceable author statement
CG9254	Y	6796 // phosphate metabolism // inferred from electronic annotation // 6812 // cation transport // inferred from electronic annotation // 6817 // phosphate transport // inferred from electronic annotation // 6858 // extracellular transport // inferred

Table 2.S1 Cont.

Gene Symbol	CRE Site within 3 kb of Promoter	Gene Ontology Biological Process
		from electronic annotation // 6810 // transport // inferred from electronic annotation
CG11880		6810 // transport // inferred from electronic annotation
Obp51a	Y	6810 // transport // inferred from electronic annotation // 7606 // sensory perception of chemical stimulus // inferred from sequence or structural similarity // 7606 // sensory perception of chemical stimulus // inferred from sequence similarity
Obp56e		6810 // transport // inferred from electronic annotation // 7606 // sensory perception of chemical stimulus // inferred from sequence or structural similarity // 7606 // sensory perception of chemical stimulus // inferred from sequence similarity
CG4323		6812 // cation transport // inferred from electronic annotation // 6810 //

Table 2.S1 Cont.

Gene Symbol	CRE Site within 3 kb of Promoter	Gene Ontology Biological Process
		transport // inferred from electronic annotation
Porin2		6820 // anion transport // inferred from electronic annotation /// 6839 // mitochondrial transport // inferred from sequence or structural similarity /// 6839 // mitochondrial transport // inferred from sequence similarity
lcs	Y	6839 // mitochondrial transport // inferred from mutant phenotype // 6810 // transport // inferred from electronic annotation
CG32079		6865 // amino acid transport // inferred from electronic annotation
path	Y	6865 // amino acid transport // inferred from electronic annotation // 40008 // regulation of growth // non-traceable author statement
CG5804	Y	6869 // lipid transport // inferred from electronic annotation // 42049 // cell acyl-CoA homeostasis // inferred from sequence or

Table 2.S1 Cont.

Gene Symbol	CRE Site within 3 kb of Promoter	Gene Ontology Biological Process
		structural similarity // 42049 // cell acyl-CoA homeostasis // inferred from sequence similarity
Tub85D		6886 // intracellular protein transport // inferred from electronic annotation // 6928 // cell motility // inferred from electronic annotation // 7017 // microtubule-based process // inferred from sequence or structural similarity // 7059 // chromosome segregation // inferred from electronic annotation // 7067 // mitosis // inferred from electronic annotation // 7018 // microtubule-based movement // inferred from electronic annotation // 51258 // protein polymerization // inferred from electronic annotation // 7017 // microtubule-based process // inferred from sequence similarity
d	Y	6886 // intracellular protein transport //

Table 2.S1 Cont.

Gene Symbol	CRE Site within 3 kb of Promoter	Gene Ontology Biological Process
		inferred from electronic annotation // 7601 // visual perception // inferred from electronic annotation // 7605 // sensory perception of sound // inferred from electronic annotation // 16192 // vesicle-mediated transport // inferred from electronic annotation
CG31624		6928 // cell motility // inferred from electronic annotation // 7010 // cytoskeleton organization and biogenesis // inferred from electronic annotation
TpnC41C		6936 // muscle contraction // inferred from electronic annotation // 19722 // calcium-mediated signaling // inferred from electronic annotation
Mbs	Y	6936 // muscle contraction // inferred from electronic annotation // 7391 // dorsal closure // inferred from mutant phenotype // 7391 // dorsal closure // non-traceable author

Table 2.S1 Cont.

Gene Symbol	CRE Site within 3 kb of Promoter	Gene Ontology Biological Process
		statement // 9993 // oogenesis (sensu Insecta) // inferred from mutant phenotype // 35317 // wing hair organization and biogenesis // inferred from mutant phenotype // 45314 // regulation of eye photoreceptor development (sensu Endopterygota) // inferred from mutant phenotype
Ag5r	Y	6952 // defense response // inferred from electronic annotation
CG17575		6952 // defense response // inferred from electronic annotation
msopa	Y	6952 // defense response // inferred from sequence or structural similarity // 6952 // defense response // inferred from sequence similarity
Ect4	Y	6955 // immune response // inferred from electronic annotation // 45087 // innate immune response // inferred from electronic annotation

Table 2.S1 Cont.

Gene Symbol	CRE Site within 3 kb of Promoter	Gene Ontology Biological Process
Atg8b	Y	7010 // cytoskeleton organization and biogenesis // inferred from electronic annotation
Act88F	Y	7010 // cytoskeleton organization and biogenesis // inferred from sequence or structural similarity // 7010 // cytoskeleton organization and biogenesis // inferred from sequence similarity
CG10859		7018 // microtubule-based movement // inferred from sequence or structural similarity // 7018 // microtubule-based movement // inferred from sequence similarity
lectin-30A	Y	7283 // spermatogenesis // inferred from electronic annotation
dj		7283 // spermatogenesis // traceable author statement // 7286 // spermatid development // non-traceable author statement // 7291 // sperm individualization // inferred from expression pattern

Table 2.S1 Cont.

Gene Symbol	CRE Site within 3 kb of Promoter	Gene Ontology Biological Process
Acp36DE	Y	7321 // sperm displacement // non-traceable author statement // 42628 // mating plug formation // traceable author statement // 45434 // negative regulation of female receptivity, post-mating // non-traceable author statement // 46692 // sperm competition // traceable author statement // 46693 // sperm storage // inferred from mutant phenotype // 46693 // sperm storage // traceable author statement // 7610 // behavior // inferred from electronic annotation
Acp53Ea		7321 // sperm displacement // non-traceable author statement // 7582 // physiological process // non-traceable author statement // 45297 // post-mating behavior // non-traceable author statement // 46692 // sperm competition // traceable author statement // 7610 //

Table 2.S1 Cont.

Gene Symbol	CRE Site within 3 kb of Promoter	Gene Ontology Biological Process
		behavior // inferred from electronic annotation
Acp26Aa	Y	7321 // sperm displacement // non-traceable author statement // 7618 // mating // inferred from electronic annotation // 18991 // oviposition // non-traceable author statement // 18991 // oviposition // traceable author statement // 30728 // ovulation // inferred from mutant phenotype // 30728 // ovulation // traceable author statement // 45297 // post-mating behavior // non-traceable author statement // 46662 // regulation of oviposition // non-traceable author statement // 46692 // sperm competition // traceable author statement // 48042 // regulation of oviposition, post-mating // traceable author statement
skpB		74 // regulation of progression through cell cycle // inferred from electronic

Table 2.S1 Cont.

Gene Symbol	CRE Site within 3 kb of Promoter	Gene Ontology Biological Process
		annotation // 6508 // proteolysis // inferred from electronic annotation // 7049 // cell cycle // inferred from electronic annotation // 7059 // chromosome segregation // inferred from electronic annotation // 7067 // mitosis // inferred from electronic annotation // 19538 // protein metabolism // inferred from electronic annotation
CG15306		74 // regulation of progression through cell cycle // inferred from electronic annotation // 7049 // cell cycle // inferred from electronic annotation
CG32371	Y	74 // regulation of progression through cell cycle // inferred from electronic annotation // 7049 // cell cycle // inferred from electronic annotation
CG17470		7498 // mesoderm development // inferred from expression pattern
janB		7548 // sex differentiation //

Table 2.S1 Cont.

Gene Symbol	CRE Site within 3 kb of Promoter	Gene Ontology Biological Process
		inferred from expression pattern
CG10852	Y	7582 // physiological process // non-traceable author statement // 45297 // post-mating behavior // non-traceable author statement // 7610 // behavior // inferred from electronic annotation
CG1262		7582 // physiological process // non-traceable author statement // 8340 // determination of adult life span // non-traceable author statement // 30162 // regulation of proteolysis // traceable author statement // 45297 // post-mating behavior // non-traceable author statement // 45861 // negative regulation of proteolysis // inferred from sequence or structural similarity // 45861 // negative regulation of proteolysis // traceable author statement // 7610 // behavior // inferred from electronic annotation // 45861 //

Table 2.S1 Cont.

Gene Symbol	CRE Site within 3 kb of Promoter	Gene Ontology Biological Process
		negative regulation of proteolysis // inferred from sequence similarity
CG12896		800 // oxygen and reactive oxygen species metabolism // inferred from electronic annotation // 6952 // defense response // inferred from electronic annotation // 7498 // mesoderm development // inferred from expression pattern
CG3699	Y	8152 // metabolism // inferred from electronic annotation
Strn-Mlck	Y	910 // cytokinesis // inferred from electronic annotation // 6468 // protein amino acid phosphorylation // inferred from sequence or structural similarity // 6468 // protein amino acid phosphorylation // non-traceable author statement // 7059 // chromosome segregation // inferred from electronic annotation // 7067 // mitosis // inferred from electronic annotation

Table 2.S1 Cont.

Gene Symbol	CRE Site within 3 kb of Promoter	Gene Ontology Biological Process
		// 7498 // mesoderm development // inferred from electronic annotation // 7507 // heart development // inferred from electronic annotation // 6468 // protein amino acid phosphorylation // inferred from electronic annotation // 7275 // development // inferred from electronic annotation // 6468 // protein amino acid phosphorylation // inferred from sequence similarity
Acp53C14a		
Acp53C14b		
CG10407		
CG10734	Y	
CG11106		
CG11591	Y	
CG11635	Y	
CG1287	Y	
CG12907	Y	
CG1324	Y	
CG13477	Y	
CG1394	Y	
CG14835		
CG1690	Y	
CG17237	Y	
CG17838	Y	
CG18170		

Table 2.S1 Cont.

Gene Symbol	CRE Site within 3 kb of Promoter	Gene Ontology Biological Process
CG18449		
CG18662		
CG2113	Y	
CG2267	Y	
CG2955	Y	
CG30039	Y	
CG30376	Y	
CG31538	Y	
CG31542		
CG32148		
CG32450		
CG32832		
CG4375		
CG4460		
CG4546		
CG5048	Y	
CG5089		
CG5107	Y	
CG9119	Y	
Mst35Ba		
Mst77F	Y	
ocn		
Summary		
169 total hits, among which 78 are positive for CRE		

Chapter 2 has been published and appears in Cell Metabolism 2008. Biao Wang, Jason Goode, Jennifer Best, Jodi Meltzer, Pablo E. Schilman, Jian Chen, Dan Garza, John B. Thomas, and Marc Montminy.

CHAPTER 3

The CREB Coactivator dTORC is Required for Cardiac Function in *Drosophila*

3.1 Abstract

The previous chapter describes the generation of a dTORC null mutant fly and the role of neuronal dTORC in stress resistance and energy balance. In this chapter we focus on the analysis of dTORC in cardiac physiology. dTORC mutant flies have increased heart rates due to a shortened diastolic interval and decreased heart diameters. These altered heart functions are accompanied by a disrupted myofibrillar structure and reduction of CREB target gene expression. Cardiac expression of dTORC rescues the observed cardiac dysfunction and muscle degeneration as well as expression of CREB transcriptional targets. Our results suggest that dTORC is acting as a CREB coactivator in a complex transcriptional program directing cardiac maintenance and repair.

3.2 Introduction

The fruit fly has long been recognized as an important genetic model system in the analysis of biological processes. Its genetic tractability, well-studied genome and the plethora of available genetic tools makes *Drosophila* the premier organism for studying complex processes in vivo. One such process in which *Drosophila* has been invaluable is cardiogenesis (Bier and

Bodmer 2004). The network of transcription factors and signaling molecules that control this process are highly conserved between flies and mammals (Olson 2006), (Cripps and Olson 2002). In fact, the early developmental stages of this process in flies and humans are strikingly similar (Tao and Schulz 2007). Both start with bilateral specification of rows of cells in the lateral mesoderm as cardiac precursors, which then migrate to the midline to form the initial heart tube (Tao and Schulz 2007). In the fly, cardiogenesis is essentially complete with formation of the beating tubular heart, whereas mammalian hearts undergo looping and further specialization. The core set of transcription factors (NK2/Tinman, GATA, Tbx, MEF2, and Hand) driving this process is the same in flies and vertebrates (Olson 2006).

Recent work has established *Drosophila melanogaster* as a powerful organism not only for studying the developmental process of cardiogenesis, but also for elucidating the mechanism of cardiac function (Ocorr, Akasaka et al. 2007) (Ocorr, Reeves et al. 2007),(Akasaka, Klinedinst et al. 2006). Fly hearts share many of the ion channels used by human hearts to maintain normal rhythmic pumping. Several studies have shown that mutations in the genes encoding these channels cause similar cardiac phenotypes in flies and humans (Ocorr, Akasaka et al. 2007) (Ocorr, Reeves et al. 2007),(Akasaka, Klinedinst et al. 2006). In one study, the *Drosophila* homolog of the human KCNQ1 gene was mutated and found to cause cardiac arrhythmias, which is similar to the phenotype observed in humans harboring mutations in this gene

(Ocorr, Reeves et al. 2007). Comparable findings have been reported for the gene encoding the KATP channel, SUR2A and for human ether-a-go-go (hERG) (Ocorr, Reeves et al. 2007), (Akasaka, Klinedinst et al. 2006). Aside from the wide range of tools available in *Drosophila*, the fly heart also offers several technical advantages inherent to the organism. *Drosophila* can tolerate very deleterious mutations affecting the heart, because it is not required for respiration. Severely impairing heart function in mammalian models causes immediate death. Furthermore, the fly heart is far simpler anatomically, being composed of only 104 myocytes (Zeitouni, Senatore et al. 2007). Also, there is little functional redundancy in the genes used to specify the development and maintenance of heart function, making genetic manipulation that much easier (Olson 2006). Given that the basic developmental and functional mechanisms of the heart are conserved between flies and mammals, and the wealth of resources available, *Drosophila melanogaster* is an ideal organism in which to study the role of TORC in the heart.

We showed in the previous chapter that dTORC mutant flies ($TORC^{25-3}$) are stress sensitive and have a reduced lifespan when compared to wild-type flies, and that dTORC is regulated by the insulin signaling pathway (Wang, Goode et al. 2008). One possible explanation for the short lifespan seen in dTORC mutant flies is rapid aging. The role of insulin-IGF signaling in organismal aging and lifespan is well established (Kenyon, Chang et al. 1993), (Bluher, Kahn et al. 2003),(Tatar, Kopelman et al. 2001), (Hwangbo,

Gershman et al. 2004) .Recent work has shown that *Drosophila* resting heart rate progressively declines and that stress-induced heart failure increases from one to seven weeks of age (Wessells, Fitzgerald et al. 2004). Furthermore, disrupting insulin signaling in the heart can reverse this age-dependent decline in cardiac function.

In this chapter, we address the potential role of dTORC in maintenance of normal cardiac function and whether the reduced lifespan seen in dTORC mutant animals is due to accelerated aging, using heart function as an indicator of relative organismal age. We found that dTORC mutant animals do not exhibit the hallmarks of flies beyond their chronological age, however they do show profound cardiac dysfunction which can be rescued by reintroducing dTORC into the mutant heart. dTORC does not appear to be required for normal development of the heart, but is necessary to maintain cardiac integrity in the adult animal. In this system, dTORC is likely acting as a coactivator in a complex transcriptional program directing cardiac maintenance and repair.

3.3 Results

dTORC is Expressed in the Heart

To establish a role for dTORC in the *Drosophila* heart we first showed that dTORC is in fact expressed in this tissue. In our previous work we mutated the dTORC gene by imprecise P-element excision resulting in a deletion (named 25-3) that removed the entire transcribed region of dTORC

(Wang, Goode et al. 2008). We performed RT-PCR analysis on RNA isolated from head and heart tissue from both wild-type and dTORC mutant flies. dTORC is expressed in both tissues, although to a lower degree in the heart of wild-type animals, and completely absent from mutants (Figure 3.1A and 3.1B). dTORC protein can also be detected in all three body compartments of wild-type flies, as well as isolated hearts, and is not detected in any tissue of dTORC mutant flies (Figure 3.1C and 3.1D).

dTORC Mutant Flies Exhibit Cardiac Dysfunction

dTORC mutant flies have an average lifespan that is about one third that of wild type. In an effort to determine whether this early death is due to premature aging, we measured resting heart rate and cardiac rhythmicity, which have been shown to decline in aging fruit flies (Wessells, Fitzgerald et al. 2004). This was done using high-speed video microscopy on surgically exposed beating hearts of adult flies (Video 3.1A and 3.1B). The resulting videos were then analyzed using specialized software to track the edges of the beating heart and make measurements of systolic/diastolic diameter and rhythmic beating over time (Figure 3.2A and 3.2B and See Materials and Methods). M-mode traces of video recordings were also generated showing details of heart edge positions (y-axis) over time (x-axis) (Figure 3.2B). In about one third of the dTORC mutant hearts, we observed a constriction of the heart in the third abdominal segment (Figure 3.2B).

Resting heart rate was determined for wild-type and dTORC mutant flies at one, two and three weeks of age (which is nearing maximal lifespan for dTORC mutants) in order to measure slowing of heart rate with age. Rather than observing a slower heart rate that might indicate premature aging, we found that dTORC mutant have a faster heart rate than age-matched wild-type flies and that heart rate declines normally with age (Figure 3.2C and 3.2E). This difference in heart rate is almost entirely due to a decreased diastolic interval in dTORC mutant flies, as systolic interval is largely unchanged (Figure 3.2E).

Although we were unable to observe the phenotypes typical of aging flies (Wessells, Fitzgerald et al. 2004), to our surprise we found that the dTORC mutant flies have a profound cardiac pathology. As well as having an increased heart rate and stenosis at the third abdominal segment, these flies show reduced systolic and diastolic diameter along the entire heart tube at all ages observed (Figure 3.2D).

dTORC Mutant Flies Exhibit Cardiac Muscle Degeneration

In order to gain some insight in to what might be causing the reduced heart size and stenosis, we dissected and stained hearts from wild-type and dTORC knockout flies to observe the myofibrillar organization. Hearts were stained with alpha-actinin, which localizes to sarcomeric Z-discs (Taghli-Lamallem, Akasaka et al. 2008), and phalloidin which binds polymerized actin

filaments. In wild-type animals, myofibrils are tightly packed and organized in a parallel alignment forming a solid muscular tube that gently tapers from anterior to posterior. Muscle fibers in dTORC mutant hearts were loosely packed, splayed and disorganized or sometimes missing when compared to hearts of wild type flies (Figure 3.3).

dTORC Cardiac Phenotype is not Developmental

Development of the *Drosophila* heart tube is a well-characterized process that involves specification, alignment, adhesion and migration of cardioblasts and pericardial cells in the dorsal mesoderm (Bodmer and Venkatesh 1998). In order to determine if dTORC is involved in the embryonic development of the heart, we examined stage 17 wild-type and dTORC mutant embyos for expression of markers involved in this process. We found no difference in the expression patterns of Neuromancer, Dystroglycan (Figure 3.4A, and 3.4D) , Zfh1, dMEF2 (Figure 3.4B and 3.4E), or Svp (Figure 3.4C and 3.4F). We also observed normal positioning and numbers of both cardioblasts and pericardial cells in dTORC mutant embryos.

Cardiac Expression of dTORC Rescues dTORC Mutant Heart Phenotypes

Using the GAL4/UAS transactivation system (Brand and Perrimon 1993), we reintroduced dTORC into the myocardial and pericardial cells of dTORC mutant flies with a Hand-Gal4 driver (Han, Yi et al. 2006). This combination drives expression of dTORC protein to high levels in the fly heart

(Figure 3.5A). Cardiac expression of dTORC is sufficient to rescue the decrease in mean systolic and diastolic diameters (Figure 3.5B) and the increase in heart rate (Figure 3.5C) observed in dTORC mutant flies (Video 3.2). It should be noted that heart diameters are actually significantly larger and that systolic interval is significantly longer in Rescue flies than WT flies, suggesting a possible gain of function when expressing dTORC to these levels in the heart.

Another measure of general cardiac health in *Drosophila* is their ability to recover from pacing induced stress (Paternostro, Vignola et al. 2001), (Wessells and Bodmer 2004). We subjected WT, KO and Rescue flies to 6 Hz electrical pacing for 30 seconds and then observed whether they recovered from cardiac fibrillation or cardiac arrest. dTORC mutant animals had a greater than four fold higher incidence of heart failure when compared to WT flies, and this was almost completely rescued by expression of dTORC in the heart (Figure 3.5D).

Staining of WT, KO, and Rescue hearts with fluorescent phalloidin revealed a complete rescue of muscle fiber degeneration in dTORC mutant animals (Figure 3.6).

Role for Serine Proteases in Maintenance of Cardiac Function

To learn more about the mechanism by which dTORC maintains normal cardiac function, we performed gene expression profiling studies on mRNAs

from hearts of WT, KO and Rescue flies. This analysis revealed 30 genes that are 1.7 fold or more upregulated when comparing WT to KO samples and Rescue to KO samples (Table 3.1). To identify genes that are likely transcriptional targets of dTORC, we chose genes with CREB binding sites within three kilobases upstream of the transcription start site for further study.

The majority of the genes identified in our microarray analysis are of unknown function. However, gene ontology analysis revealed a strong enrichment of genes with serine protease activity (Figure 3.7). Two of the most strongly upregulated genes with CREB binding sites, CG31823 and CG31821, have predicted serine carboxypeptidase activity. Expression levels of both of these transcripts in WT, KO and Rescue hearts were validated by quantitative RT-PCR analysis (Figure 3.8A).

To determine whether the genes that are downregulated in dTORC mutant hearts and upregulated in Rescue hearts are directly modulated by dTORC, we made luciferase reporters using their promoters. Both the CG31823 and CG31821 reporters are responsive to cAMP elevation by forskolin (Figure 3.8B). Furthermore, expression of wild-type dTORC, and increasingly, a phosphorylation-defective, constitutively-active S157A-S294A dTORC greatly increase activity of these reporters in HEK293T cells (Figure 3.8B). Coexpression of the CREB dominant-negative polypeptide ACREB, or mutation of the CREB binding sites in the promoter, completely abolishes

reporter activity suggesting that these promoters are regulated by CREB and dTORC (Figure 3.8B).

3.4 Discussion

TORCs have been shown to maintain energy balance during fasting and to protect against oxidative stress (Dentin, Liu et al. 2007), (Koo, Flechner et al. 2005), (Wang, Goode et al. 2008). We were surprised to find that dTORC also plays a role in heart function. We found that flies deficient for dTORC protein have increased heart rates reminiscent of mammalian regular tachycardia. Tachycardia can be very deleterious to the heart because the increased heart rate leads to increased oxygen demand and excess work for the myocardium. dTORC mutant flies also exhibit smaller heart diameters which further results in less efficient pumping of hemolymph and more stress on the heart. The result of this increased stress is apparent when examining the integrity of the cardiac muscle fibers. dTORC mutant flies were found to have severe degeneration of the muscles of the heart tube.

The cardiac phenotypes observed in dTORC mutant animals could be completely reversed by expressing dTORC specifically in the cardiac tissue. It should be noted that unlike neuronal dTORC's ability to rescue starvation and oxidative stress sensitivity, expression of dTORC in neurons had no effect on any of the cardiac defects observed in mutants. Taken together, these data suggest that dTORC acts cell autonomously in the *Drosophila* heart.

Gene expression profiling revealed that dTORC is required for expression of a set of genes of mostly unknown functions. However, several of these genes are predicted to be serine-type proteases. Two genes of particular interest (CG31823 and CG31821) due to their high sensitivity to dTORC and presence of CREB binding sites in their promoters, are orthologs of a mammalian gene known as serine caboxypeptidase 1 (SCPEP1). CG31823 and CG31821 are 34% and 31% identical, respectively, to SCPEP1 at the primary amino acid sequence level, and the substrate binding domain and catalytic triad that characterizes the family are well conserved. SCPEP1 is most highly expressed in the kidney, heart and aorta in mammals (Lee, Streb et al. 2006) where it is believed to be involved, along with other serine carboxypeptidases Cathepsin-A (CathA) and vitellogenic-like carboxypeptidase (CPVL), in degradation of vascular peptides such as endothelin-1 (ET-1) (Pshezhetsky and Hinek 2009). This is of particular interest to the present study because ET-1 and CathA have well established roles in the pathogenesis of cardiovascular diseases (Yanagisawa and Masaki 1989), (Kyllerman, Mansson et al. 1993), (Nordborg, Kyllerman et al. 1997). CathA has also been shown to be involved in the assembly of elastin fibers on the extracellular microfibrillar scaffold (Hinek, Pshezhetsky et al. 2006). We have seen that pericardin, an elastin-like molecule that surrounds the *Drosophila* heart, appears disorganized in dTORC mutant flies (Figure 3.S1). Immunoblotting pericardin reveals higher levels in the dTORC mutant flies

which may represent protein trapped in endosomes due to decreased expression of serine carboxypeptidases (Figure 3.S1). A recent study has also shown that mice lacking SCPEP1 are deficient in vascular remodeling and smooth muscle cell proliferation (Lee, Chen et al. 2009). Future studies should reveal whether *Drosophila* CG31823 and CG31821 are functional homologs of these mammalian serine carboxypeptidases.

3.5 Materials and Methods

Generation and Maintenance of Fly Stocks

All *Drosophila melanogaster* lines were maintained on Cornmeal, Molasses and Yeast Medium at 25°C or room temperature. The 24B-Gal4, Hand-Gal4 and Tin-Gal4 lines were all obtained from Rolf Bodmer. TORC null mutant and UAS-TORC flies were generated as previously reported (Wang, Goode et al. 2008). Rescue experiments were carried out by crossing UAS-TORC;$TORC^{25\text{-}3}$ flies to Gal4; $TORC^{25\text{-}3}$ flies.

Recording of *Drosophila* Heart Activity

Age matched adult *Drosophila* were anesthetized with FlyNap (Carolina Biological Supply Company) and secured dorsal-side down in petroleum jelly. Hearts were prepared for imaging by removing the legs and head and cutting the ventral cuticle of the fly. All internal viscera except the heart was removed and fat was suctioned off with a pulled glass capillary attached to a vacuum source. Dissections were done while flies were bathed in an oxygenated, adult

artificial hemolymph solution (108 mM $NaCl_2$, 5 mM KCl, 2 mM $CaCl_2$, 8 mM $MgCl_2$,1 mM NaH_2PO_4, 4 mM $NaHCO_3$, 15 mM HEPES, 10 mM sucrose, and 5 mM trehalose, at pH 7.1). Recordings of heart activity were acquired at room temperature using a Hamamatsu EM-CCD digital camera (McBain Instruments) mounted on a Leica DM-LFSA microscope with a 10× water immersion lens (McBain Instruments) and Simple PCI image capture software (Compix Imaging System).

Analysis of Heart Recordings

Videos of beating *Drosophila* hearts were analyzed with a custom software package developed in Matlab by the Giles and Bodmer labs (Fink, Callol-Massot et al. 2009). Briefly: a combination of two algorithms is used to detect movement of the heart edges. The first algorithm measures changes in average light intensity for each frame as frame brightness tends to decrease with contraction. The second algorithm tracks changes in individual pixel intensities from frame to frame. This allows detection of areas of movement as dark pixels “move” across the lighter background. Systolic interval, diastolic interval, heart period, etc. can be determined from these movements. Systolic and diastolic diameters are measured by manually locating the heart edges during contraction and relaxation respectively.

Anitbodies, Immunohistochemistry and Western Blotting

Whole flies or dissected tissues were crushed in lysis buffer (50 mM Tris-HCl (pH 7.5), 100 mM NaCl, 50 mM NaF, 5 mM EDTA, 1% Triton X-100, and 1X protease inhibitors) with a blue plastic pestle in a tight fitting tube. Lysates were centrifuged at 18,000 x g for 10 minutes and supernatants were reserved for SDS-PAGE analysis. Hearts were prepared for immunostaining as described for recording activity and then treated with 10mM EGTA and 4% paraformaldehyde to fix. Fixed hearts were left in the abdomens and washed with PBSTx (phosphate-buffered saline, 0.1% Triton X-100). Dissected abdomens were incubated with primary antibodies diluted in PBTx for 2 hours at room temperature or overnight at 4 degrees C and then washed in PBTx and incubated in secondary antibodies diluted in PBTx. After washing in PBTx, abdomens were trimmed to allow full view of fixed hearts and mounted on glass slides in Vectashield + DAPI (Vector Laboratories). Images were collected on an Axiovision Z1 fitted with an ApoTome (Zeiss). Primary Antibodies used were alpha-actinin at 1:100 (J. Saide), Neuromancer at 1:50 (R. Bodmer), Dystroglycan at 1:1000 (A. Wodarz), Zfh1 at 1:1000 (R. Bodmer), dMEF2 at 1:2000 (E. Olson), Svp at 1:200 (R Cripps), Heat-shock protein 70 at 1:10,000 (Sigma-Aldrich) and dTORC which were raised in rabbits against a synthetic TORC peptide (GRSVGVGPMRRPSERK). Sera were collected and purified using a peptide affinity resin. Secondary antibodies used were Goat anti-rabbit-HRP at 1:10,000 (Bio Rad), Goat anti-mouse-HRP at 1:10,000 (Bio Rad), Alexa Fluor 488 goat anti-mouse at 1:500 (Invitrogen),

Alexa Fluor 568 donkey anti-rabbit at 1:500 (Invitrogen), Cy5 goat anti-guinea pig at 1:500 (Abcam). Phalloidin-TRITC was at used at 1 μM to stain polymerized actin.

Electrical Pacing Stress Assays

Pacing assays are carried out on glass slides onto which copper wires have been soldered on either side, and then covered in aluminum foil (Wessells and Bodmer 2004). Conductive electrode jelly is spread on each strip of aluminum foil, leaving a space of about 2 mm between the lines of jelly. Adult flies are anesthetized with FlyNap (Carolina Biological Supply) and positioned dorsal side up so that their head is in one side of the jelly and the tip of their abdomen is in the other. Therefore the fly acts as an electrical bridge between the two electrodes. The copper wires are then attached to leads from a square wave stimulator. Hearts are paced at 40 V and 6 Hz for 30 s and monitored with a dissecting microscope. Heart failure rate is defined as the percentage of flies that fail to recover from cardiac arrest or fibrillation after 2 min.

Microarrays

Total RNA was isolated with TRIzol (Invitrogen) from 30 dissected hearts from of one week old Hand-Gal4;+/+ (WT), Hand-Gal4;dTORC$^{25\text{-}3}$ (KO), and Hand-Gal4/UAS-dTORC;dTORC$^{25\text{-}3}$ (Rescue) flies**.** RNA was further purified using the RNA Clean & Concentrator kit (Zymo Research) and then

reverse transcribed and amplified with the Ovation RNA Amplification kit (NuGEN) by following the manufacturer's instructions. Amplified cDNA was then fragmented and labeled using the FL-Ovation cDNA Biotin Module V2 (NuGEN) and prepared for hybridization using the Hybridization Wash Stain kit (Affymetrix) according to the manufacturer's instructions. Samples were hybridized to GeneChip *Drosophila* Genome 2.0 Arrays (Affymetrix). All experiments were performed in duplicate. Arrays were analyzed with Expression Console software (Affymetrix).

Gene Ontology Analysis

Gene lists were ranked by fold expression of Rescue/WT samples and WT/KO samples and analyzed for enriched gene ontology (GO) terms using the GOrilla gene ontology tool (Eden, Navon et al. 2009).

qPCR Measurement

Fly hearts were collected and RNA was extracted using TRIzol (Invitrogen). Total RNA was reverse-transcribed by Superscript II transcriptase (Invitrogen) and the generated cDNA used for real time PCR (Roche LightCycler 480 Real-Time PCR system, SYBRGreen), using 2 ng of cDNA template and a primer concentration of 400 nM. Values were normalized to rp49.

Cell Culture, Transfection and Luciferase Assays

HEK293T cells were maintained in Dulbecco's Modified Eagle's Medium (DMEM) with 10% fetal calf serum and 1% Penicillin/Streptinomycin and passaged every third day as described previously (Ravnskjaer, Kester et al. 2007). Transfections were carried out with Lipofectamine 2000 (Invitrogen) according to the manufacturer's instructions. Twenty-four hours after transfection, cells were treated with forskolin (10 μM) or vehicle (DMSO) for four hours. Cells were then lysed and and supernatants were reserved to perform luciferase and Beta-galactosidase assays as described previously (Conkright, Guzman et al. 2003).

3.6 Figures

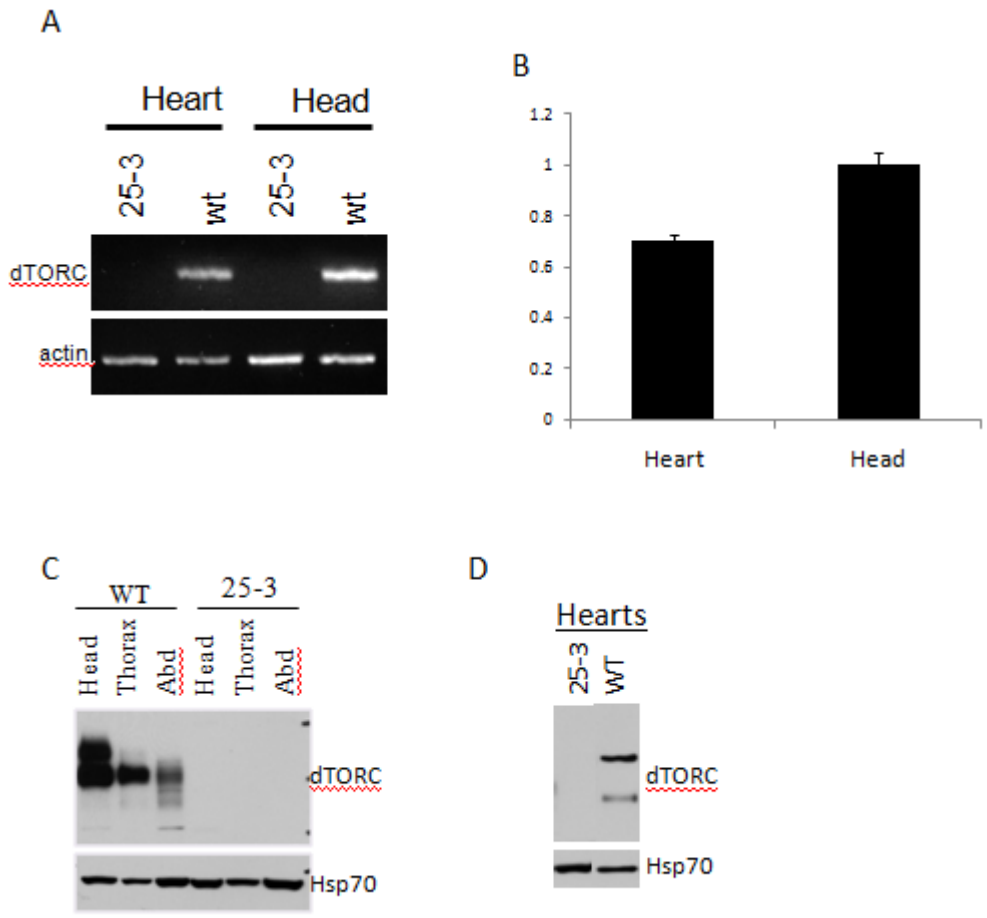

Figure 3.1. *Drosophila* TORC is Expressed in the Heart

A. RT-PCR analysis of total RNA isolated from heart or head tissue from wild-type (wt) or dTORC mutant (25-3) flies. B. Quantification of amount of RNA in Heart tissue relative to Head, normalized to actin expression. C. Immunoblot of dTORC protein showing relative expression levels in the three main body compartments of wild-type(wt) or dTORC mutant (25-3) flies. D. Immunoblot of dTORC protein in isolated hearts from wild-type or dTORC mutant (25-3) flies. Heat-shock protein 70 (Hsp70) is shown for total protein loading control.

Figure 3.2. dTORC Mutant Flies Exhibit Cardiac Dysfunction

A. Representative screenshot of the custom Optical Heartbeat Analysis software package that is used to analyze recordings of beating *Drosophila* hearts. Screenshot shows contraction prediction by the Frame Brightness algorithm (top), and the Pixel Movement algorithm (middle) mapped onto a one pixel wide slice of the movie for each frame known as an M-mode (bottom). B. Representative M-modes for wild-type and knockout hearts at both the anterior and posterior third abdominal segment showing severe constriction in the knockout hearts. C. Mean heart period for wild-type (WT) and TORC mutant flies (25-3) at one, two and three weeks of age showing normal slowing of heart rate with age. D. Diastolic and Systolic heart diameters for male and female, wild type and knockout flies at one, two, and three weeks of age. E. Top: Heart rate for wild type and dTORC mutant flies at one, two and three weeks of age. Bottom Left: Time spent in diastole (diastolic interval) for wild-type and dTORC mutant (KO) flies at one, two and three weeks of age. Bottom Right: Time spent in systole (systolic interval) for wild-type and dTORC mutant (KO) flies at one, two and three weeks of age. Error bars indicate S.E.M. Significance claimed for all pair wise comparisons indicates t-test < 0.05. One-way ANOVA with Dunnet's post test was used for all mutliple comparisons.

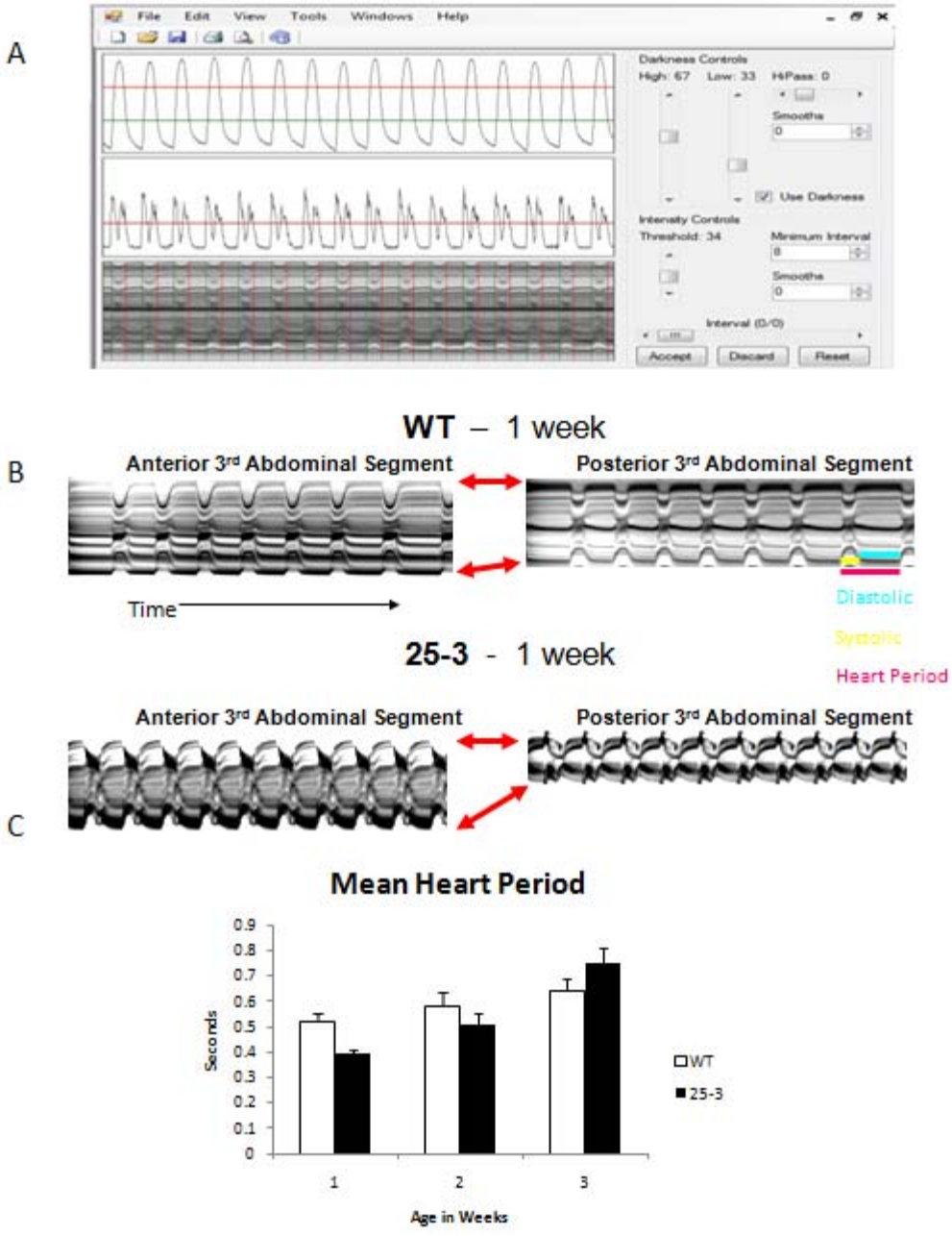
A
File Edit View Tools Windows Help
Darkness Controls
High: 67 Low: 33 HiPass: 0
Smooths
Use Darkness
Intensity Controls
Threshold: 34
Minimum Interval
Smooths
Interval (D/D)
Accept
Discard
Reset
B
WT – 1 week
Anterior 3rd Abdominal Segment
Posterior 3rd Abdominal Segment
Time
Diastolic
Systolic
Heart Period
25-3 - 1 week
Anterior 3rd Abdominal Segment
Posterior 3rd Abdominal Segment
C
Mean Heart Period
Seconds
0.9
0.8
0.7
0.6
0.5
0.4
0.3
0.2
0.1
0
1
2
3
Age in Weeks
WT
25-3

Figure 3.2

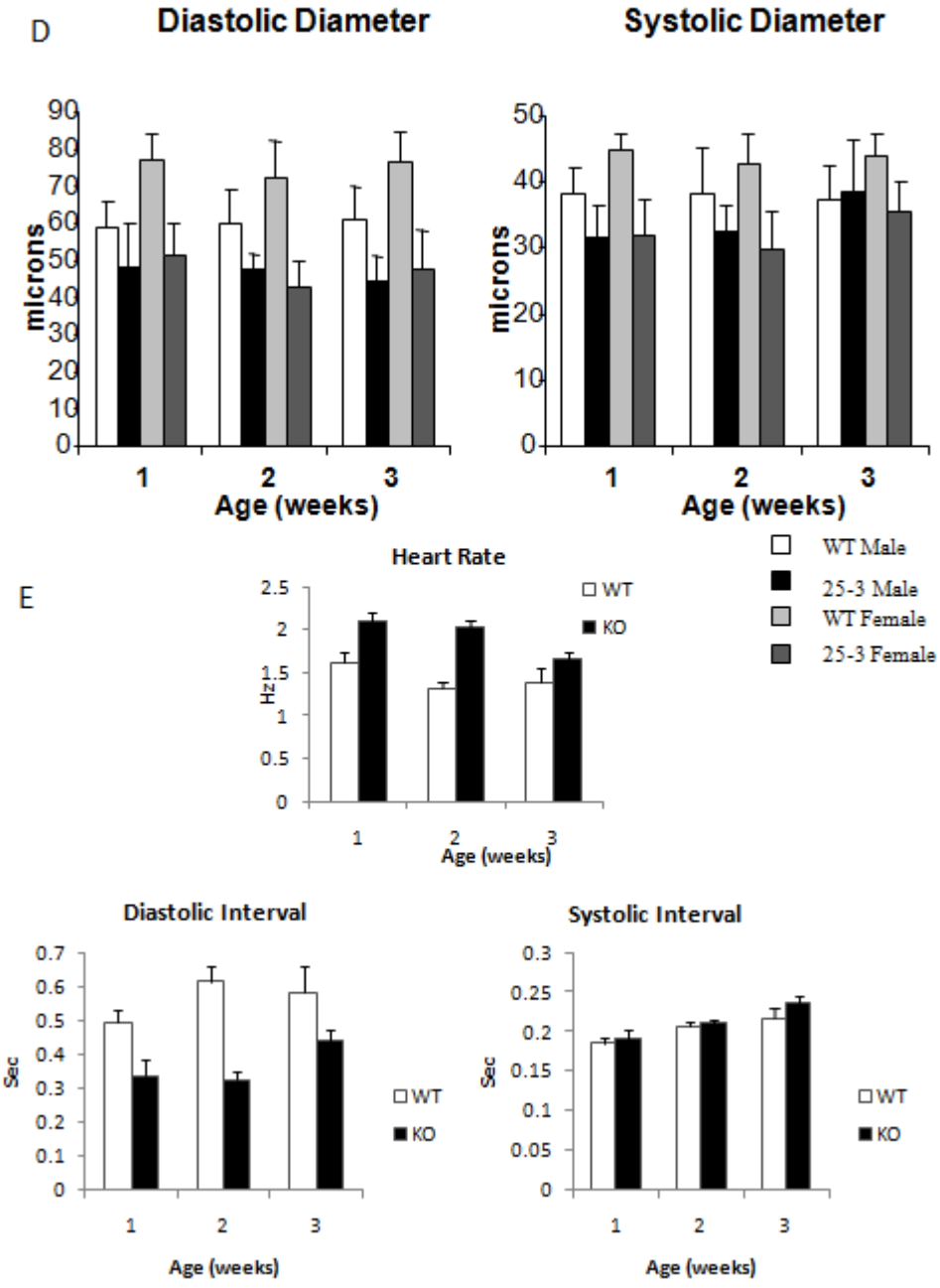

Figure 3.2 (cont.)

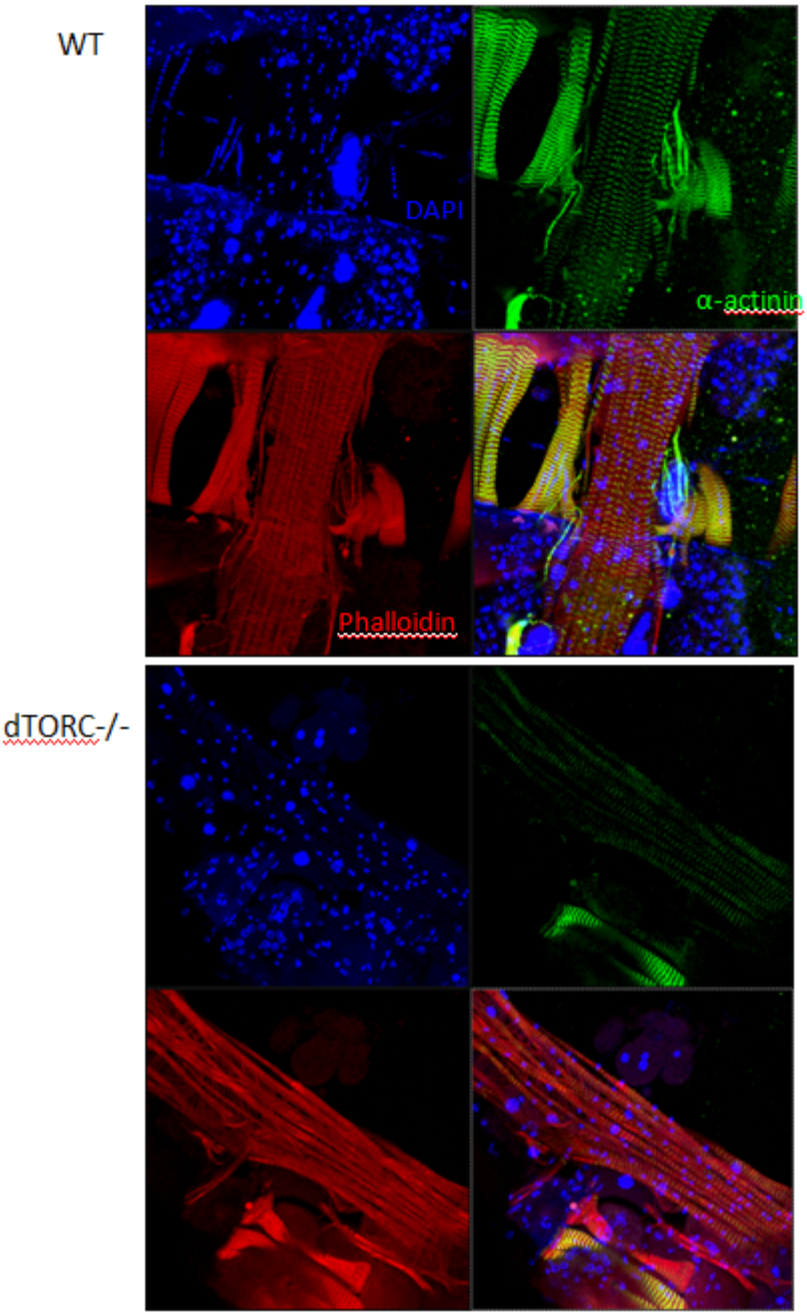

Figure 3.3. dTORC Mutant Flies Display Cardiac Muscle Degeneration

Wild-type (top) and dTORC knockout (bottom) hearts stained with phalloidin (red) to show polymerized actin, alpha-actinin (green) which marks sarcomeric Z-lines, and DAPI to show nuclei.

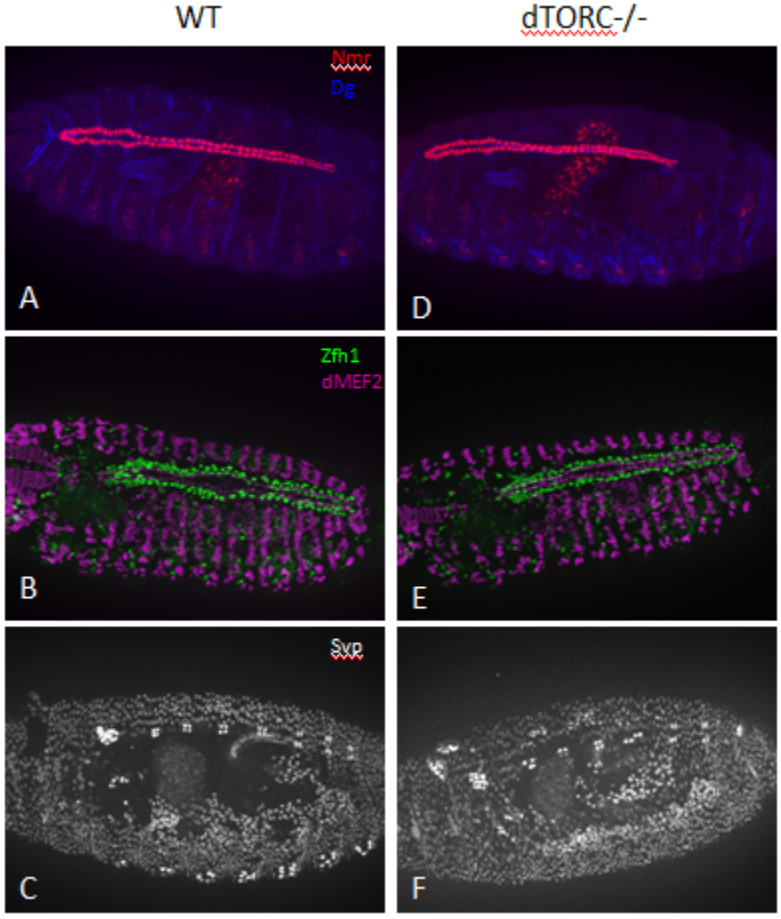

Figure 3.4. dTORC Cardiac Phenotype is not Developmental

All panels show stage 17 embryos with anterior to the right. A,D. Wild-type and dTORC mutant embryos stained for Neuromancer (Nmr) which labels cardioblast nuclei (red), and dystroglycan (Dg) which labels the basal domain of epithelial cells (blue). B,E. Zfh1(green) labels the nuclei of pericardial cells and dMEF2 (purple) stains all muscle nuclei. C,F. Svp labels a subset pericardial cells as well as many other cells throughout the developing embryo. All panels show normal cardiac developmental morphology.

Figure 3.5. Expression of dTORC in the Heart Reverses Cardiac Dysfunction in dTORC Mutant Flies

A. Western blot of dTORC in abdomens of one week old Hand-Gal4;+/+ (WT), Hand-Gal4;dTORC$^{25\text{-}3}$ (KO), and Hand-Gal4/UAS-dTORC;dTORC$^{25\text{-}3}$ (Rescue) flies. B. Mean diastolic and systolic diameters of one week old Hand-Gal4;+/+ (WT), Hand-Gal4;dTORC$^{25\text{-}3}$ (KO), and Hand-Gal4/UAS-dTORC;dTORC$^{25\text{-}3}$ (Rescue) flies. C. Mean heart rates, diastolic and systolic intervals of one week old Hand-Gal4;+/+ (WT), Hand-Gal4;dTORC$^{25\text{-}3}$ (KO), and Hand-Gal4/UAS-dTORC;dTORC$^{25\text{-}3}$ (Rescue) flies D. Percentage of one week old Hand-Gal4;+/+ (WT), Hand-Gal4;dTORC$^{25\text{-}3}$ (KO), and Hand-Gal4/UAS-dTORC;dTORC$^{25\text{-}3}$ (Rescue) flies showing heart failure after electrical pacing at 6 Hz for 30 seconds. Error bars indicate S.E.M. One-way ANOVA with Dunnet's post test ($p<0.05$) was used for all mutliple comparisons.

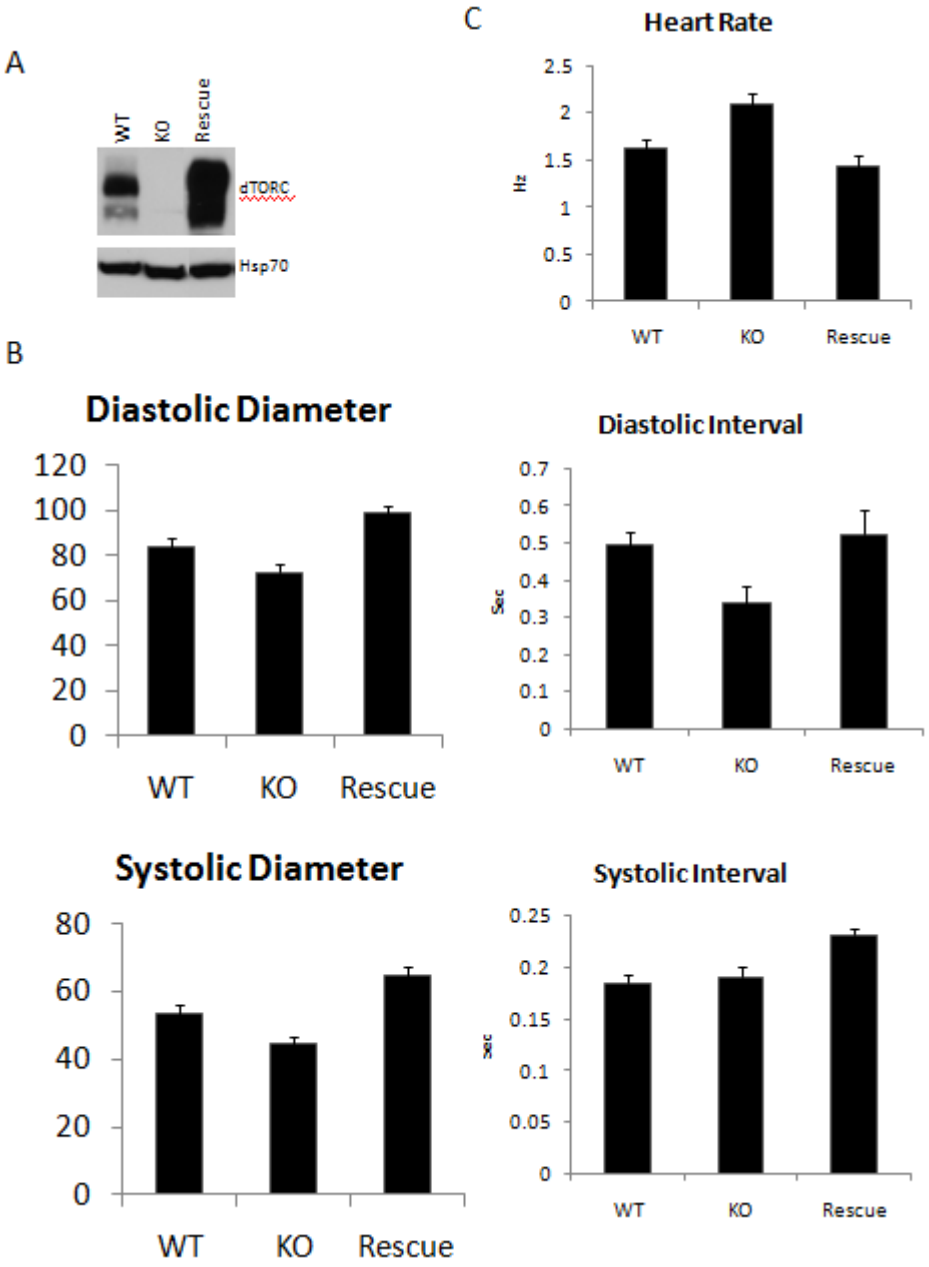
A
WT
KO
Rescue
dTORC
Hsp70
C
Heart Rate
Hz
2.5
2
1.5
1
0.5
0
WT
KO
Rescue
B
Diastolic Diameter
120
100
80
60
40
20
0
WT
KO
Rescue
Diastolic Interval
Sec
0.7
0.6
0.5
0.4
0.3
0.2
0.1
0
WT
KO
Rescue
Systolic Diameter
80
60
40
20
0
WT
KO
Rescue
Systolic Interval
Sec
0.25
0.2
0.15
0.1
0.05
0
WT
KO
Rescue

Figure 3.5

D

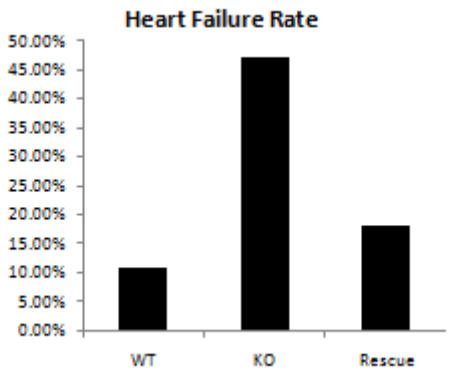

Figure 3.5 (cont.)

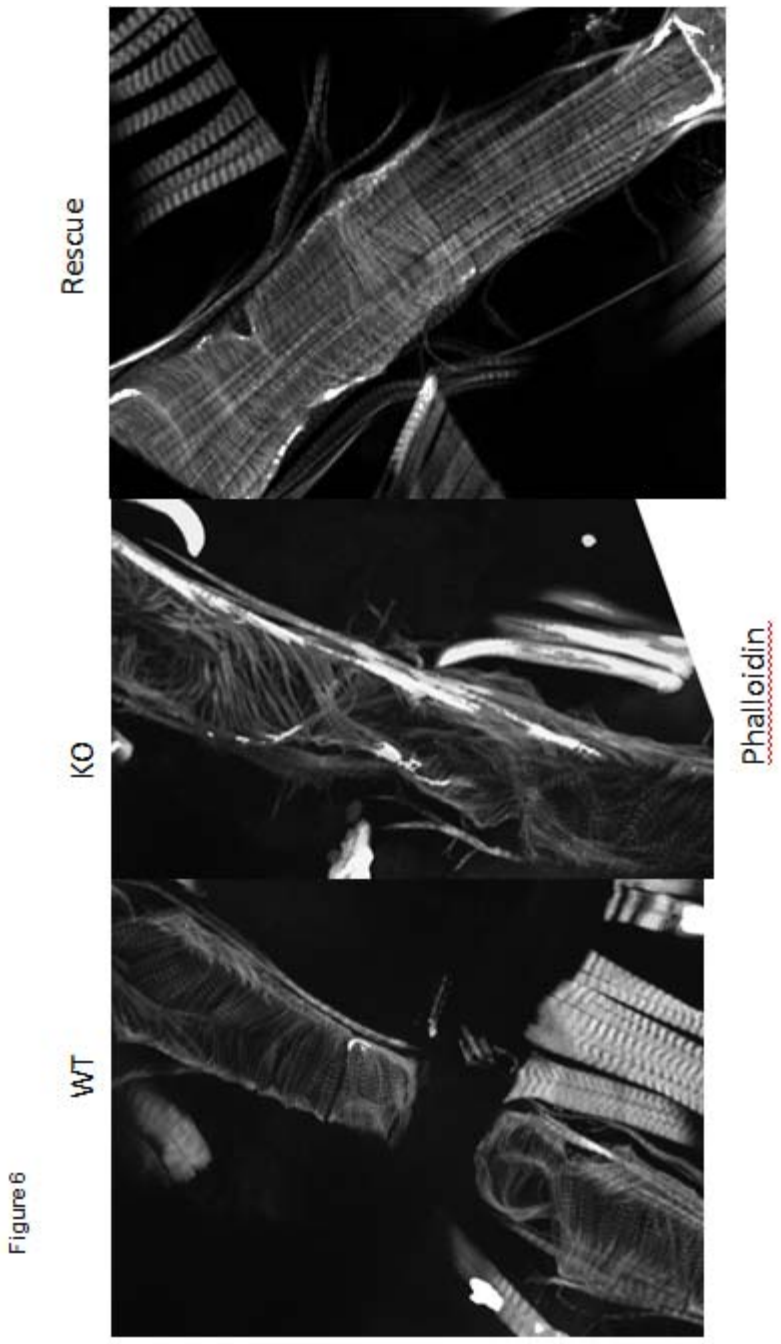

Figure 3.6. Expression of dTORC in the Heart Rescues Cardiac Muscle Degeneration

Phalloidin staining of one week old Hand-Gal4;+/+ (WT), Hand-Gal4;dTORC$^{25-3}$ (KO), and Hand-Gal4/UAS-dTORC;dTORC$^{25-3}$ (Rescue) flies showing muscle fiber structure in the third to fourth abdominal segment.

Figure 3.7. Role for Serine Proteases in dTORC Mutant Cardiac Phenotype

Gene ontology analysis showing strong enrichment of serine proteases in list of genes whose expression are downregulated in Hand-Gal4;dTORC$^{25\text{-}3}$ (KO)flies and upregulated in Hand-Gal4/UAS-dTORC;dTORC$^{25\text{-}3}$ (Rescue).

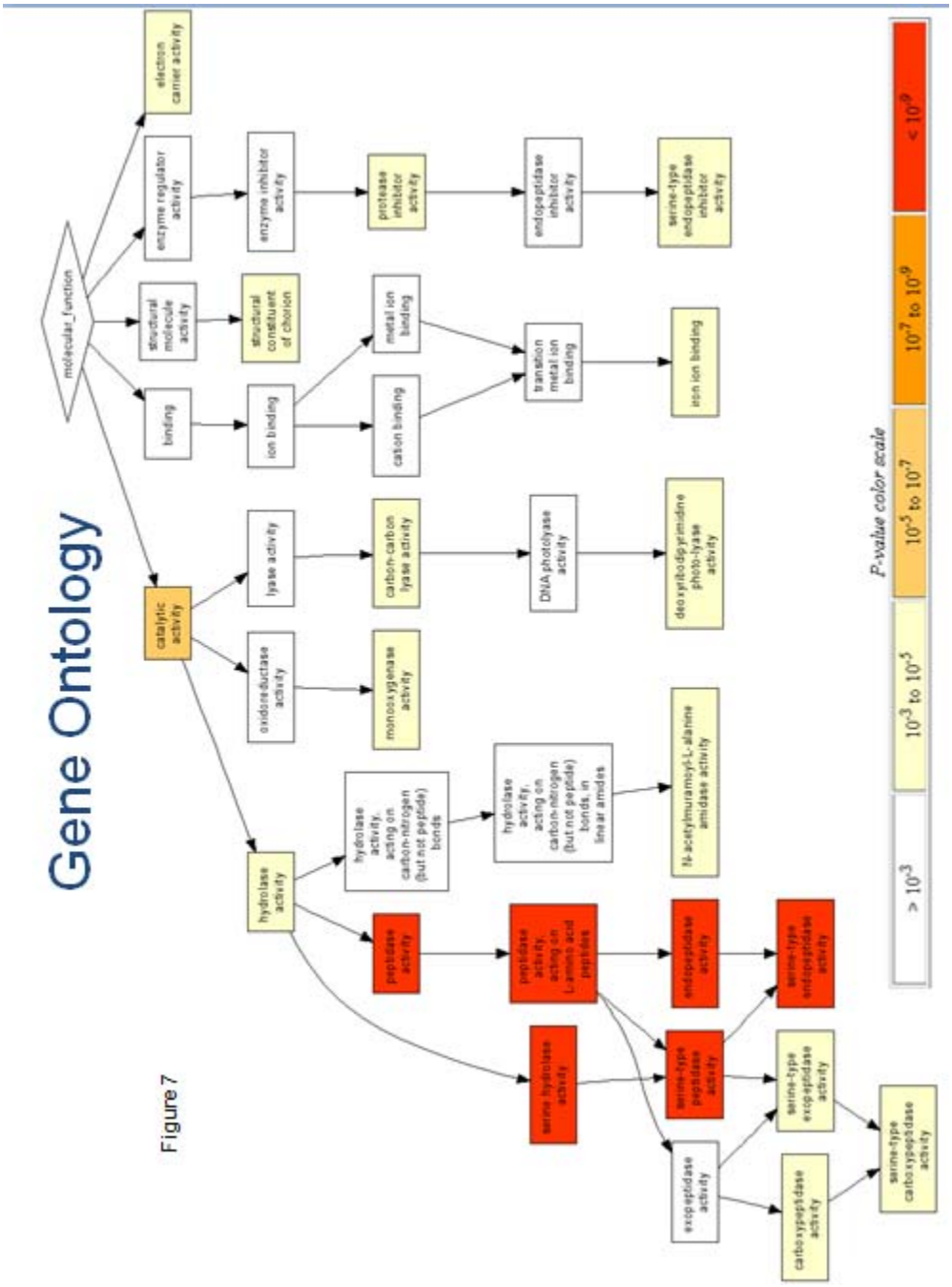
Gene Ontology
molecular_function
electron carrier activity
enzyme regulator activity
enzyme inhibitor activity
protease inhibitor activity
endopeptidase inhibitor activity
serine-type endopeptidase inhibitor activity
structural molecule activity
structural constituent of chorion
binding
ion binding
metal ion binding
cation binding
transition metal ion binding
iron ion binding
catalytic activity
lyase activity
carbon-carbon lyase activity
DNA photolyase activity
deoxyribodipyrimidine photo-lyase activity
oxidoreductase activity
monooxygenase activity
hydrolase activity
hydrolase activity, acting on carbon-nitrogen (but not peptide) bonds
hydrolase activity, acting on carbon-nitrogen (but not peptide) bonds, in linear amides
N-acetylmuramoyl-L-alanine amidase activity
peptidase activity
peptidase activity, acting on L-amino acid peptides
endopeptidase activity
serine-type endopeptidase activity
serine hydrolase activity
serine-type peptidase activity
exopeptidase activity
serine-type exopeptidase activity
carboxypeptidase activity
serine-type carboxypeptidase activity
P-value color scale
> 10^-3
10^-3 to 10^-5
10^-5 to 10^-7
10^-7 to 10^-9
< 10^-9

Figure 7

Figure 3.8. CREB/dTORC Drives Expression of a Pair of Serine Carboxypeptidases in the *Drosophila* Heart.

A. qPCR analysis of CG31823, CG31821, and dTORC gene expression in hearts of one week old Hand-Gal4;+/+ (WT), Hand-Gal4;dTORC$^{25\text{-}3}$ (KO), and Hand-Gal4/UAS-dTORC;dTORC$^{25\text{-}3}$ (Rescue) flies. B. Top: Effect of wild-type (dTORC) or constitutively active (S157A-S294A) dTORC on CG31823 or CG31821 promoter-luciferase reporter constructs in HEK293T cells. Effects of forskolin (FSK) and the dominant negative CREB inhibitor ACREB is also shown. Bottom: Effect on luciferase reporter activity of mutating the two cAMP Response Elements in the CG31823 promoter-luciferase construct.

A

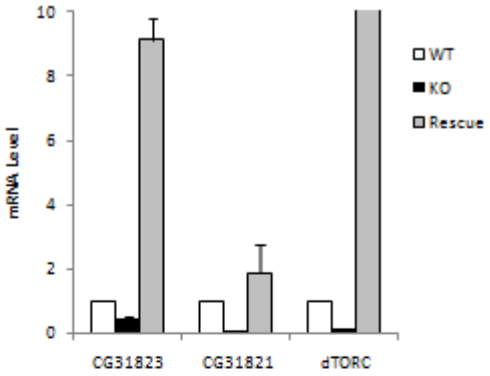
10
8
6
4
2
0
mRNA Level
WT
KO
Rescue
CG31823
CG31821
dTORC

B

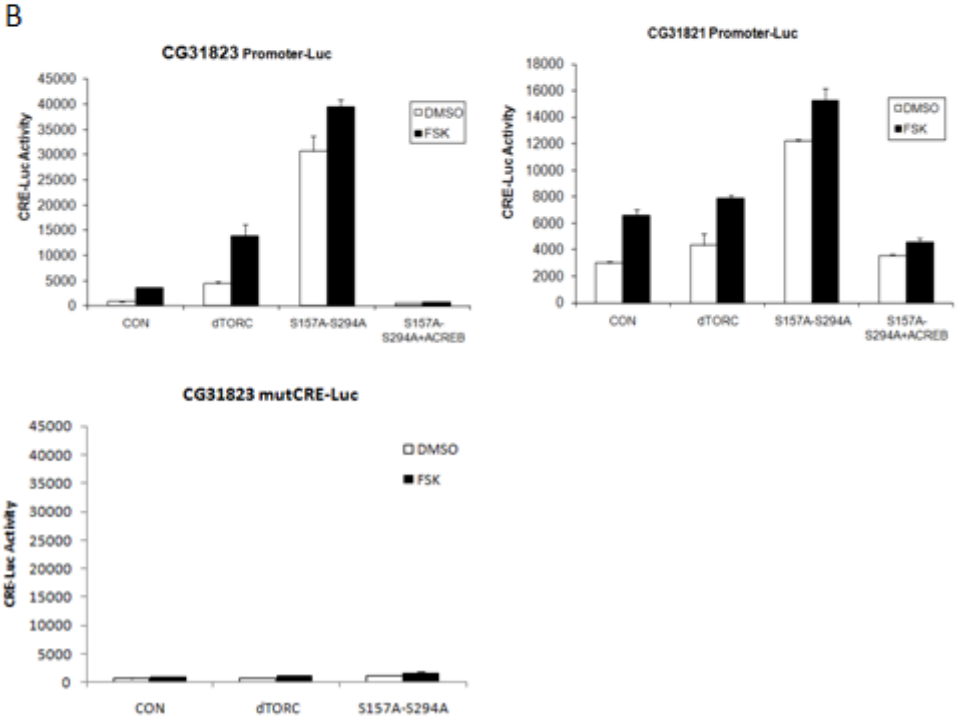
CG31823 Promoter-Luc
CRE-Luc Activity
DMSO
FSK
CON
dTORC
S157A-S294A
S157A-S294A+ACREB
CG31821 Promoter-Luc
CRE-Luc Activity
DMSO
FSK
CON
dTORC
S157A-S294A
S157A-S294A+ACREB
CG31823 mutCRE-Luc
CRE-Luc Activity
DMSO
FSK
CON
dTORC
S157A-S294A

Table 3.1. List of Genes That are Downregulated in dTORC Mutant Flies and Rescued by Reintroduction of dTORC in the Heart
Table lists genes that are at least 1.7 fold upregulated when comparing WT to KO samples and Rescue to KO samples in both replicates. The column labeled CRE indicates a conserved cAMP Response Elements within 3 kilobases of the transcription start site.

Gene Title	Gene Symbol	CRE	Family Description
Odorant-binding protein 46a	Obp46a	Yes	UNKNOWN
CG18853 /// photolyase	CG18853 /// phr	No	DEOXYRIBODIPYRIMIDINE PHOTO LYASE EC_4.1.99.3 DNA PHOTOLYASE PHOTOREACTIVATING ENZYME
CG31823	CG31823	Yes	RETINOID INDUCIBLE SERINE CARBOXYPEPTIDASE PRECURSOR EC_3.4.16.- SERINE CARBOXYPEPTIDASE 1
photolyase	phr	No	DEOXYRIBODIPYRIMIDINE PHOTO LYASE EC_4.1.99.3 DNA PHOTOLYASE PHOTOREACTIVATING ENZYME
CG11170	CG11170	Yes	AMBIGUOUS
CG9616	CG9616	Yes	AMBIGUOUS
CG31821	CG31821	Yes	RETINOID INDUCIBLE SERINE CARBOXYPEPTIDASE PRECURSOR EC_3.4.16.- SERINE CARBOXYPEPTIDASE 1
Ornithine decarboxylase 2	Odc2	Yes	ORNITHINE DECARBOXYLASE EC_4.1.1.17 ODC
CG30090	CG30090	Yes	PRECURSOR
maltase	LvpH	Yes	MALTASE PRECURSOR EC_3.2.1.20

Table 3.1 cont.

Gene Title	Gene Symbol	CRE	Family Description
CG18477 /// CG31780	CG18477 /// CG31780	Yes	SERINE PROTEINASE STUBBLE EC_3.4.21.- STUBBLE STUBBLOID [CONTAINS: SERINE PROTEINASE STUBBLE NON CATALYTIC CHAIN; SERINE PROTEINASE STUBBLE CATALYTIC CHAIN]
yellow-d	yellow-d	Yes	PRECURSOR
CG1583	GIIIspla2	Yes	PHOSPHOLIPASE A2 EC_3.1.1.4 PHOSPHATIDYLCHOLINE 2 ACYLHYDROLASE
aldose 1-epimerase /// CG32444	CG32444 /// DsimCG32444	Yes	ALDOSE 1 EPIMERASE EC_5.1.3.3 GALACTOSE MUTAROTASE
CG30360	CG30360	Yes	MALTASE PRECURSOR EC_3.2.1.20
CG12512	CG12512	Yes	AMBIGUOUS
CG4537	CG4537	Yes	FK506 BINDING EC_5.2.1.8 PEPTIDYL PROLYL CIS TRANS ISOMERASE PPIASE ROTAMASE KDA FKBP FKBP 12 IMMUNOPHILIN FKBP12
CG3604	CG3604	Yes	TISSUE FACTOR PATHWAY INHIBITOR PRECURSOR TFPI
CG11236 /// CG11236	CG11236 /// DsimCG11236	Yes	D AMINO ACID OXIDASE EC_1.4.3.3 DAMOX DAO DAAO
Borealin	borr	Yes	BOREALIN BOREALIN RELATED
CG3513	CG3513	No	TISSUE FACTOR PATHWAY INHIBITOR PRECURSOR TFPI
CG12112	CG12112	Yes	AMBIGUOUS
CG4408	CG4408	Yes	CARBOXYPEPTIDASE PRECURSOR
CG6164	CG6164	Yes	UNKNOWN
CG15358	CG15358	No	ACCESSORY GLAND ACP29AB PRECURSOR

Table 3.1 cont.

Gene Title	Gene Symbol	CRE	Family Description
CG5999	CG5999	Yes	UDP GLUCURONOSYLTRANSFERASE PRECURSOR EC_2.4.1.17 UDPGT
CG7730	CG7730	No	AMBIGUOUS

Video 3.1. dTORC Mutant Flies Show Cardiac Constriction and Increased Heart Rate

A. Video of wild-type, one week old adult *Drosophila* heart. B. dTORC mutant, one week old adult *Drosophila* heart.

Video 3.2. Cardiac dTORC Expression Rescues Increased Heart Rate and Decreased Heart Size

A. Video of Hand-Gal4;dTORC$^{25\text{-}3}$ (KO) adult *Drosophila* heart at one week old. B. Hand-Gal4/UAS-dTORC;dTORC$^{25\text{-}3}$ (Rescue) adult *Drosophila* heart at one week old.

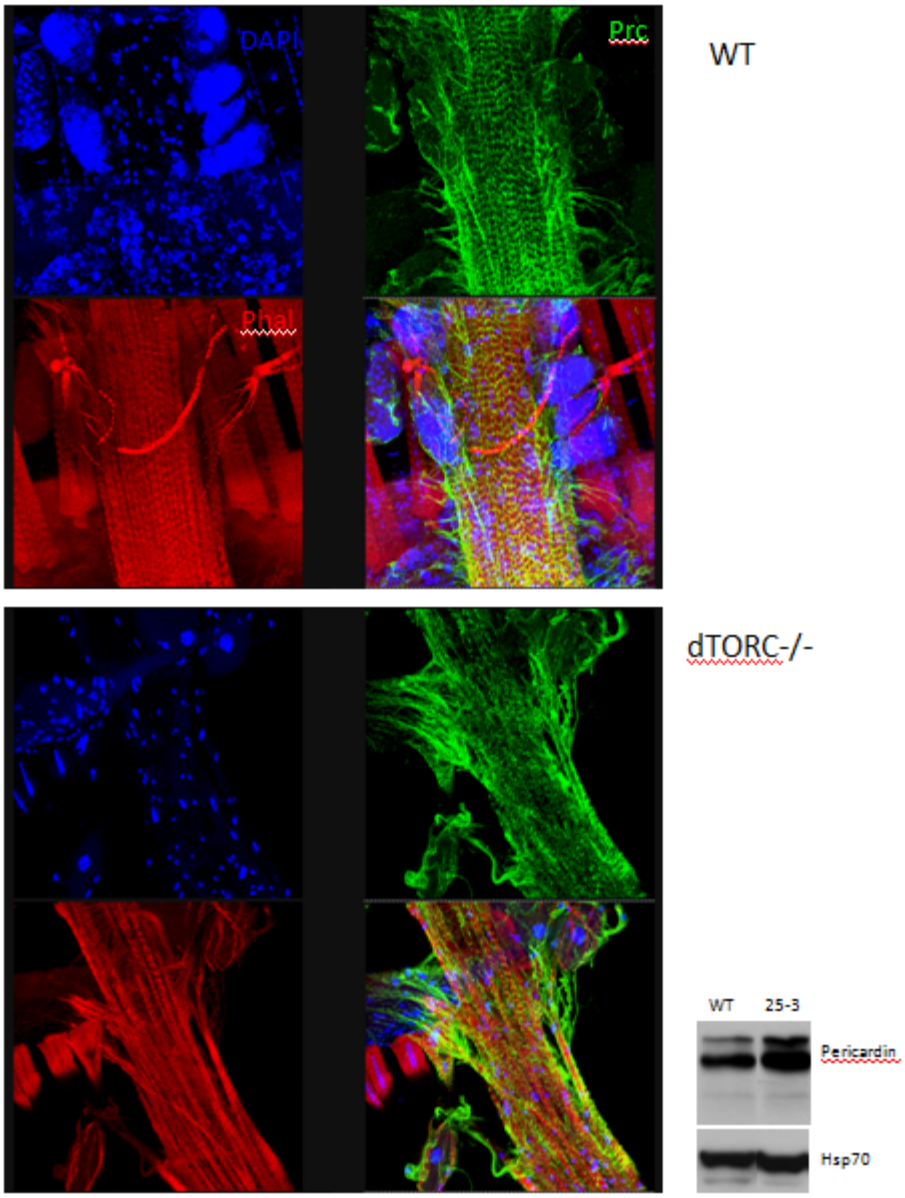

Figure 3.S1. Pericardin Matrix is Disorganized in dTORC Mutant Flies

Wild-type (top) and dTORC knockout (bottom) hearts stained with Pericardin (green) which is an elastin-like molecule that surrounds the heart, phalloidin (red) which stains polymerized actin to show myofibrillar structure, and DAPI(blue) to show nuclei. An immunoblot (lower right) shows expression levels of Pericardin in wild-type (WT) and dTORC mutant (25-3) flies.

CHAPTER 4 Discussion

4.1 TORC in Metabolic Control

This work represents the first study of a completely TORC null organism. *Drosophila* TORC (dTORC) is highly similar to its mammalian counterparts in several key regulatory domains, including the CREB binding domain, transactivation domain, calcineurin binding domain, and two regulatory phosphorylation sites. Not surprisingly, our work showed that dTORC is regulated in much the same way as mammalian TORCs.

TORCs are sequestered in the cytoplasm via a phosphorylation-dependent interaction with 14-3-3 proteins and translocate to the nucleus, where they coactivate transcription of CREB target genes, following dephosphorylation in response to the second messengers, cAMP and calcium. TORC mutant flies are very sensitive to starvation and have severely reduced glycogen and lipid stores. Work done in mammals has revealed that TORC2 plays an important role in regulating gluconeogenesis in the liver. Surprisingly, we found that the metabolic phenotypes observed in flies were not due to TORC function in the fat body, which is the functional equivalent of the liver and fat tissue in the fly. In fact, expression of dTORC exclusively in the fat body tends to reduce lipid stores, which would be predicted to exacerbate the starvation sensitivity phenotype. It should be noted, that a second tissue in flies, the oenocytes, have been ascribed hepatocyte-like functions (Gutierrez,

Wiggins et al. 2007). In fasting conditions, oenocytes uptake lipids released from the fat body and process them for energy. Additionally, oenocytes express the microsomal lipid ω hydrolase, Cyp4g1, which we found to be downregulated in the heads of dTORC mutant flies. While we did not examine the role of dTORC in this tissue, it is unlikely that the metabolic phenotype of dTORC mutants can be attributed to aberrant oenocyte function. The primary role of oenocytes appears to be metabolizing fat; a process which is entirely functional in dTORC mutant flies. Nevertheless, the role of dTORC in this tissue should be examined, given its hepatocyte-like function.

We found that dTORC is expressed most strongly in the fly brain, and that neuronal expression of a dTORC transgene could fully rescue the starvation sensitivity of the mutant. The fly brain contains a set of neuroendocrine cells responsible for producing insulin, the insulin-producing cells or IPCs. The brain is closely apposed to a compound neuroendocrine organ that produces adipokinetic hormone (AKH), the fly equivalent of mammalian glucagon. One possible mechanism for the neuronal role of dTORC in regulating energy stores, would be through affecting the production of insulin-like peptides or AKH. However, we found that expression of insulin-like peptides in dTORC mutant flies is largely unchanged. Additionally, ablation of the insulin-producing cells does not affect the starvation sensitivity of dTORC mutant or wild-type flies. Arguing against the role of dTORC in regulating AKH production, we found that expression of a dTORC transgene

specifically in the AKH producing cells is unable to rescue the metabolic phenotypes observed in dTORC mutant flies.

So how might neuronal dTORC regulate metabolic stress resistance? One possibility is through the regulation of other neuropeptides. In *Drosophila*, there are at lease thirty genes that encode neuropeptide precursors (Nassel 2002). Neuropeptides can act locally as neuromodulators in the central nervous system, or act at a distance as circulating hormones. In some cases, the same peptide will exhibit both behaviors. dTORC mutant flies may be deficient in one or several of these neuropeptides, which could lead to dysregulation of peripheral metabolic tissues (such as the fat body). While we did not identify any obvious candidate neuropeptides in our gene expression studies, we also cannot rule out their misexpression in dTORC mutant flies. Many of the annotated neuropeptide precursors were below the detection threshold on our GeneChips. This is not surprising, given that some neuropeptides are expressed in as few as two neurons in the *Drosophila* brain (Nassel 2002). Still, some neuropeptides that were detected on the microarrays (e.g. pigment-dispersing factor, PDF), showed reduced expression in dTORC mutant flies, but were excluded by our strict criteria for selecting potential dTORC target genes. Neuropeptide F, the putative insect ortholog of mammalian neuropeptide Y, was found by quantitative PCR, to be downregulated in our dTORC mutant flies. Additionally, the NPF promoter contains CRE binding sites and can be activated by cAMP and dTORC in

reporter assays. The possibility that NPF is regulated by dTORC is interesting because neuronal mouse TORC1 was shown to regulate Cartpt, a peptide that completely blocks the feeding response induced by NPY. Indeed, TORC1 mutant mice are hyperphagic and become obese, due to leptin insensitivity. NPF has also been shown to positively regulate feeding in *Drosophila* (Wu, Wen et al. 2003). However, if down regulation of NPF is contributing to the metabolic phenotype in dTORC mutants, it is likely acting through another mechanism, as we observed no difference in feeding between wild-type and mutant animals. Furthermore, flies do not appear to possess homologs for leptin or leptin receptor, suggesting that metabolic feedback to the brain is different in some ways between flies and mammals. Still, the possibility that neuronal TORC controls metabolism through the same neuronal circuit (even though the direction of regulation may be opposite) in flies and mammals is intriguing and warrants further study.

Rather than activating the transcription of neuropeptides themselves, TORC may instead regulate the genes responsible for processing or secretion. A large number of the genes identified in our gene profiling analysis as downregulated in dTORC mutant heads, are annotated as proteases or inhibitors of proteases. With the exception of two serpins (Spn2 and Spn3), all of these genes were identified solely by sequence analysis, so nothing is known about their expression or function. The maturation of neuropeptides is often controlled by proteases that cleave a propeptide to release the active

form. These processing proteases can be controlled by protease inhibitors, such as the serpins (serine protease inhibitors). Indeed, *Drosophila* express serpins that have been shown to regulate neuropeptide maturation (Osterwalder, Kuhnen et al. 2004). In addition to their role in regulating proteases, serpins can also serve as hormone carriage proteins. Transcortin and thyroxine-binding globulin (TBG) are primarily responsible for carrying cortisol and the thyroid hormones T3 and T4, respectively in the bloodstream. Other serpins are themselves propeptide hormones. The plasma serpin, angiotensinogen is cleaved by the enzyme renin to release the hormone precursor, Angiotensin I. These examples illustrate several plausible mechanisms by which the proteases and protease inhibitors, which are downregulated in dTORC mutants, might contribute to the metabolic phenotype.

Neuronal dTORC may also promote metabolic health through the more general process of protecting the brain from oxidative damage. Starvation and compounds that promote the formation of reactive oxygen species, (e.g. paraquat, hydrogen peroxide); induce dTORC to activate the expression of catalase. Catalase is an enzyme that catalyzes the decomposition of hydrogen peroxide to oxygen and water. Catalase can also use hydrogen peroxide to oxidize toxins such as alcohols or formaldehyde. Hydrogen peroxide is produced by many metabolic processes, and can be harmful to the cell if not rapidly decomposed. Excessive reactive oxygen species (ROS) have been

linked to apoptosis and cognitive decline in neurodegenerative diseases. Although we did not detect any gross abnormality in brain structure or excessive apoptosis by terminal deoxynucleotidyl transferase dUTP nick end labeling (TUNEL) assay, oxidative damage could have more subtle effects on dTORC mutant neurons. In neurodegenerative disorders such as Alzheimer's disease, synaptic defects can be detected before cell death ensues (Selkoe 2002). It is possible that the brains of dTORC mutant flies are subtly damaged by oxidative stress.

Even in the absence of oxidative stress damage, dTORC mutant neurons may display defects in synaptic activity. In mouse hippocampal neurons, activation of the CREB target gene, brain-derived neurotrophic factor (BDNF), which is involved in enhancing synaptic transmission, requires the activity-dependent nuclear translocation of TORC1 (Zhou, Wu et al. 2006), (Kovacs, Steullet et al. 2007). Moreover, expression of a dominant-negative TORC1 polypeptide blocked the maintenance of late-phase long-term potentiation (L-LTP), while overexpression of TORC1 lowered the threshold for L-LTP induction (Zhou, Wu et al. 2006), (Kovacs, Steullet et al. 2007). Brains of dTORC mutant flies may exhibit dysfunctional neuronal activity, due to loss of CREB target gene activation, which could impinge on metabolic regulation through innervation of peripheral tissues or hormone production.

Similar to TORC1 mutant mice, dTORC mutant flies exhibit reduced fertility. While the complete or partial loss of fertility in TORC1 mutant mice

appears to be due to uterine abnormalities, the reduced fecundity of dTORC mutant flies is not accompanied by any obvious physical defect in the reproductive organs. Cursory examinations of the ovaries and testes revealed largely normal organs. dTORC mutant males when mated to wild-type females, show normal fertility. Initial matings of dTORC mutant females usually results in several days of egg laying, followed by a complete cessation, whereas wild-type flies will typically lay eggs throughout their lifespan, although at greatly reduced numbers as they age. Nearly all dTORC mutant embryos hatch into first instar larvae, and progress to pupation at a normal rate. A fraction of dTORC mutant pupae fail to complete metamorphosis and eclosion, suggesting that dTORC may play a role at this point in the fly life cycle. The reduction in fecundity of dTORC mutant females may be secondary to the decreased energy stores as starved flies will reduce their egg production (David, Van Herrewege et al. 1971). The increased activity of FOXO observed in dTORC mutant flies might also be the cause of reduced egg production, as overexpression of FOXO in *Drosophila* fat body has been shown to reduce fecundity (Giannakou, Goss et al. 2004). Despite the differences observed in the reproductive phenotypes between the mouse and fly, the fact that TORC appears to regulate this process in both organisms, warrants further study.

Studies in mice have suggested that TORC activity is required in the hypothalamus and hippocampus (Altarejos, Goebel et al. 2008) (Zhou, Wu et

al. 2006; Kovacs, Steullet et al. 2007), which raises the question, in which neurons is dTORC required to control energy homeostasis and fertility? All attempts to localize endogenous dTORC by RNA in situ hybridization or immunohistochemistry, were unsuccessful. Therefore, the exact expression pattern of dTORC is unknown. We used pan-neuronal expression of dTORC to rescue the metabolic phenotype, and observed that restricting expression to only the insulin-producing or AKH-producing neurons, failed to rescue the dTORC mutant phenotype. We imagine that dTORC is required only in a subset of neurons to control energy balance, but it is also plausible that dTORC is essential for all neurons. One way to distinguish between these possibilities is to attempt to rescue the metabolic phenotype of the dTORC mutant flies, by driving expression of dTORC in subsets of neurons using any number of GAL4 driver lines. Although, the functional characterization of various brain regions in the fly is not as well established as mammals, several sets of neurons stand out as possible candidates for energy regulation. These include the serotonergic and dopaminergic neurons, which are known to regulate metabolism and stress in mammals and worms, and insulin signaling in the fly (Akana 2008), (Ashrafi 2007; Kaplan, Zimmermann et al. 2008). Other potential players are the c673a-Gal4 and fruitless-Gal4 neurons which have been shown to regulate metabolism in flies (Al-Anzi, Sapin et al. 2009). Perhaps a better method for elucidating the neurons which require dTORC activity, is to attempt to recreate the metabolic phenotype by inactivating

dTORC in various neuronal populations by expressing a dominant-negative dTORC transgene or dTORC RNAi. This strategy has the advantage of being less time consuming, because a large number of GAL4 lines could be screened with single genetic crosses.

Our studies show that TORC is used in flies and mammals to control energy balance and fertility. However, in flies the brain is the major site of TORC action and controls both metabolism and fertility. This is in contrast to mammals in which TORC in the liver controls glucose homeostasis, while neuronal TORC regulates feeding behavior and fertility. This difference might be explained by a divergence in the anatomy of insects and mammals. For example, the islet β cells in the pancreas of mammals produce insulin, while in flies this function is carried out by neuroendocrine cells in the brain. Future studies of dTORC in the *Drosophila* brain may offer further insights into the evolution of these metabolic control systems, and reveal new roles for the mammalian brain.

4.2 TORC in Cardiac Function

dTORC mutant flies have severely reduced average and maximal lifespans when compared to wild-type controls. Insulin signaling is known to regulate lifespan, potentially by modulating the aging process, in many organisms including worms, flies, and rodents (Taguchi and White 2008). Given that dTORC is regulated by insulin signaling, one plausible explanation

for the short lives of dTORC mutant flies is accelerated aging. Fruit flies exhibit an insulin-dependent decline in cardiac function that correlates well with chronological age (Wessells, Fitzgerald et al. 2004). We sought to use cardiac function as a proxy for age to determine whether dTORC mutant flies age faster than controls. We did observe an increased electrical pacing-induced heart failure rate in dTORC mutants that could be rescued by expressing dTORC specifically in heart tissue. However, we did not observe any abnormality in the decline in heart rate that is characteristic of aging flies. On the contrary, we found that dTORC mutant flies on average have faster resting heart rates than controls at all ages tested. These results would obfuscate the use of these heart function assays to determine the physiological age of the dTORC mutant. It should be noted that expression of FOXO, specifically in the heart tissue, was found to prevent the aging-related cardiac decline of heart rate and increase in heart failure rate (Wessells, Fitzgerald et al. 2004). This suggests that FOXO may not be able to protect heart function in the absence of dTORC as the dTORC mutants have increased FOXO activity, but still exhibit abnormally high failure rates. However, we did not test for increased FOXO activity specifically in the heart. It is still possible that the abrogation of aging-related cardiac decline found by reducing insulin signaling could be acting, in part, through dTORC. Testing the effects of insulin signaling mutants on heart rate and heart failure rate in the dTORC mutant background may reveal whether dTORC is involved in this process.

Although we were unable to observe a rapid aging phenotype in the dTORC mutant, we did find that they exhibit significant cardiac dysfunction. In addition to the increased heart rate and pacing-induced failure rate, dTORC mutants have a narrower heart tube and myofibrillar disorganization that may be responsible for the localized loss of contractility observed in some individual flies. All of these phenotypes could be reversed by expression of dTORC specifically in the heart, while neuronal expression had no effect, suggesting that dTORC acts independently in at least two separate tissues in the fly.

Mammalian TORC has not yet been implicated in heart function; however the CREB family members, CREB1 and CREM, have been shown to regulate cardiac physiology. Mice expressing a Ser133Ala mutant CREB transgene in the heart developed dilated cardiomyopathy with increased end diastolic and systolic dimensions, and died prematurely due to congestive heart failure and hepatic congestion (Fentzke, Korcarz et al. 1998). These phenotypes appear to be opposite to what we observed in dTORC mutant flies. There are several plausible explanations for this discrepancy. First, the Ser133Ala CREB mutant may not be a true dominant negative, as is often assumed. TORC has been shown to activate transcription of CRE-reporters and CREB target genes even in the absence of Ser133 phosphorylatable CREB (Conkright, Canettieri et al. 2003), (Xu, Kasper et al. 2007). Therefore loss of TORC and CREB Ser157Ala overexpression likely alter the

transcription profile in different ways. For example, CREB regulates expression of the repressor of CRE transcription, ICER, which has been shown to regulate cardiac hypertrophy and apoptosis (Tomita, Nazmy et al. 2003). ICER transcription requires TORC, but is relatively insensitive to disruption of the KID/KIX interaction (Xu, Kasper et al. 2007). The differential regulation of this gene may partly explain the difference in phenotype between flies and mice. Another potential reason for the discrepancy in phenotype observed in these two species, may simply be the differences in anatomy. The *Drosophila* heart is a tubular structure made up of a single layer of myocardial cells, which pumps hemolymph in an open circulatory system. Unlike the mouse heart, this organ is not subject to fluid pressure and is not responsible for circulating oxygen. Therefore, the fly heart is likely responding to different physiological cues and may manifest disease is slightly different ways. The CREB Ser133Ala mutant mouse hearts also displayed both hypertrophic and atrophied myocytes, as well as interstitial fibrosis. These phenotypes may be analogous to the disarrayed myofibrillar structure and increased expression of pericardin observed in dTORC mutant hearts.

Another transcription factor known to regulate heart function is the nuclear factor of activated T-cells (NFAT). NFAT is a widely expressed family of transcription factors that are regulated by calcium signaling. In a manner analogous to TORC regulation, inactive NFAT is sequestered in the cytoplasm via a phosphorylation-dependent interaction with 14-3-3. Upon a rise in

intracellular Ca2+, NFAT is dephosphorylated by calcineurin and translocates to the nucleus where it activates transcription in conjunction with other transcription factors (Crabtree and Olson 2002), (Chow and Davis 2000). NFAT signaling is required in development for the formation of cardiac valves, as well as patterning of the vasculature (Crabtree and Olson 2002). However, NFAT has also been shown to play a role in the function of the adult heart. During the hypertrophic response in mammals, fetal cardiac genes are re-expressed and drive growth of the heart. These genes are activated by a NFAT in combination with the GATA motif-binding transcription factor GATA4. Indeed, overexpression of a constitutively active NFAT polypeptide in the mouse heart can induce cardiac hypertrophy (Crabtree and Olson 2002). An even more severe hypertrophic response, leading to dilated cardiomyopathy and death, is observed in mice expressing constitutively active calcineurin in the heart (Crabtree and Olson 2002). This suggests that calcineurin dephosphorylates substrates in addition to NFAT in driving the hypertrophic response. TORC is a plausible candidate. However, invertebrates do not possess calcineurin-responsive NFAT homologs (Graef, Gastier et al. 2001). Given the common regulatory mechanism and hypertrophic-like response observed when overexpressing dTORC in the fly heart, it is intriguing to speculate that TORC may substitute for NFAT in lower organisms.

Detailed analysis of the physiology of the adult *Drosophila* heart has only recently been possible due to the advent of new experimental

procedures. Several mutants which affect cardiac function and myofibrillar organization have recently been identified. The dTORC mutant phenotype is distinct from each of these, but shares some characteristics as will be discussed below.

Dystrophin is a protein localized to the cytoplasmic surface of the muscle sarcolemma that helps connect the cytoskeleton of muscle fibers to the extracellular matrix. Mutations in the dystrophin gene in humans have been linked to several muscular dystrophies. *Drosophila* dystrophin mutants were found to have dilated hearts with myofribrillar disorganization and reduced lifespans (Taghli-Lamallem, Akasaka et al. 2008). They also exhibited increased heart rates compared to wild-type flies. While the phenotype of these flies is distinct from the dTORC mutant, they do share some of the same defects (reduced life span, myofibrillar disarray, and tachycardia), suggesting that investigation of a link between these two proteins may be warranted.

Sestrins are evolutionarily conserved proteins which accumulate in cells in response to stress. Their expression leads to activation of AMPK and inhibition of the target of rapamycin (TOR) (Budanov and Karin 2008).Transcription of the single *Drosophila* homolog of sestrins (dSesn) is activated by FOXO in response to oxidative stress (Lee, Budanov et al. 2010). Sestrin-null mutant flies exhibit decreased heart rate, cardiac arrhythmia, dilated hearts and disorganized cardiac myofibrils. Additionally, dSesn mutants accumulate lipids to higher levels than wild-type flies. Many of these

phenotypes could be alleviated by pharmacological activation of AMPK with aminoimidazole carboxyamide ribonucleotide (AICAR) (Lee, Budanov et al. 2010). Given that dTORC mutants exhibit many phenotypes that are opposite to those observed in dSesn mutant flies, it is possible that dTORC is acting downstream of dSesn, and is hyperactivated in the dSesn mutant due to decreased AMPK activity. Indeed, RNAi knockdown of AMPK has been shown to decrease heart rate (Lee, Budanov et al. 2010), similar to what we observed by overexpressing dTORC in the heart. However, unlike in mammals, AMPK has not yet been shown to regulate dTORC in the fly. Future studies should reveal whether this pathway is conserved in *Drosophila*.

A genome wide RNAi screen for cell-autonomous regulators of cardiac function in *Drosophila*, revealed that the transcriptional regulator, NOT3, is involved in this process. Knockdown of NOT3 caused cardiac dilation and myofibrillar disarray. This was accompanied by reduced expression of the sarcoplasmic/endoplasmic reticulum calcium ATPase (Serca2a), myosin heavy chain (mhc), and the potassium channel KCNQ. Furthermore, a P-element insertion in the Not3 locus caused embryonic lethality with a defect in heart tube organization. NOT3 mutant mice were also found to develop severe cardiomyopathy in response to cardiac stress (Neely, Kuba et al. 2010). If dTORC impinges on NOT3 signaling in the heart, it is likely only in the post-developmental stage as the dTORC mutant phenotype manifests only in the adult heart.

Screening a set of molecularly-defined genomic deficiencies for abnormal heart function in *Drosophila*, found the serine protease rhomboid 3 (rho3) is involved in controlling heart size in the adult fly (Yu, Lee et al. 2010). Rho3 processes the epidermal growth factor (EGF)-like ligand, Spitz, which is involved in the development of many tissues including the musculature (Yu, Lee et al. 2010). This study found that the observed enlargement of the adult heart was due to deficiencies in EGF receptor (EGFR) signaling. One intriguing possibility is that dTORC is negatively regulated by EGFR signaling, and the increased heart size in dTORC overexpressing flies is caused by overwhelming this regulation. In fact, dTORC contains a conserved, putative D-domain docking site for the extracellular signal-regulated kinase (ERK) which is activated by EGFR signaling. Determining whether the dTORC mutant can suppress the rho3 mutant heart phenotype should determine whether dTORC is in the EGFR pathway.

Our studies identified a number of potential TORC target genes that are specifically regulated in the fly heart. The majority of these genes are of completely unknown function. Transgenic overexpression and RNAi mediated knockdown of these genes should reveal what role they play in the dTORC mutant phenotype. Furthermore, genetic interaction experiments will illuminate to what degree dTORC is involved in the phenotypes of other *Drosophila* mutants which display cardiac dysfunction.

4.3 Concluding Remarks

Despite the large evolutionary separation between flies and mice, our studies have revealed that the mechanisms regulating TORC are largely unchanged. We have also found that TORC is involved in the control of energy balance and reproduction in both flies and mammals, albeit in different ways. Generation of a completely TORC-null animal allowed us to uncover a potential new role for TORC in cardiac physiology. The fact that flies express only one TORC gene and that dTORC-null mutants are viable and fertile allows for the study of the role this gene in all aspects of organismal physiology. These results should serve as a platform from which to investigate the role of TORC in other organisms.

REFERENCES

Ahn, S., M. Olive, S. Aggarwal, D. Krylov, D. Ginty and C. Vinson (1998). "A dominant negative inhibitor of CREB reveals that it is a general mediator stimulus-dependent transcription of c-fos." Molec. Cell. Biol. **18**: 967-977.

Akana, S. F. (2008). "Feeding and stress interact through the serotonin 2C receptor in developing mice." Physiol Behav **94**(4): 569-579.

Akasaka, T., S. Klinedinst, K. Ocorr, E. L. Bustamante, S. K. Kim and R. Bodmer (2006). "The ATP-sensitive potassium (KATP) channel-encoded dSUR gene is required for Drosophila heart function and is regulated by tinman." Proc Natl Acad Sci U S A **103**(32): 11999-12004.

Al-Anzi, B., V. Sapin, C. Waters, K. Zinn, R. J. Wyman and S. Benzer (2009). "Obesity-blocking neurons in Drosophila." Neuron **63**(3): 329-341.

Altarejos, J. Y., N. Goebel, M. D. Conkright, H. Inoue, J. Xie, C. M. Arias, P. E. Sawchenko and M. Montminy (2008). "The Creb1 coactivator Crtc1 is required for energy balance and fertility." Nat Med **14**(10): 1112-1117.

Amelio, A. L., M. Caputi and M. D. Conkright (2009). "Bipartite functions of the CREB co-activators selectively direct alternative splicing or transcriptional activation." Embo J **28**(18): 2733-2747.

Ashrafi, K. (2007). "Obesity and the regulation of fat metabolism." WormBook: 1-20.

Barco, A., J. M. Alarcon and E. R. Kandel (2002). "Expression of constitutively active CREB protein facilitates the late phase of long-term potentiation by enhancing synaptic capture." Cell **108**(5): 689-703.

Bartsch, D., M. Ghirardi, P. A. Skehel, K. A. Karl, S. P. Herder, M. Chen, C. H. Bailey and E. R. Kandel (1995). "Aplysia CREB2 represses long-term facilitation: relief of repression converts transient facilitation into long-term functional and structural change." Cell **83**(6): 979-992.

Belvin, M. P., H. Zhou and J. C. Yin (1999). "The Drosophila dCREB2 gene affects the circadian clock." Neuron **22**(4): 777-787.

Benito, E. and A. Barco (2010). "CREB's control of intrinsic and synaptic plasticity: implications for CREB-dependent memory models." Trends Neurosci **33**(5): 230-240.

Bier, E. and R. Bodmer (2004). "Drosophila, an emerging model for cardiac disease." Gene **342**(1): 1-11.

Bittinger, M. A., E. McWhinnie, J. Meltzer, V. Iourgenko, B. Latario, X. Liu, C. H. Chen, C. Song, D. Garza and M. Labow (2004). "Activation of cAMP response element-mediated gene expression by regulated nuclear transport of TORC proteins." Curr Biol **14**(23): 2156-2161.

Bleckmann, S. C., J. A. Blendy, D. Rudolph, A. P. Monaghan, W. Schmid and G. Schutz (2002). "Activating transcription factor 1 and CREB are important for cell survival during early mouse development." Mol Cell Biol **22**(6): 1919-1925.

Blendy, J. A., K. H. Kaestner, G. F. Weinbauer, E. Nieschlag and G. Schutz (1996). "Severe impairment of spermatogenesis in mice lacking the CREM gene." Nature **380**(6570): 162-165.

Bluher, M., B. B. Kahn and C. R. Kahn (2003). "Extended longevity in mice lacking the insulin receptor in adipose tissue." Science **299**(5606): 572-574.

Bodmer, R. and T. V. Venkatesh (1998). "Heart development in Drosophila and vertebrates: conservation of molecular mechanisms." Dev Genet **22**(3): 181-186.

Bodor, J., Z. Fehervari, B. Diamond and S. Sakaguchi (2007). "ICER/CREM-mediated transcriptional attenuation of IL-2 and its role in suppression by regulatory T cells." Eur J Immunol **37**(4): 884-895.

Bonni, A., D. D. Ginty, H. Dudek and M. E. Greenberg (1995). "Serine 133-phosphorylated CREB induces transcription via a cooperative mechanism that may confer specificity to neurotrophin signals." Mol Cell Neurosci **6**(2): 168-183.

Bourtchuladze, R., B. Frenguelli, J. Blendy, D. Cioffi, G. Schutz and A. J. Silva (1994). "Deficient long-term memory in mice with a targeted mutation of the cAMP-responsive element-binding protein." Cell **79**(1): 59-68.

Brand, A. H. and N. Perrimon (1993). "Targeted gene expression as a means of altering cell fates and generating dominant phenotypes." Development **118**(2): 401-415.

Breuillaud, L., O. Halfon, P. J. Magistretti, F. P. Pralong and J. R. Cardinaux (2009). "Mouse fertility is not dependent on the CREB coactivator Crtc1." Nat Med **15**(9): 989-990; author reply 991.

Brindle, P., S. Linke and M. Montminy (1993). "Protein-kinase-A-dependent activator in transcription factor CREB reveals new role for CREM repressors." Nature **364**(6440): 821-824.

Broughton, S. J., M. D. Piper, T. Ikeya, T. M. Bass, J. Jacobson, Y. Driege, P. Martinez, E. Hafen, D. J. Withers, S. J. Leevers and L. Partridge (2005). "Longer lifespan, altered metabolism, and stress resistance in Drosophila from ablation of cells making insulin-like ligands." Proc Natl Acad Sci U S A **102**(8): 3105-3110.

Budanov, A. V. and M. Karin (2008). "p53 target genes sestrin1 and sestrin2 connect genotoxic stress and mTOR signaling." Cell **134**(3): 451-460.

Canettieri, G., S. Coni, M. Della Guardia, V. Nocerino, L. Antonucci, L. Di Magno, R. Screaton, I. Screpanti, G. Giannini and A. Gulino (2009). "The coactivator CRTC1 promotes cell proliferation and transformation via AP-1." Proc Natl Acad Sci U S A **106**(5): 1445-1450.

Canettieri, G., S. H. Koo, R. Berdeaux, J. Heredia, S. Hedrick, X. Zhang and M. Montminy (2005). "Dual role of the coactivator TORC2 in modulating hepatic glucose output and insulin signaling." Cell Metab **2**(5): 331-338.

Chen, L., D. C. Rio, G. G. Haddad and E. Ma (2004). "Regulatory role of dADAR in ROS metabolism in Drosophila CNS." Brain Res Mol Brain Res **131**(1-2): 93-100.

Chow, C. W. and R. J. Davis (2000). "Integration of calcium and cyclic AMP signaling pathways by 14-3-3." Mol Cell Biol **20**(2): 702-712.

Chrivia, J. C., R. P. Kwok, N. Lamb, M. Hagiwara, M. R. Montminy and R. H. Goodman (1993). "Phosphorylated CREB binds specifically to the nuclear protein CBP." Nature **365**(6449): 855-859.

Clancy, D. J., D. Gems, L. G. Harshman, S. Oldham, H. Stocker, E. Hafen, S. J. Leevers and L. Partridge (2001). "Extension of life-span by loss of CHICO, a Drosophila insulin receptor substrate protein." Science **292**(5514): 104-106.

Conkright, M. D., G. Canettieri, R. Screaton, E. Guzman, L. Miraglia, J. B. Hogenesch and M. Montminy (2003). "TORCs: transducers of regulated CREB activity." Mol Cell **12**(2): 413-423.

Conkright, M. D., E. Guzman, L. Flechner, A. I. Su, J. B. Hogenesch and M. Montminy (2003). "Genome-wide analysis of CREB target genes reveals a core promoter requirement for cAMP responsiveness." Mol Cell **11**(4): 1101-1108.

Crabtree, G. R. and E. N. Olson (2002). "NFAT signaling: choreographing the social lives of cells." Cell **109 Suppl**: S67-79.

Cripps, R. M. and E. N. Olson (2002). "Control of cardiac development by an evolutionarily conserved transcriptional network." Dev Biol **246**(1): 14-28.

David, J., J. Van Herrewege and P. Fouillet (1971). "Quantitative under-feeding of Drosophila: effects on adult longevity and fecundity." Exp Gerontol **6**(3): 249-257.

de Groot, R. P., J. den Hertog, J. R. Vandenheede, J. Goris and P. Sassone-Corsi (1993). "Multiple and cooperative phosphorylation events regulate the CREM activator function." Embo J **12**(10): 3903-3911.

Dentin, R., S. Hedrick, J. Xie, J. Yates, 3rd and M. Montminy (2008). "Hepatic glucose sensing via the CREB coactivator CRTC2." Science **319**(5868): 1402-1405.

Dentin, R., Y. Liu, S. H. Koo, S. Hedrick, T. Vargas, J. Heredia, J. Yates, 3rd and M. Montminy (2007). "Insulin modulates gluconeogenesis by inhibition of the coactivator TORC2." Nature **449**(7160): 366-369.

Djawdan, M., A. K. Chippindale, M. R. Rose and T. J. Bradley (1998). "Metabolic reserves and evolved stress resistance in Drosophila melanogaster." Physiol Zool **71**(5): 584-594.

Doi, J., H. Takemori, X. Z. Lin, N. Horike, Y. Katoh and M. Okamoto (2002). "Salt-inducible kinase represses cAMP-dependent protein kinase-mediated activation of human cholesterol side chain cleavage cytochrome P450 promoter through the CREB basic leucine zipper domain." J Biol Chem **277**(18): 15629-15637.

Dong, Y., T. Green, D. Saal, H. Marie, R. Neve, E. J. Nestler and R. C. Malenka (2006). "CREB modulates excitability of nucleus accumbens neurons." Nat Neurosci **9**(4): 475-477.

Eden, E., R. Navon, I. Steinfeld, D. Lipson and Z. Yakhini (2009). "GOrilla: a tool for discovery and visualization of enriched GO terms in ranked gene lists." BMC Bioinformatics **10**: 48.

Fentzke, R. C., C. E. Korcarz, R. M. Lang, H. Lin and J. M. Leiden (1998). "Dilated cardiomyopathy in transgenic mice expressing a dominant-negative CREB transcription factor in the heart." J Clin Invest **101**(11): 2415-2426.

Ferreri, K., G. Gill and M. Montminy (1994). "The cAMP-regulated transcription factor CREB interacts with a component of the TFIID complex." Proc Natl Acad Sci U S A **91**(4): 1210-1213.

Fink, M., C. Callol-Massot, A. Chu, P. Ruiz-Lozano, J. C. Izpisua Belmonte, W. Giles, R. Bodmer and K. Ocorr (2009). "A new method for detection and quantification of heartbeat parameters in Drosophila, zebrafish, and embryonic mouse hearts." Biotechniques **46**(2): 101-113.

Finsterwald, C., H. Fiumelli, J. R. Cardinaux and J. L. Martin (2010). "Regulation of dendritic development by BDNF requires activation of CRTC1 by glutamate." J Biol Chem **285**(37): 28587-28595.

Foulkes, N. S., J. Borjigin, S. H. Snyder and P. Sassone-Corsi (1997). "Rhythmic transcription: the molecular basis of circadian melatonin synthesis." Trends Neurosci **20**(10): 487-492.

Foulkes, N. S., E. Borrelli and P. Sassone-Corsi (1991). "CREM gene: use of alternative DNA-binding domains generates multiple antagonists of cAMP-induced transcription." Cell **64**(4): 739-749.

Foulkes, N. S. and P. Sassone-Corsi (1992). "More is better: activators and repressors from the same gene." Cell **68**(3): 411-414.

Fridell, Y. W., A. Sanchez-Blanco, B. A. Silvia and S. L. Helfand (2005). "Targeted expression of the human uncoupling protein 2 (hUCP2) to adult neurons extends life span in the fly." Cell Metab **1**(2): 145-152.

Fu, A. and R. A. Screaton (2008). "Using kinomics to delineate signaling pathways: control of CRTC2/TORC2 by the AMPK family." Cell Cycle **7**(24): 3823-3828.

Gau, D., T. Lemberger, C. von Gall, O. Kretz, N. Le Minh, P. Gass, W. Schmid, U. Schibler, H. W. Korf and G. Schutz (2002). "Phosphorylation of CREB Ser142 regulates light-induced phase shifts of the circadian clock." Neuron **34**(2): 245-253.

Gershman, B., O. Puig, L. Hang, R. M. Peitzsch, M. Tatar and R. S. Garofalo (2007). "High-resolution dynamics of the transcriptional response to nutrition in Drosophila: a key role for dFOXO." Physiol Genomics **29**(1): 24-34.

Giannakou, M. E., M. Goss, M. A. Junger, E. Hafen, S. J. Leevers and L. Partridge (2004). "Long-lived Drosophila with overexpressed dFOXO in adult fat body." Science **305**(5682): 361.

Giannakou, M. E. and L. Partridge (2007). "Role of insulin-like signalling in Drosophila lifespan." Trends Biochem Sci **32**(4): 180-188.

Girardet, C., W. H. Walker and J. F. Habener (1996). "An alternatively spliced polycistronic mRNA encoding cyclic adenosine 3',5'-monophosphate (cAMP)-responsive transcription factor CREB (cAMP response element-binding protein) in human testis extinguishes expression of an internally translated inhibitor CREB isoform." Mol Endocrinol **10**(7): 879-891.

Gonzalez, G. A., P. Menzel, J. Leonard, W. H. Fischer and M. R. Montminy (1991). "Characterization of motifs which are critical for activity of the cyclic AMP-responsive transcription factor CREB." Mol Cell Biol **11**(3): 1306-1312.

Gonzalez, G. A. and M. R. Montminy (1989). "Cyclic AMP stimulates somatostatin gene transcription by phosphorylation of CREB at serine 133." Cell **59**(4): 675-680.

Graef, I. A., J. M. Gastier, U. Francke and G. R. Crabtree (2001). "Evolutionary relationships among Rel domains indicate functional diversification by recombination." Proc Natl Acad Sci U S A **98**(10): 5740-5745.

Gutierrez, E., D. Wiggins, B. Fielding and A. P. Gould (2007). "Specialized hepatocyte-like cells regulate Drosophila lipid metabolism." Nature **445**(7125): 275-280.

Hagiwara, M., A. Alberts, P. Brindle, J. Meinkoth, J. Feramisco, T. Deng, M. Karin, S. Shenolikar and M. Montminy (1992). "Transcriptional attenuation following cAMP induction requires PP-1-mediated dephosphorylation of CREB." Cell **70**(1): 105-113.

Hai, T. W., F. Liu, W. J. Coukos and M. R. Green (1989). "Transcription factor ATF cDNA clones: an extensive family of leucine zipper proteins able to selectively form DNA-binding heterodimers." Genes Dev **3**(12B): 2083-2090.

Han, Z., P. Yi, X. Li and E. N. Olson (2006). "Hand, an evolutionarily conserved bHLH transcription factor required for Drosophila cardiogenesis and hematopoiesis." Development **133**(6): 1175-1182.

Hendricks, J. C., J. A. Williams, K. Panckeri, D. Kirk, M. Tello, J. C. Yin and A. Sehgal (2001). "A non-circadian role for cAMP signaling and CREB activity in Drosophila rest homeostasis." Nat Neurosci **4**(11): 1108-1115.

Herzig, S., S. Hedrick, I. Morantte, S. H. Koo, F. Galimi and M. Montminy (2003). "CREB controls hepatic lipid metabolism through nuclear hormone receptor PPAR-gamma." Nature **426**(6963): 190-193.

Herzig, S., F. Long, U. S. Jhala, S. Hedrick, R. Quinn, A. Bauer, D. Rudolph, G. Schutz, C. Yoon, P. Puigserver, B. Spiegelman and M. Montminy (2001). "CREB regulates hepatic gluconeogenesis through the coactivator PGC-1." Nature **413**(6852): 179-183.

Hinek, A., A. V. Pshezhetsky, M. von Itzstein and B. Starcher (2006). "Lysosomal sialidase (neuraminidase-1) is targeted to the cell surface in a multiprotein complex that facilitates elastic fiber assembly." J Biol Chem **281**(6): 3698-3710.

Hinke, S. A., K. Hellemans and F. C. Schuit (2004). "Plasticity of the beta cell insulin secretory competence: preparing the pancreatic beta cell for the next meal." J Physiol **558**(Pt 2): 369-380.

Hishiki, T., T. Ohshima, T. Ego and K. Shimotohno (2007). "BCL3 acts as a negative regulator of transcription from the human T-cell leukemia virus type 1 long terminal repeat through interactions with TORC3." J Biol Chem **282**(39): 28335-28343.

Hoeffler, J. P., T. E. Meyer, G. Waeber and J. F. Habener (1990). "Multiple adenosine 3',5'-cyclic [corrected] monophosphate response element DNA-binding proteins generated by gene diversification and alternative exon splicing." Mol Endocrinol **4**(6): 920-930.

Hollander, J. A., H. I. Im, A. L. Amelio, J. Kocerha, P. Bali, Q. Lu, D. Willoughby, C. Wahlestedt, M. D. Conkright and P. J. Kenny (2010). "Striatal microRNA controls cocaine intake through CREB signalling." Nature **466**(7303): 197-202.

Honjo, K. and K. Furukubo-Tokunaga (2005). "Induction of cAMP response element-binding protein-dependent medium-term memory by appetitive gustatory reinforcement in Drosophila larvae." J Neurosci **25**(35): 7905-7913.

Hurst, H. C., N. F. Totty and N. C. Jones (1991). "Identification and functional characterisation of the cellular activating transcription factor 43 (ATF-43) protein." Nucleic Acids Res **19**(17): 4601-4609.

Hwangbo, D. S., B. Gershman, M. P. Tu, M. Palmer and M. Tatar (2004). "Drosophila dFOXO controls lifespan and regulates insulin signalling in brain and fat body." Nature **429**(6991): 562-566.

Iijima-Ando, K. and J. C. Yin (2005). "Transgenic cAMP response element reporter flies for monitoring circadian rhythms." Methods Enzymol **393**: 302-315.

Iijima, K., L. Zhao, C. Shenton and K. Iijima-Ando (2009). "Regulation of energy stores and feeding by neuronal and peripheral CREB activity in Drosophila." PLoS ONE **4**(12): e8498.

Impey, S., S. R. McCorkle, H. Cha-Molstad, J. M. Dwyer, G. S. Yochum, J. M. Boss, S. McWeeney, J. J. Dunn, G. Mandel and R. H. Goodman (2004). "Defining the CREB regulon: a genome-wide analysis of transcription factor regulatory regions." Cell **119**(7): 1041-1054.

Iourgenko, V., W. Zhang, C. Mickanin, I. Daly, C. Jiang, J. M. Hexham, A. P. Orth, L. Miraglia, J. Meltzer, D. Garza, G. W. Chirn, E. McWhinnie, D. Cohen, J. Skelton, R. Terry, Y. Yu, D. Bodian, F. P. Buxton, J. Zhu, C. Song and M. A. Labow (2003). "Identification of a family of cAMP response element-binding protein coactivators by genome-scale functional analysis in mammalian cells." Proc Natl Acad Sci U S A **100**(21): 12147-12152.

Ja, W. W., G. B. Carvalho, E. M. Mak, N. N. de la Rosa, A. Y. Fang, J. C. Liong, T. Brummel and S. Benzer (2007). "Prandiology of Drosophila and the CAFE assay." Proc Natl Acad Sci U S A **104**(20): 8253-8256.

Jansson, D., A. C. Ng, A. Fu, C. Depatie, M. Al Azzabi and R. A. Screaton (2008). "Glucose controls CREB activity in islet cells via regulated phosphorylation of TORC2." Proc Natl Acad Sci U S A **105**(29): 10161-10166.

Jaskoll, T., K. Htet, G. Abichaker, F. J. Kaye and M. Melnick (2010). "CRTC1 expression during normal and abnormal salivary gland development supports a precursor cell origin for mucoepidermoid cancer." Gene Expr Patterns.

Jin, J., F. D. Smith, C. Stark, C. D. Wells, J. P. Fawcett, S. Kulkarni, P. Metalnikov, P. O'Donnell, P. Taylor, L. Taylor, A. Zougman, J. R. Woodgett, L. K. Langeberg, J. D. Scott and T. Pawson (2004). "Proteomic, functional, and domain-based analysis of in vivo 14-3-3 binding proteins involved in cytoskeletal regulation and cellular organization." Curr Biol **14**(16): 1436-1450.

Johannessen, M., M. P. Delghandi and U. Moens (2004). "What turns CREB on?" Cell Signal **16**(11): 1211-1227.

Junger, M. A., F. Rintelen, H. Stocker, J. D. Wasserman, M. Vegh, T. Radimerski, M. E. Greenberg and E. Hafen (2003). "The Drosophila forkhead transcription factor FOXO mediates the reduction in cell number associated with reduced insulin signaling." J Biol **2**(3): 20.

Kaplan, D. D., G. Zimmermann, K. Suyama, T. Meyer and M. P. Scott (2008). "A nucleostemin family GTPase, NS3, acts in serotonergic neurons to regulate insulin signaling and control body size." Genes Dev **22**(14): 1877-1893.

Kawasaki, H., R. Eckner, T. P. Yao, K. Taira, R. Chiu, D. M. Livingston and K. K. Yokoyama (1998). "Distinct roles of the co-activators p300 and CBP in retinoic-acid-induced F9-cell differentiation." Nature **393**(6682): 284-289.

Kenyon, C., J. Chang, E. Gensch, A. Rudner and R. Tabtiang (1993). "A C. elegans mutant that lives twice as long as wild type." Nature **366**(6454): 461-464.

Kim, S. K. and E. J. Rulifson (2004). "Conserved mechanisms of glucose sensing and regulation by Drosophila corpora cardiaca cells." Nature **431**(7006): 316-320.

Kobayashi, M. and K. Kawakami (1995). "ATF-1CREB heterodimer is involved in constitutive expression of the housekeeping Na,K-ATPase alpha 1 subunit gene." Nucleic Acids Res **23**(15): 2848-2855.

Koo, S. H., L. Flechner, L. Qi, X. Zhang, R. A. Screaton, S. Jeffries, S. Hedrick, W. Xu, F. Boussouar, P. Brindle, H. Takemori and M. Montminy (2005). "The CREB coactivator TORC2 is a key regulator of fasting glucose metabolism." Nature **437**(7062): 1109-1111.

Kornhauser, J. M., C. W. Cowan, A. J. Shaywitz, R. E. Dolmetsch, E. C. Griffith, L. S. Hu, C. Haddad, Z. Xia and M. E. Greenberg (2002). "CREB transcriptional activity in neurons is regulated by multiple, calcium-specific phosphorylation events." Neuron **34**(2): 221-233.

Kovacs, K. A., P. Steullet, M. Steinmann, K. Q. Do, P. J. Magistretti, O. Halfon and J. R. Cardinaux (2007). "TORC1 is a calcium- and cAMP-sensitive coincidence detector involved in hippocampal long-term synaptic plasticity." Proc Natl Acad Sci U S A **104**(11): 4700-4705.

Kramer, J. M., J. T. Davidge, J. M. Lockyer and B. E. Staveley (2003). "Expression of Drosophila FOXO regulates growth and can phenocopy starvation." BMC Dev Biol **3**: 5.

Kvietikova, I., R. H. Wenger, H. H. Marti and M. Gassmann (1995). "The transcription factors ATF-1 and CREB-1 bind constitutively to the hypoxia-inducible factor-1 (HIF-1) DNA recognition site." Nucleic Acids Res **23**(22): 4542-4550.

Kyllerman, M., J. E. Mansson, O. Westphal, N. Conradi and H. Nellstrom (1993). "Infantile galactosialidosis presenting with congenital adrenal hyperplasia and renal hypertension." Pediatr Neurol **9**(4): 318-322.

Laoide, B. M., N. S. Foulkes, F. Schlotter and P. Sassone-Corsi (1993). "The functional versatility of CREM is determined by its modular structure." Embo J **12**(3): 1179-1191.

Le Lay, J., G. Tuteja, P. White, R. Dhir, R. Ahima and K. H. Kaestner (2009). "CRTC2 (TORC2) contributes to the transcriptional response to fasting in the liver but is not required for the maintenance of glucose homeostasis." Cell Metab **10**(1): 55-62.

Lee, G. and J. H. Park (2004). "Hemolymph sugar homeostasis and starvation-induced hyperactivity affected by genetic manipulations of the adipokinetic hormone-encoding gene in Drosophila melanogaster." Genetics **167**(1): 311-323.

Lee, J. H., A. V. Budanov, E. J. Park, R. Birse, T. E. Kim, G. A. Perkins, K. Ocorr, M. H. Ellisman, R. Bodmer, E. Bier and M. Karin (2010). "Sestrin as a feedback inhibitor of TOR that prevents age-related pathologies." Science **327**(5970): 1223-1228.

Lee, K. A., T. Y. Hai, L. SivaRaman, B. Thimmappaya, H. C. Hurst, N. C. Jones and M. R. Green (1987). "A cellular protein, activating transcription factor, activates transcription of multiple E1A-inducible adenovirus early promoters." Proc Natl Acad Sci U S A **84**(23): 8355-8359.

Lee, T. H., J. Chen and J. M. Miano (2009). "Functional characterization of a putative serine carboxypeptidase in vascular smooth muscle cells." Circ Res **105**(3): 271-278.

Lee, T. H., J. W. Streb, M. A. Georger and J. M. Miano (2006). "Tissue expression of the novel serine carboxypeptidase Scpep1." J Histochem Cytochem **54**(6): 701-711.

Lighton, J. R. (1991). Measurements on insects. Oxford, Pergamon Press.

Lighton, J. R. and R. J. Turner (2004). "Thermolimit respirometry: an objective assessment of critical thermal maxima in two sympatric desert harvester ants, Pogonomyrmex rugosus and P. californicus." J Exp Biol **207**(Pt 11): 1903-1913.

Liu, Y., R. Dentin, D. Chen, S. Hedrick, K. Ravnskjaer, S. Schenk, J. Milne, D. J. Meyers, P. Cole, J. Yates, 3rd, J. Olefsky, L. Guarente and M. Montminy (2008). "A fasting inducible switch modulates gluconeogenesis via activator/coactivator exchange." Nature **456**(7219): 269-273.

Long, F., E. Schipani, H. Asahara, H. Kronenberg and M. Montminy (2001). "The CREB family of activators is required for endochondral bone development." Development **128**(4): 541-550.

Lonze, B. E. and D. D. Ginty (2002). "Function and regulation of CREB family transcription factors in the nervous system." Neuron **35**(4): 605-623.

Lopez de Armentia, M., D. Jancic, R. Olivares, J. M. Alarcon, E. R. Kandel and A. Barco (2007). "cAMP response element-binding protein-mediated gene expression increases the intrinsic excitability of CA1 pyramidal neurons." J Neurosci **27**(50): 13909-13918.

Loriaux, M. M., R. G. Brennan and R. H. Goodman (1994). "Modulatory function of CREB.CREM alpha heterodimers depends upon CREM alpha phosphorylation." J Biol Chem **269**(46): 28839-28843.

Matsumoto, M., A. Pocai, L. Rossetti, R. A. Depinho and D. Accili (2007). "Impaired regulation of hepatic glucose production in mice lacking the forkhead transcription factor foxo1 in liver." Cell Metab **6**(3): 208-216.

Mayr, B. and M. Montminy (2001). "Transcriptional regulation by the phosphorylation-dependent factor CREB." Nat Rev Mol Cell Biol **2**(8): 599-609.

Mazzucchelli, C. and P. Sassone-Corsi (1999). "The inducible cyclic adenosine monophosphate early repressor (ICER) in the pituitary intermediate lobe: role in the stress response." Mol Cell Endocrinol **155**(1-2): 101-113.

Meinkoth, J. L., M. R. Montminy, J. S. Fink and J. R. Feramisco (1991). "Induction of a cyclic AMP-responsive gene in living cells requires the nuclear factor CREB." Mol Cell Biol **11**(3): 1759-1764.

Mockett, R. J., A. C. Bayne, L. K. Kwong, W. C. Orr and R. S. Sohal (2003). "Ectopic expression of catalase in Drosophila mitochondria increases stress resistance but not longevity." Free Radic Biol Med **34**(2): 207-217.

Molina, C. A., N. S. Foulkes, E. Lalli and P. Sassone-Corsi (1993). "Inducibility and negative autoregulation of CREM: an alternative promoter directs the expression of ICER, an early response repressor." Cell **75**(5): 875-886.

Montminy, M. (1997). "Transcriptional regulation by cyclic AMP." Annu Rev Biochem **66**: 807-822.

Montminy, M. R. and L. M. Bilezikjian (1987). "Binding of a nuclear protein to the cyclic-AMP response element of the somatostatin gene." Nature **328**(6126): 175-178.

Montminy, M. R., K. A. Sevarino, J. A. Wagner, G. Mandel and R. H. Goodman (1986). "Identification of a cyclic-AMP-responsive element within the rat somatostatin gene." Proc Natl Acad Sci U S A **83**(18): 6682-6686.

Murata, T., Y. Sato, S. Nakayama, A. Kudoh, S. Iwahori, H. Isomura, M. Tajima, T. Hishiki, T. Ohshima, M. Hijikata, K. Shimotohno and T. Tsurumi (2009). "TORC2, a coactivator of cAMP-response element-binding protein, promotes Epstein-Barr virus reactivation from latency through interaction with viral BZLF1 protein." J Biol Chem **284**(12): 8033-8041.

Nakajima, T., C. Uchida, S. F. Anderson, C. G. Lee, J. Hurwitz, J. D. Parvin and M. Montminy (1997). "RNA helicase A mediates association of CBP with RNA polymerase II." Cell **90**(6): 1107-1112.

Nantel, F., L. Monaco, N. S. Foulkes, D. Masquilier, M. LeMeur, K. Henriksen, A. Dierich, M. Parvinen and P. Sassone-Corsi (1996). "Spermiogenesis deficiency and germ-cell apoptosis in CREM-mutant mice." Nature **380**(6570): 159-162.

Nassel, D. R. (2002). "Neuropeptides in the nervous system of Drosophila and other insects: multiple roles as neuromodulators and neurohormones." Prog Neurobiol **68**(1): 1-84.

Neely, G. G., K. Kuba, A. Cammarato, K. Isobe, S. Amann, L. Zhang, M. Murata, L. Elmen, V. Gupta, S. Arora, R. Sarangi, D. Dan, S. Fujisawa, T. Usami, C. P. Xia, A. C. Keene, N. N. Alayari, H. Yamakawa, U. Elling, C. Berger, M. Novatchkova, R. Koglgruber, K. Fukuda, H. Nishina, M. Isobe, J. A. Pospisilik, Y. Imai, A. Pfeufer, A. A. Hicks, P. P. Pramstaller, S. Subramaniam, A. Kimura, K. Ocorr, R. Bodmer and J. M. Penninger (2010). "A global in vivo Drosophila RNAi screen identifies NOT3 as a conserved regulator of heart function." Cell **141**(1): 142-153.

Nordborg, C., M. Kyllerman, N. Conradi and J. E. Mansson (1997). "Early-infantile galactosialidosis with multiple brain infarctions: morphological, neuropathological and neurochemical findings." Acta Neuropathol **93**(1): 24-33.

Ocorr, K., T. Akasaka and R. Bodmer (2007). "Age-related cardiac disease model of Drosophila." Mech Ageing Dev **128**(1): 112-116.

Ocorr, K., N. L. Reeves, R. J. Wessells, M. Fink, H. S. Chen, T. Akasaka, S. Yasuda, J. M. Metzger, W. Giles, J. W. Posakony and R. Bodmer (2007). "KCNQ potassium channel mutations cause cardiac arrhythmias in Drosophila that mimic the effects of aging." Proc Natl Acad Sci U S A **104**(10): 3943-3948.

Okamoto, M., H. Takemori and Y. Katoh (2004). "Salt-inducible kinase in steroidogenesis and adipogenesis." Trends Endocrinol Metab **15**(1): 21-26.

Olson, E. N. (2006). "Gene regulatory networks in the evolution and development of the heart." Science **313**(5795): 1922-1927.

Osterwalder, T., A. Kuhnen, W. M. Leiserson, Y. S. Kim and H. Keshishian (2004). "Drosophila serpin 4 functions as a neuroserpin-like inhibitor of subtilisin-like proprotein convertases." J Neurosci **24**(24): 5482-5491.

Parker, D., U. S. Jhala, I. Radhakrishnan, M. B. Yaffe, C. Reyes, A. I. Shulman, L. C. Cantley, P. E. Wright and M. Montminy (1998). "Analysis of an activator:coactivator complex reveals an essential role for secondary structure in transcriptional activation." Mol Cell **2**(3): 353-359.

Paternostro, G., C. Vignola, D. U. Bartsch, J. H. Omens, A. D. McCulloch and J. C. Reed (2001). "Age-associated cardiac dysfunction in Drosophila melanogaster." Circ Res **88**(10): 1053-1058.

Perazzona, B., G. Isabel, T. Preat and R. L. Davis (2004). "The role of cAMP response element-binding protein in Drosophila long-term memory." J Neurosci **24**(40): 8823-8828.

Pruitt, K. D., J. Harrow, R. A. Harte, C. Wallin, M. Diekhans, D. R. Maglott, S. Searle, C. M. Farrell, J. E. Loveland, B. J. Ruef, E. Hart, M. M. Suner, M. J. Landrum, B. Aken, S. Ayling, R. Baertsch, J. Fernandez-Banet, J. L. Cherry, V. Curwen, M. Dicuccio, M. Kellis, J. Lee, M. F. Lin, M. Schuster, A. Shkeda, C. Amid, G. Brown, O. Dukhanina, A. Frankish, J. Hart, B. L. Maidak, J. Mudge, M. R. Murphy, T. Murphy, J. Rajan, B. Rajput, L. D. Riddick, C. Snow, C. Steward, D. Webb, J. A. Weber, L. Wilming, W. Wu, E. Birney, D. Haussler, T. Hubbard, J. Ostell, R. Durbin and D. Lipman (2009). "The consensus coding sequence (CCDS) project: Identifying a common protein-coding gene set for the human and mouse genomes." Genome Res **19**(7): 1316-1323.

Pshezhetsky, A. V. and A. Hinek (2009). "Serine carboxypeptidases in regulation of vasoconstriction and elastogenesis." Trends Cardiovasc Med **19**(1): 11-17.

Puig, O., M. T. Marr, M. L. Ruhf and R. Tjian (2003). "Control of cell number by Drosophila FOXO: downstream and feedback regulation of the insulin receptor pathway." Genes Dev **17**(16): 2006-2020.

Qi, L., M. Saberi, E. Zmuda, Y. Wang, J. Altarejos, X. Zhang, R. Dentin, S. Hedrick, G. Bandyopadhyay, T. Hai, J. Olefsky and M. Montminy (2009). "Adipocyte CREB promotes insulin resistance in obesity." Cell Metab **9**(3): 277-286.

Quinn, P. G. (1993). "Distinct activation domains within cAMP response element-binding protein (CREB) mediate basal and cAMP-stimulated transcription." J Biol Chem **268**(23): 16999-17009.

Radhakrishnan, I., G. C. Perez-Alvarado, D. Parker, H. J. Dyson, M. R. Montminy and P. E. Wright (1997). "Solution structure of the KIX domain of CBP bound to the transactivation domain of CREB: a model for activator:coactivator interactions." Cell **91**(6): 741-752.

Ravnskjaer, K., H. Kester, Y. Liu, X. Zhang, D. Lee, J. R. Yates, 3rd and M. Montminy (2007). "Cooperative interactions between CBP and TORC2 confer selectivity to CREB target gene expression." Embo J.

Ravnskjaer, K., H. Kester, Y. Liu, X. Zhang, D. Lee, J. R. Yates, 3rd and M. Montminy (2007). "Cooperative interactions between CBP and TORC2 confer selectivity to CREB target gene expression." Embo J **26**(12): 2880-2889.

Rehfuss, R. P., K. M. Walton, M. M. Loriaux and R. H. Goodman (1991). "The cAMP-regulated enhancer-binding protein ATF-1 activates transcription in response to cAMP-dependent protein kinase A." J Biol Chem **266**(28): 18431-18434.

Riccio, A., S. Ahn, C. M. Davenport, J. A. Blendy and D. D. Ginty (1999). "Mediation by a CREB family transcription factor of NGF-dependent survival of sympathetic neurons." Science **286**(5448): 2358-2361.

Robertson, H. M., C. R. Preston, R. W. Phillis, D. M. Johnson-Schlitz, W. K. Benz and W. R. Engels (1988). "A stable genomic source of P element transposase in Drosophila melanogaster." Genetics **118**(3): 461-470.

Rudolph, D., A. Tafuri, P. Gass, G. J. Hammerling, B. Arnold and G. Schutz (1998). "Impaired fetal T cell development and perinatal lethality in mice lacking the cAMP response element binding protein." Proc Natl Acad Sci U S A **95**(8): 4481-4486.

Ruppert, S., T. J. Cole, M. Boshart, E. Schmid and G. Schutz (1992). "Multiple mRNA isoforms of the transcription activator protein CREB: generation by alternative splicing and specific expression in primary spermatocytes." Embo J **11**(4): 1503-1512.

Ryu, D., K. J. Oh, H. Y. Jo, S. Hedrick, Y. N. Kim, Y. J. Hwang, T. S. Park, J. S. Han, C. S. Choi, M. Montminy and S. H. Koo (2009). "TORC2 regulates hepatic insulin signaling via a mammalian phosphatidic acid phosphatase, LIPIN1." Cell Metab **9**(3): 240-251.

Sakai, T., T. Tamura, T. Kitamoto and Y. Kidokoro (2004). "A clock gene, period, plays a key role in long-term memory formation in Drosophila." Proc Natl Acad Sci U S A **101**(45): 16058-16063.

Screaton, R. A., M. D. Conkright, Y. Katoh, J. L. Best, G. Canettieri, S. Jeffries, E. Guzman, S. Niessen, J. R. Yates, 3rd, H. Takemori, M. Okamoto and M. Montminy (2004). "The CREB coactivator TORC2 functions as a calcium- and cAMP-sensitive coincidence detector." Cell **119**(1): 61-74.

Selkoe, D. J. (2002). "Alzheimer's disease is a synaptic failure." Science **298**(5594): 789-791.

Shaw, R. J., K. A. Lamia, D. Vasquez, S. H. Koo, N. Bardeesy, R. A. Depinho, M. Montminy and L. C. Cantley (2005). "The kinase LKB1 mediates glucose homeostasis in liver and therapeutic effects of metformin." Science **310**(5754): 1642-1646.

Sheng, M., M. A. Thompson and M. E. Greenberg (1991). "CREB: a Ca(2+)-regulated transcription factor phosphorylated by calmodulin-dependent kinases." Science **252**(5011): 1427-1430.

Spiegelman, B. M. and R. Heinrich (2004). "Biological control through regulated transcriptional coactivators." Cell **119**(2): 157-167.

Struhl, K. (1998). "Histone acetylation and transcriptional regulatory mechanisms." Genes Dev **12**(5): 599-606.

Struthers, R. S., W. W. Vale, C. Arias, P. E. Sawchenko and M. R. Montminy (1991). "Somatotroph hypoplasia and dwarfism in transgenic mice expressing a non-phosphorylatable CREB mutant." Nature **350**(6319): 622-624.

Sun, P., H. Enslen, P. S. Myung and R. A. Maurer (1994). "Differential activation of CREB by Ca2+/calmodulin-dependent protein kinases type II and type IV involves phosphorylation of a site that negatively regulates activity." Genes Dev **8**(21): 2527-2539.

Svensson, M. J. and J. Larsson (2007). "Thioredoxin-2 affects lifespan and oxidative stress in Drosophila." Hereditas **144**(1): 25-32.

Taghli-Lamallem, O., T. Akasaka, G. Hogg, U. Nudel, D. Yaffe, J. S. Chamberlain, K. Ocorr and R. Bodmer (2008). "Dystrophin deficiency in Drosophila reduces lifespan and causes a dilated cardiomyopathy phenotype." Aging Cell **7**(2): 237-249.

Taguchi, A. and M. F. White (2008). "Insulin-like signaling, nutrient homeostasis, and life span." Annu Rev Physiol **70**: 191-212.

Takemori, H., M. Kanematsu, J. Kajimura, O. Hatano, Y. Katoh, X. Z. Lin, L. Min, T. Yamazaki, J. Doi and M. Okamoto (2007). "Dephosphorylation of TORC initiates expression of the StAR gene." Mol Cell Endocrinol **265-266**: 196-204.

Tao, Y. and R. A. Schulz (2007). "Heart development in Drosophila." Semin Cell Dev Biol **18**(1): 3-15.

Tatar, M., A. Kopelman, D. Epstein, M. P. Tu, C. M. Yin and R. S. Garofalo (2001). "A mutant Drosophila insulin receptor homolog that extends life-span and impairs neuroendocrine function." Science **292**(5514): 107-110.

Tomita, H., M. Nazmy, K. Kajimoto, G. Yehia, C. A. Molina and J. Sadoshima (2003). "Inducible cAMP early repressor (ICER) is a negative-feedback regulator of cardiac hypertrophy and an important mediator of cardiac myocyte apoptosis in response to beta-adrenergic receptor stimulation." Circ Res **93**(1): 12-22.

Tonon, G., S. Modi, L. Wu, A. Kubo, A. B. Coxon, T. Komiya, K. O'Neil, K. Stover, A. El-Naggar, J. D. Griffin, I. R. Kirsch and F. J. Kaye (2003). "t(11;19)(q21;p13) translocation in mucoepidermoid carcinoma creates a novel fusion product that disrupts a Notch signaling pathway." Nat Genet **33**(2): 208-213.

Van Handel, E. (1985). "Rapid determination of glycogen and sugars in mosquitoes." J Am Mosq Control Assoc **1**(3): 299-301.

Van Handel, E. (1985). "Rapid determination of total lipids in mosquitoes." J Am Mosq Control Assoc **1**(3): 302-304.

Vander, A. J., J. H. Sherman and D. S. Luciano (1998). Human physiology : the mechanisms of body function. Boston, Mass., WCB McGraw-Hill.

Vo, N. and R. H. Goodman (2001). "CREB-binding protein and p300 in transcriptional regulation." J Biol Chem **276**(17): 13505-13508.

Wadzinski, B. E., W. H. Wheat, S. Jaspers, L. F. Peruski, Jr., R. L. Lickteig, G. L. Johnson and D. J. Klemm (1993). "Nuclear protein phosphatase 2A dephosphorylates protein kinase A-phosphorylated CREB and regulates CREB transcriptional stimulation." Mol Cell Biol **13**(5): 2822-2834.

Walker, W. H., C. Girardet and J. F. Habener (1996). "Alternative exon splicing controls a translational switch from activator to repressor isoforms of transcription factor CREB during spermatogenesis." J Biol Chem **271**(33): 20145-21050.

Wang, B., J. Goode, J. Best, J. Meltzer, P. E. Schilman, J. Chen, D. Garza, J. B. Thomas and M. Montminy (2008). "The insulin-regulated CREB coactivator TORC promotes stress resistance in Drosophila." Cell Metab **7**(5): 434-444.

Wang, Y., H. Inoue, K. Ravnskjaer, K. Viste, N. Miller, Y. Liu, S. Hedrick, L. Vera and M. Montminy (2010). "Targeted disruption of the CREB coactivator Crtc2 increases insulin sensitivity." Proc Natl Acad Sci U S A **107**(7): 3087-3092.

Wang, Y., L. Vera, W. H. Fischer and M. Montminy (2009). "The CREB coactivator CRTC2 links hepatic ER stress and fasting gluconeogenesis." Nature **460**(7254): 534-537.

Wang, Z., M. Iwasaki, F. Ficara, C. Lin, C. Matheny, S. H. Wong, K. S. Smith and M. L. Cleary (2010). "GSK-3 promotes conditional association of CREB and its coactivators with MEIS1 to facilitate HOX-mediated transcription and oncogenesis." Cancer Cell **17**(6): 597-608.

Wessells, R. J. and R. Bodmer (2004). "Screening assays for heart function mutants in Drosophila." Biotechniques **37**(1): 58-60, 62, 64 passim.

Wessells, R. J., E. Fitzgerald, J. R. Cypser, M. Tatar and R. Bodmer (2004). "Insulin regulation of heart function in aging fruit flies." Nat Genet **36**(12): 1275-1281.

Wu, Q., T. Wen, G. Lee, J. H. Park, H. N. Cai and P. Shen (2003). "Developmental control of foraging and social behavior by the Drosophila neuropeptide Y-like system." Neuron **39**(1): 147-161.

Wu, Z., X. Huang, Y. Feng, C. Handschin, P. S. Gullicksen, O. Bare, M. Labow, B. Spiegelman and S. C. Stevenson (2006). "Transducer of regulated CREB-binding proteins (TORCs) induce PGC-1alpha transcription and mitochondrial biogenesis in muscle cells." Proc Natl Acad Sci U S A **103**(39): 14379-14384.

Xing, L., V. K. Gopal and P. G. Quinn (1995). "cAMP response element-binding protein (CREB) interacts with transcription factors IIB and IID." J Biol Chem **270**(29): 17488-17493.

Xing, L. and P. G. Quinn (1994). "Three distinct regions within the constitutive activation domain of cAMP regulatory element-binding protein (CREB) are required for transcription activation." J Biol Chem **269**(46): 28732-28736.

Xu, W., L. H. Kasper, S. Lerach, T. Jeevan and P. K. Brindle (2007). "Individual CREB-target genes dictate usage of distinct cAMP-responsive coactivation mechanisms." Embo J **26**(12): 2890-2903.

Yanagisawa, M. and T. Masaki (1989). "Molecular biology and biochemistry of the endothelins." Trends Pharmacol Sci **10**(9): 374-378.

Yao, T. P., S. P. Oh, M. Fuchs, N. D. Zhou, L. E. Ch'ng, D. Newsome, R. T. Bronson, E. Li, D. M. Livingston and R. Eckner (1998). "Gene dosage-dependent embryonic development and proliferation defects in mice lacking the transcriptional integrator p300." Cell **93**(3): 361-372.

Yin, J. C., M. Del Vecchio, H. Zhou and T. Tully (1995). "CREB as a memory modulator: induced expression of a dCREB2 activator isoform enhances long-term memory in Drosophila." Cell **81**(1): 107-115.

Yin, J. C., J. S. Wallach, M. Del Vecchio, E. L. Wilder, H. Zhou, W. G. Quinn and T. Tully (1994). "Induction of a dominant negative CREB transgene specifically blocks long-term memory in Drosophila." Cell **79**(1): 49-58.

Yin, J. C., J. S. Wallach, E. L. Wilder, J. Klingensmith, D. Dang, N. Perrimon, H. Zhou, T. Tully and W. G. Quinn (1995). "A Drosophila CREB/CREM homolog encodes multiple isoforms, including a cyclic AMP-dependent protein kinase-responsive transcriptional activator and antagonist." Mol Cell Biol **15**(9): 5123-5130.

Yu, L., T. Lee, N. Lin and M. J. Wolf (2010). "Affecting Rhomboid-3 function causes a dilated heart in adult Drosophila." PLoS Genet **6**(5): e1000969.

Zeitouni, B., S. Senatore, D. Severac, C. Aknin, M. Semeriva and L. Perrin (2007). "Signalling pathways involved in adult heart formation revealed by gene expression profiling in Drosophila." PLoS Genet **3**(10): 1907-1921.

Zhang, X., D. T. Odom, S. H. Koo, M. D. Conkright, G. Canettieri, J. Best, H. Chen, R. Jenner, E. Herbolsheimer, E. Jacobsen, S. Kadam, J. R. Ecker, B. Emerson, J. B. Hogenesch, T. Unterman, R. A. Young and M. Montminy (2005). "Genome-wide analysis of cAMP-response element binding protein occupancy, phosphorylation, and target gene activation in human tissues." Proc Natl Acad Sci U S A **102**(12): 4459-4464.

Zhou, Y., H. Wu, S. Li, Q. Chen, X. W. Cheng, J. Zheng, H. Takemori and Z. Q. Xiong (2006). "Requirement of TORC1 for late-phase long-term potentiation in the hippocampus." PLoS ONE **1**: e16.

Zinke, I., C. S. Schutz, J. D. Katzenberger, M. Bauer and M. J. Pankratz (2002). "Nutrient control of gene expression in Drosophila: microarray analysis of starvation and sugar-dependent response." Embo J **21**(22): 6162-6173.